DRAFT

3-Dimensional Hydrodynamic and Water Quality Model of Lake Thunderbird, Oklahoma

EFDC Water Quality Model Setup, Calibration and Load Allocation

Tasks 1A, 1B, 1C and 1D

MARK DERICHSWEILER, ENGINEERING MANAGER
OKLAHOMA DEPT. ENVIRONMENTAL QUALITY
WATER QUALITY DIVISION
PO BOX 1677
OKLAHOMA CITY, OKLAHOMA 73101-1677

PURCHASE ORDER NO: 2929012225
March 30, 2012

DYNAMIC SOLUTIONS, LLC
6421 DEANE HILL DRIVE
KNOXVILLE, TENNESSEE 37919

Dynamic Solutions LLC

Table of Contents

List of Figures

List of Tables

List of Acronyms and Abbreviations

ADCP	Acoustic Doppler Continuous Profiler
BUMP	Beneficial Uses Monitoring Program
Chl-a	Chlorophyll-a
COD	Chemical Oxygen Demand
COE	United States Army Corps of Engineers
COMCD	Central Oklahoma Master Conservancy District
CST	Central Standard Time Zone
DO	Dissolved Oxygen
DOC	Dissolved Organic Carbon
DOM	Dissolved Organic Matter
DON	Dissolved Organic Nitrogen
DOP	Dissolved Organic Phosphorus
DSLLC	Dynamic Solutions, LLC
EFDC	Environmental Fluid Dynamics Code
EPA	Environmental Protection Agency
HSPF	Hydrologic Simulation Fortran Program
HUC	Hydrologic Unit Code for Catalog Units
LPOC	Labile particulate organic carbon
LPON	Labile particulate organic nitrogen
LPOP	Labile particulate organic phosphorus
MSL	Mean Sea Level
NAD83	North American Datum of 1983
NAVD88	North American Vertical Datum of 1988
NGVD29	National Geodetic Vertical Datum of 1929
NLW	Nutrient Limited Waterbody
NPS	Nonpoint Source
OCC	Oklahoma Conservation Commission
ODEQ	Oklahoma Department of Environmental Quality
OWRB	Oklahoma Water Resources Board
POC	Particulate Organic Carbon
POM	Particulate Organic Matter
PON	Particulate Organic Nitrogen
POP	Particulate Organic Phosphorus
RMS	Root Mean Square
RMSE	Root Mean Square Error
RPOC	Refractory particulate organic carbon
RPON	Refractory particulate organic nitrogen
RPOP	Refractory particulate organic phosphorus
SOD	Sediment Oxygen Demand

SWS	Sensitive Water Supply
TKN	Total Kjedhal Nitrogen (Total Organic Nitrogen + Ammonia-N)
TMDL	Total Maximum Daily Load
TN	Total Nitrogen
TOC	Total Organic Carbon
TON	Total Organic Nitrogen
TOP	Total Organic Phosphorus
TP	Total Phosphorus
TPO4	Total Phosphate
TSI	Trophic State Index
TSS	Total Suspended Solids
USGS	United States Geological Survey
UTM	Universal Transverse Mercator (map projection)
WQMP	Water Quality Management Plan
WWAC	Warm Water Aquatic Community

Section 1 INTRODUCTION, PURPOSE, AND SCOPE

1.1 Introduction

Lake Thunderbird (OK Waterbody Identification Number OK520810000020_00) is a 6,070-acre reservoir lake located at 35.222344 degrees north latitude and –97.257328 degrees west longitude in Cleveland County, Oklahoma within the Little River drainage basin (HUC8 11090203) (**Figure 1**). The lake was constructed in 1965 and is owned by the U.S. Bureau of Reclamation. The lake is on Oklahoma's 2008 303 (d) list for impaired beneficial uses of public/private water supply and warm water aquatic community life. Causes of impairment have been identified as low oxygen levels, high algae biomass levels, and high turbidity (ODEQ, 2008). Lake Thunderbird is classified as a Nutrient Limited Watershed in Oklahoma Water Quality Standards based on Carlson's Trophic State Index (TSI) (Carlson, 1977). Precise sources of nutrient loading that are causally related to nutrient enrichment are unknown, although it is generally thought that nonpoint source loading from watershed runoff of nutrients, sediments and organic matter is the cause. Lake Thunderbird, an important recreational lake for fishing and boating, is also identified as a Sensitive Water Supply (SWS) since the lake serves as a public water supply for the cities of Norman, Midwest City and Del City. With the three major municipalities of Norman, Midwest City and Oklahoma City in the watershed, this area is one of the fastest growing regions in Oklahoma. With considerable urban development over the past decade and continued urban development forecast by local governments, there is concern about the need for appropriate mitigation of the ecological impact of nonpoint sources of pollutant loading from the watershed to Lake Thunderbird.

1.2 Purpose

The Oklahoma Department of Environmental Quality (ODEQ) will develop a TMDL or a watershed-based water quality management plan (WQMP) in lieu of a TMDL for Lake Thunderbird. An important component of the plan will be the identification of potential load reductions needed to control loading of nutrients, organic matter and sediments to attain compliance with water quality targets for restoration of Lake Thunderbird to its designated beneficial uses. The technical foundation for the determination of the required load reductions will be based on a surface water model framework that includes, (a) a watershed hydrology and runoff model linked for input to, (b) a lake hydrodynamic and water quality model. The Hydrologic Simulation Program Fortran (HSPF) model (Bicknell et al., 2001) has been selected as the watershed model of choice for the Lake Thunderbird project. The Environmental Fluid Dynamics Code (EFDC) model (Hamrick, 1992; 1996; Park et al., 2000) has been selected as the hydrodynamic and water quality model of choice for the Lake Thunderbird project.

The linked watershed and lake model framework, calibrated to data collected from April 2008 through April 2009, will be used by ODEQ to assess the effectiveness of alternative BMPs and other load reduction scenarios needed to attain compliance with Oklahoma water quality standards and defined water quality targets for turbidity, chlorophyll-a, Trophic State Index (TSI) and dissolved oxygen for Lake Thunderbird. The calibrated HSPF watershed runoff and EFDC hydrodynamic and water quality model of the watershed and Lake Thunderbird will provide ODEQ with a scientifically defensible surface water model framework that can be used to support the development of a TMDL or a water quality management plan for Lake Thunderbird by ODEQ.

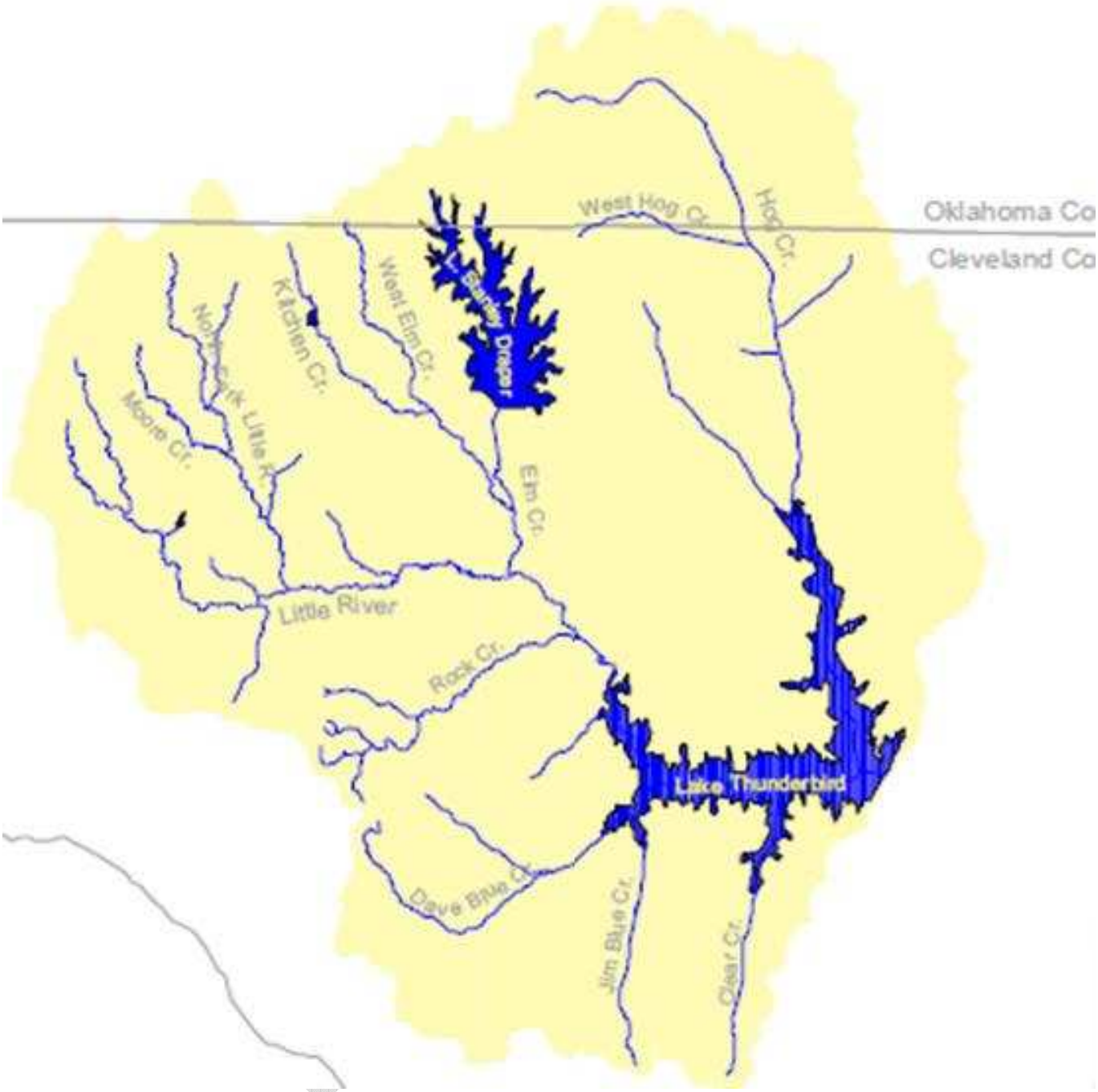

Figure 1 – Lake Thunderbird and location within upper reaches of the Little River watershed

The EFDC hydrodynamic and water quality model of Lake Thunderbird has been linked to results generated by the HSPF watershed model developed by ODEQ. A technical report documenting data sources, computational grid development, model setup and calibration of the EFDC hydrodynamic model of Lake Thunderbird was submitted to ODEQ in June 2011 (Dynamic Solutions, 2011) as a deliverable of the ODEQ contract for Tasks 1A, 1B(b) and 1B(c). The calibrated EFDC hydrodynamic model and the HSPF watershed model have been used to support the development of the EFDC water quality model of Lake Thunderbird in this next phase of this project. This report documents the data sources, model setup, water quality

model calibration and results of load allocation scenarios as the deliverable of the ODEQ contract for Tasks 1A, 1B, 1C, 1D, Task 2 and Task 3.

1.3 Scope

The scope of services for Task 1A, 1B, 1C, Task 2 and Task 3 included the following elements:

- Setup and develop data linkages between the ODEQ developed HSPF watershed runoff model and the EFDC lake model of hydrodynamics and water quality. The HSPF model results are used to provide streamflow, water temperature, suspended solids (TSS), organic carbon, nutrients (N,P), algae biomass, and dissolved oxygen as input data for the EFDC lake model;

- Provide peer review and technical support to ODEQ for the HSPF watershed model;

- Develop a curvilinear computational grid based on available bathymetric data from Oklahoma Water Resources Board (OWRB) and shoreline and topography data available from the United States Geological Survey (USGS);

- Analyze, process, and format available data to describe municipal water supply withdrawals from Central Oklahoma Master Conservancy District (COMCD);

- Analyze, process and format lake surface elevation, storage volume and release flow measured at the dam at Station NRMO2 by the US Army Corps of Engineers Tulsa District;

- Analyze, process and format wind and meteorological input data from Oklahoma MesoNet at Station NRMN;

- Analyze, process, and format available station data to describe time series and vertical profiles of water temperature, suspended solids, turbidity, dissolved oxygen, nutrients (N,P) and algae biomass as chlorophyll-a from OWRB;

- Analyze, process, and format available station data to describe sediment bed distributions of solids, nitrogen and phosphorus from OWRB;

- Process all data in formats required for input to the EFDC model for setup of the hydrodynamic, sediment transport, water quality and sediment diagenesis model;

- Calibrate the hydrodynamic and water quality model for the 374 day period from 18 April 2008 through 27 April 2009 to records for water level elevation, water temperature, suspended solids, dissolved oxygen, organic carbon, nutrients (N,P) and algae biomass as chlorophyll-a at eight (8) station locations in Lake Thunderbird;

- Analyze, process and present calibrated water quality model results to show comparisons to water quality targets for dissolved oxygen, anoxic volume of the lake, chlorophyll-a, Trophic State Index (TSI) and turbidity;

- Based on calibrated HSPF and EFDC models, compile mass balance budgets to compare external watershed loading of inorganic solids, organic carbon and nutrients

from the HSPF model and internal loading of nutrients across the sediment-water interface from the EFDC sediment diagenesis model;

- Using the calibrated HSPF watershed and EFDC lake models simulate the in-lake response to load allocation scenarios based on 50%, 75%, 85% and 95% reduction of inorganic solids, organic carbon and nutrients from the watershed to the lake;

- Using the selected load allocation scenario that provides the most likely compliance with one, or more, of the water quality targets with a series of sequential EFDC model spinup runs, derive a final set of initial conditions for the sediment diagenesis model that reflects approximate equilibrium conditions for the selected load reduction scenario;

- Using initial conditions for the sediment diagenesis model derived from the final lake model spinup run, simulate lake water quality response to the selected load reduction scenario;

- Prepare and submit draft and final technical reports documenting the development, calibration and application of the Lake Thunderbird EFDC hydrodynamic and water quality model.

1.4 Model Domain and Data Sources

Lake Thunderbird, a 6,070-acre reservoir in Cleveland County, Oklahoma is located approximately 35 miles southeast of Oklahoma City. **Figure 1** depicts Lake Thunderbird's location in the upper portion of the Little River watershed (HUC8 11090203). The upper watershed drains 255 square miles into Lake Thunderbird. **Figure 2** depicts the EFDC model domain and computational grid developed for Lake Thunderbird.

Data sources used for development of the Lake Thunderbird EFDC model included routine lake and tributary monitoring by Oklahoma Water Resources Board (OWRB) and the Oklahoma Conservation Commission (OCC); lake level and storage volume monitoring by the USGS and the U.S. Army Corps of Engineers (COE); and meteorological data from rain gages co-located with tributary sampling sites and the Oklahoma MesoNet network. Under Oklahoma's Beneficial Use Monitoring Program (BUMP), water quality samples were collected quarterly at seven station locations in Lake Thunderbird from October 2006 through June 2007 by OWRB (2008). Using Acoustic Doppler Continuous Profiler (ADCP), detailed lake data was also collected by OWRB in June 2001 to map bathymetry of Lake Thunderbird. In support of this effort to develop the HSPF watershed and EFDC lake model for Lake Thunderbird, an intensive one-year monitoring program was implemented by ODEQ to collect weekly samples from April 2008 through April 2009. Sediment bed data was also collected by ODEQ at five stations in the lake in July 2008 and December 2008 to provide solids and nutrient data needed to support development of the sediment diagenesis model. The data collected by ODEQ was used for development and calibration of the EFDC hydrodynamic, sediment transport, water quality and sediment diagenesis model.

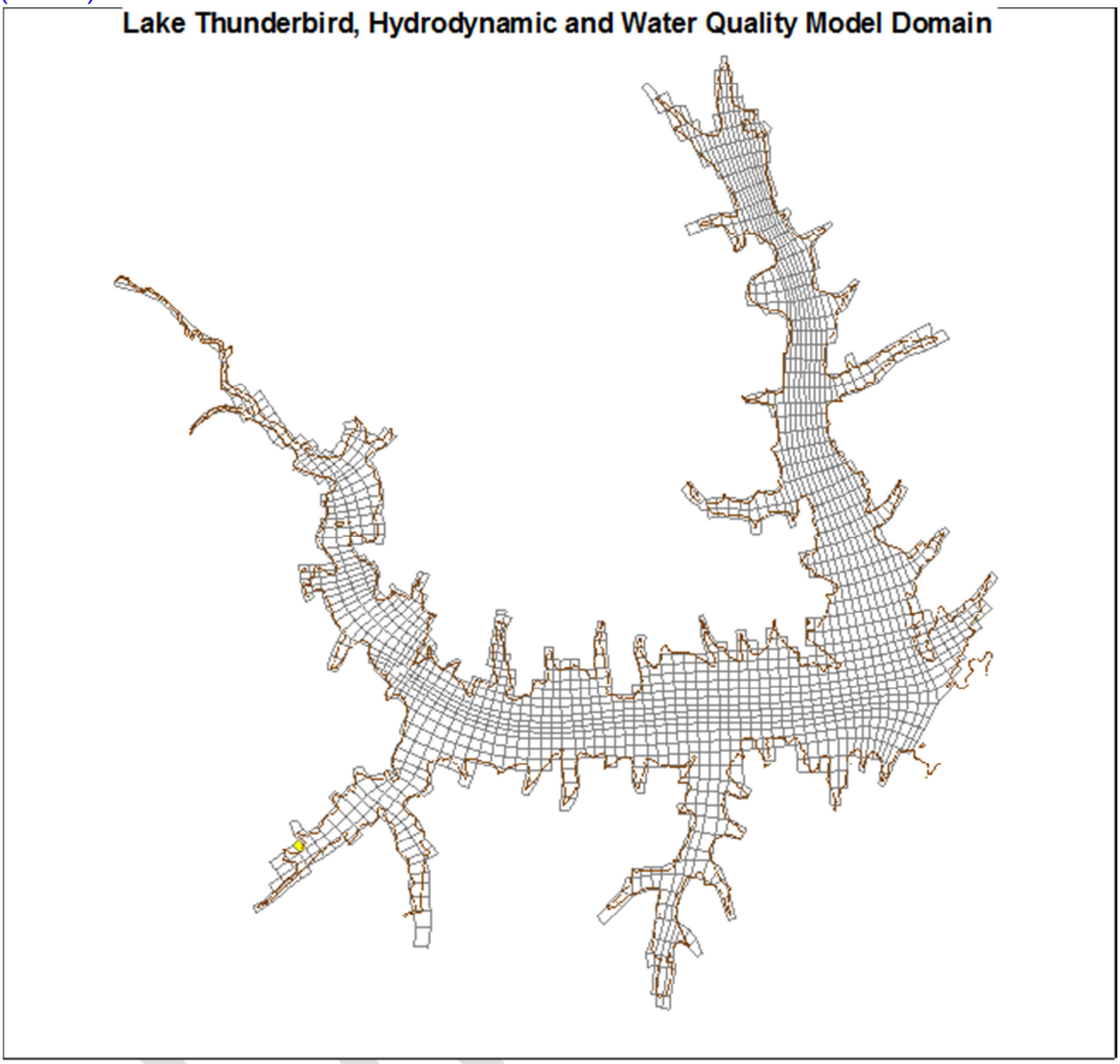

Figure 2 – EFDC model domain overlaid on 316.8 meter normal pool elevation contour for Lake Thunderbird.

Section 2 MODEL DEVELOPMENT

2.1 Overview of the EFDC Model

The Environmental Fluid Dynamics Code (EFDC) is a general-purpose surface water modeling package for simulating three-dimensional (3-D) circulation, mass transport, sediments and biogeochemical processes in surface waters including rivers, lakes, estuaries, reservoirs, nearshore and continental shelf-scale coastal systems. The EFDC model was originally developed at the Virginia Institute of Marine Science for estuarine and coastal applications (Hamrick, 1992; 1996). Over the past decade, the US Environmental Protection Agency (EPA) has continued to support its development, and EFDC is now part of a family of public domain surface water models recommended by EPA to support water quality investigations. In addition to state of the art hydrodynamics with salinity, water temperature and dye tracer simulation capabilities, EFDC can also simulate cohesive and non-cohesive sediment transport, the transport and fate of toxic contaminants in the water and sediment bed, and water quality interactions that include dissolved oxygen, nutrients, organic carbon, algae and bacteria. A state of the art sediment diagenesis model (Di Toro, 2001) is coupled with the water quality model (Park et al., 2000). Special enhancements to the hydrodynamic code, such as vegetation resistance, drying and wetting, hydraulic structure representation, wave-current boundary layer interaction, and wave-induced currents, allow refined modeling of tidal systems, wetland and marsh systems, controlled-flow systems, and near-shore wave-induced currents and sediment transport. The EFDC code has been extensively tested, documented and used in more than 100 surface water modeling studies (Ji, 2008). The EFDC model is currently used by university, government, engineering and environmental consulting organizations worldwide.

Dynamic Solutions, LLC (DSLLC), has developed a version of the EFDC code that streamlines the modeling process and provides links to DSLLC's pre- and post-processing software tool EFDC_Explorer5 (Craig, 2011). The DSLLC version of the EFDC code is open source and DSLLC coordinates with EPA to provide ongoing updates and enhancements to both DSLLC's version of EFDC as well as the version of the EFDC code provided by EPA.

2.2 Grid Development

In order to accurately describe the physical properties of Lake Thunderbird, a curvilinear horizontal computational grid was developed using the Delft Hydraulics grid generation software Delf3D-RGFGRID (Delft Hydraulics, 2007). The hydrodynamic and water quality model includes a total of 1,660 horizontal grids in the model domain (**Figure 2**). The EFDC model grid was configured with six (6) vertical layers to represent observed stratification of the lake. Each layer represented 1/6 of the total water depth for each cell.

2.3 Shoreline and Bathymetry

The OWRB provided bottom bathymetry survey data for Lake Thunderbird. This data set was used to interpolate and assign bathymetry for the computational grid of the EFDC model (**Figure 3)**. Details of model bathymetry in the vicinity of the dam are shown in **Figure 4** with an overlay of OWRB 5-ft contour intervals. The model domain was bounded by the normal pool elevation of 316.8 meters as shown by the black outline of the lake shoreline. The wetting and drying feature of the EFDC model was used to represent cells as dry when lake water surface elevation is less than the bottom elevation of a grid cell. Horizontal projection for the XY data

used to define shoreline and grid coordinates is UTM Zone 14 as meters with a horizontal datum of NAD83. Vertical datum used for the model is NAVD88 as meters relative to mean sea level. The causeway across the southwestern area of the Little River arm of the lake was represented in the model grid as a barrier to flow by removing selected model grid cells to force flow to be transported around the roadway.

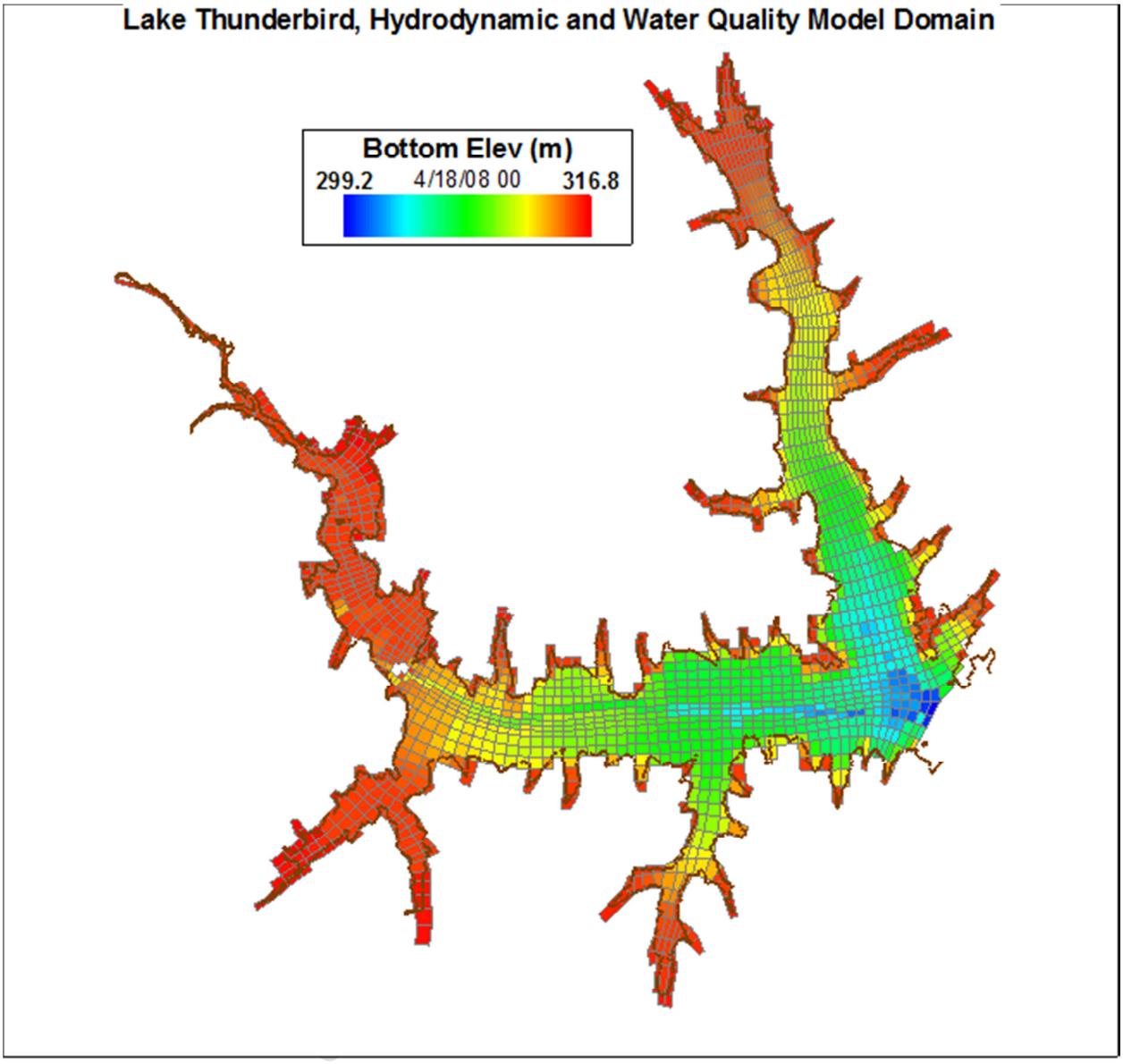

Figure 3 – Bathymetric map,grid cell bottom elevation in meters above MSL, NAVD88.

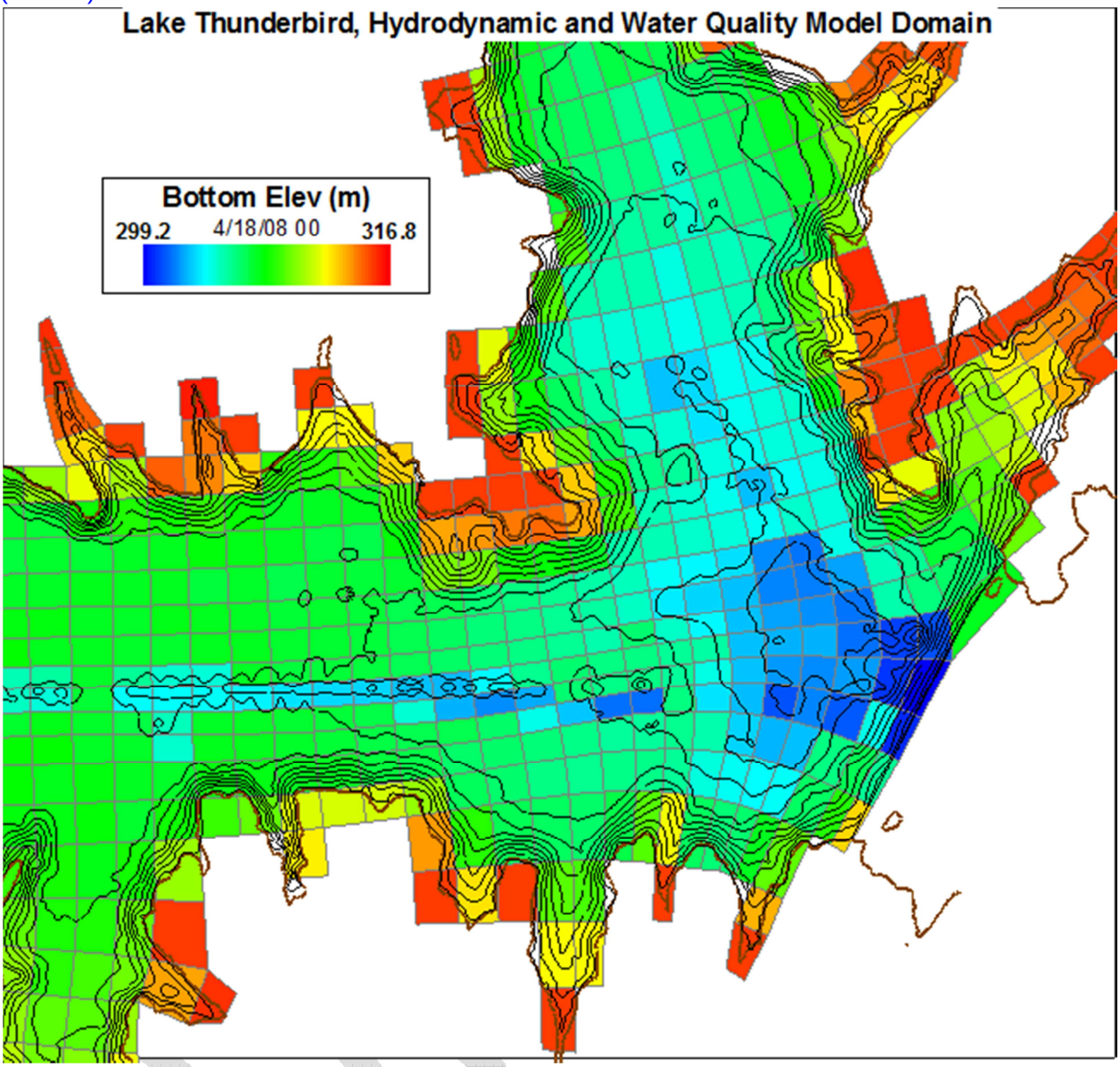

Figure 4 – Detail of bathymetry near dam in meters above MSL, NAVD88. OWRB contour lines are at 5-ft intervals.

2.4 Boundary Conditions

External flow boundary conditions from the HSPF model were assigned to grid cells based on physical location and the specific boundary condition represented in the lake model. The lake model was developed with 36 flow boundaries to define water coming into the lake from the HSPF watershed model and 2 flow boundaries to account for water removed from the lake by COMCD water supply withdrawals and releases of water at the dam. **Figure 1** shows the watershed area and streams represented in the HSPF model that drain into Lake Thunderbird. Simulated streamflow and runoff, water temperature, suspended solids, organic carbon, nutrients, dissolved oxygen and algae biomass records, aggregated to daily records from the 1-hr interval provided by the HSPF model, was used to assign flow boundaries for 18 tributaries

and 18 NPS catchments for input to the lake model. **Figure 5** shows the HSPF watershed model locations that provided the flow and water quality data for input to the lake model.

Flow boundaries also included water supply withdrawals at a common intake location from the reservoir for the municipalities of Norman, Midwest City and Del City. Water supply withdrawal data was provided by Central Oklahoma Master Conservancy District (COMCD). Flow release records at the dam (designated by the COE as Station NRM02) were recorded by the U.S. Army Corps of Engineers. In order to obtain input flow data for the model that agreed with the COE estimate of total inflow to the lake, a time series flow balance was derived from the difference between the COE inflow estimate, water supply withdrawals and the sum of the HSPF simulated flows. The derived flow balance data was assigned to eight grid cells around the perimeter of the lake.

Flow boundaries also included water supply withdrawals at a common intake location from the reservoir for the municipalities of Norman, Midwest City and Del City. Water supply withdrawal data was provided by Central Oklahoma Master Conservancy District (COMCD). Flow release records at the dam (designated by the COE as Station NRM02) were recorded by the U.S. Army Corps of Engineers. In order to obtain input flow data for the model that agreed with the COE estimate of total inflow to the lake, a time series flow balance was derived from the difference between the COE inflow estimate, water supply withdrawals and the sum of the HSPF simulated flows. The derived flow balance data was assigned to eight grid cells around the perimeter of the lake.

Figure 6 shows the EFDC model grid with the boundary condition locations identified as black squares for each boundary group. HSPF_ID codes and stream names of the boundary locations are given in Table 1. As can be seen in **Figure 6**, the HSPF boundary inflow locations were assigned near the normal pool elevation contour of 316.8 m as indicated by the black line. Table 1 lists the 39 model flow boundary indexes with the number of EFDC cells assigned for the boundary and the HSPF_ID corresponding to that location on **Figure 5**.

Table 1. Lake Thunderbird EFDC model flow boundaries and data source.

BC	HSPF_ID	NAME	Data	Cells	Filename
1	28_NPS	Little-River	HSPF	3	LOC_28_NPS.PLT
2	29_NPS	Little-River	HSPF	3	LOC_29_NPS.PLT
3	39_NPS	Little-River	HSPF	3	LOC_39_NPS.PLT
4	40_NPS	Rock-Creek	HSPF	3	LOC_40_NPS.PLT
5	41_NPS	Little-River	HSPF	3	LOC_41_NPS.PLT
6	43_NPS	Little-River	HSPF	3	LOC_43_NPS.PLT
7	64_TRIB	Little-River	HSPF	1	LOC_64_TRIB.PLT
8	27_TRIB	Elm-Creek	HSPF	1	LOC_27_TRIB.PLT
9	30_TRIB	unknown	HSPF	1	LOC_30_TRIB.PLT

BC	HSPF_ID	NAME	Data	Cells	Filename
10	42_TRIB	unknown	HSPF	1	LOC_42_TRIB.PLT
11	44_TRIB	Little-River	HSPF	1	LOC_44_TRIB.PLT
12	65_TRIB	Rock-Creek	HSPF	1	LOC_65_TRIB.PLT
13	47_TRIB	unknown	HSPF	1	LOC_47_TRIB.PLT
14	48_NPS	Little-River	HSPF	5	LOC_48_NPS.PLT
15	54_NPS	Distributed	HSPF	6	LOC_54_NPS.PLT
16	55_NPS	Distributed	HSPF	6	LOC_55_NPS.PLT
17	56_NPS	Dave-Blue-Creek	HSPF	4	LOC_56_NPS.PLT
18	58_TRIB	unknown	HSPF	1	LOC_58_TRIB.PLT
19	59_TRIB	Dave-Blue-Creek	HSPF	1	LOC_59_TRIB.PLT
20	57_TRIB	Jim-Blue-Creek	HSPF	2	LOC_57_TRIB.PLT
21	52_NPS	Little-River	HSPF	10	LOC_52_NPS.PLT
22	53_TRIB	Clear-Creek	HSPF	1	LOC_53_TRIB.PLT
23	50_NPS	Little-River	HSPF	8	LOC_50_NPS.PLT
24	51_NPS	Distributed	HSPF	5	LOC_51_NPS.PLT
25	49_NPS	Hog-Creek	HSPF	6	LOC_49_NPS.PLT
26	45_NPS	Distributed	HSPF	5	LOC_45_NPS.PLT
27	46_TRIB	Willow-Branch	HSPF	2	LOC_46_TRIB.PLT
28	37_NPS	Distributed	HSPF	6	LOC_37_NPS.PLT
29	38_TRIB	unknown	HSPF	1	LOC_38_TRIB.PLT
30	24_TRIB	unknown	HSPF	2	LOC_24_TRIB.PLT
31	23_NPS	Distributed	HSPF	4	LOC_23_NPS.PLT
32	22_TRIB	unknown	HSPF	2	LOC_22_TRIB.PLT
33	20_TRIB	unknown	HSPF	1	LOC_20_TRIB.PLT
34	19_NPS	Distributed	HSPF	3	LOC_19_NPS.PLT

BC	HSPF_ID	NAME	Data	Cells	Filename
35	17_TRIB	unknown	HSPF	2	LOC_17_TRIB.PLT
36	18_TRIB	Hog-Creek	HSPF	1	LOC_18_TRIB.PLT
37	INFLOW_1	Flow Balance	INFLOW	8	ACOE_2007_2009(INFLOW&HSPF&WATERSUPPLY).csv
38	OUTFLOW_1	Water-Supply	OUTFLOW	1	COMCD-DailyLog-Data-2003-Withdrawal(Total-COMCD3)INT-HR-EFDC-FMT.CSV
39	OUTFLOW_2	Dam	OUTFLOW	1	ACOE_LakeLevel_2007_2009(RELEASE-FLOW)INT-EFDC-FMT.DAT

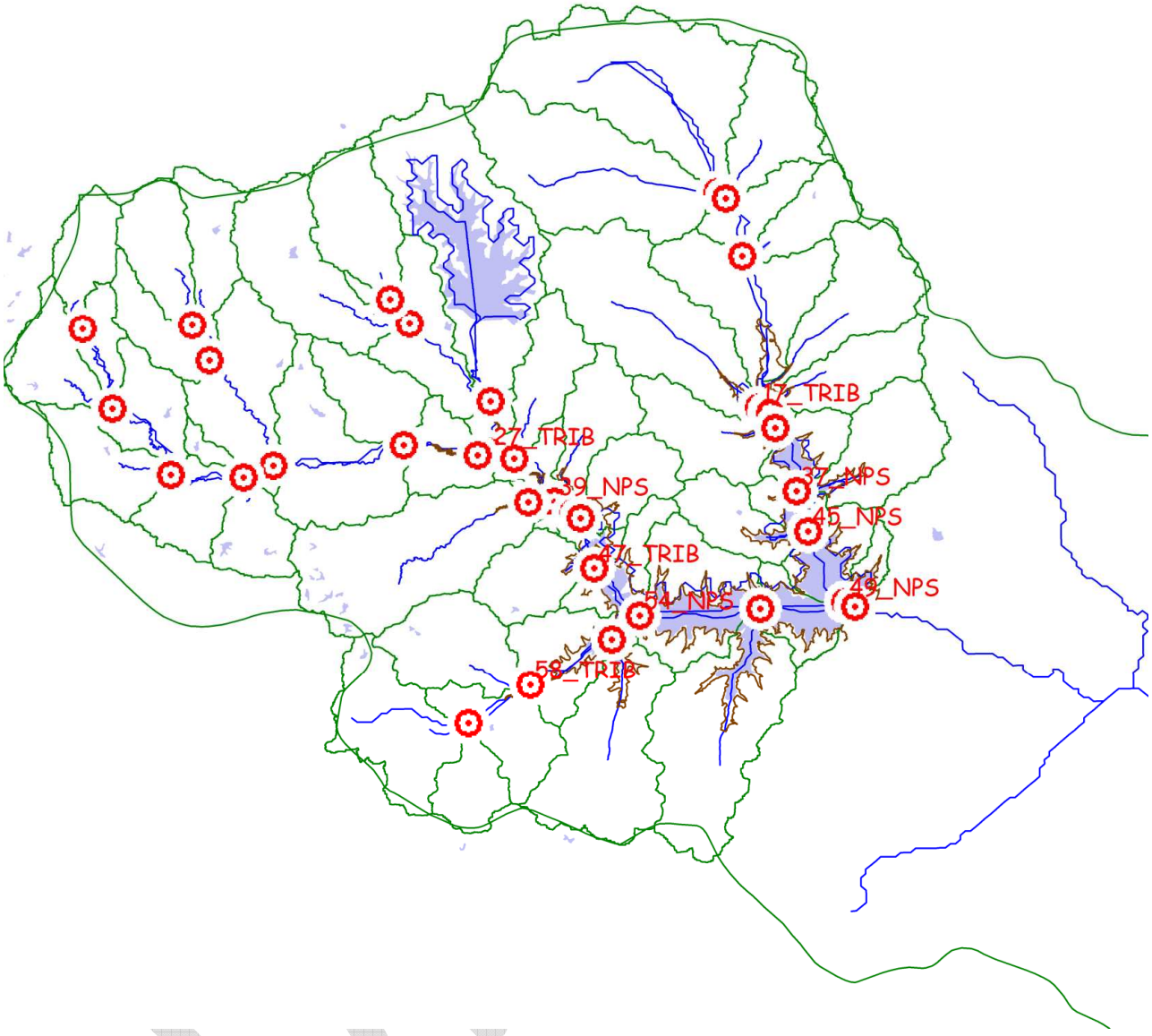

Figure 5 – HSPF tributary outlets and NPS catchment locations.

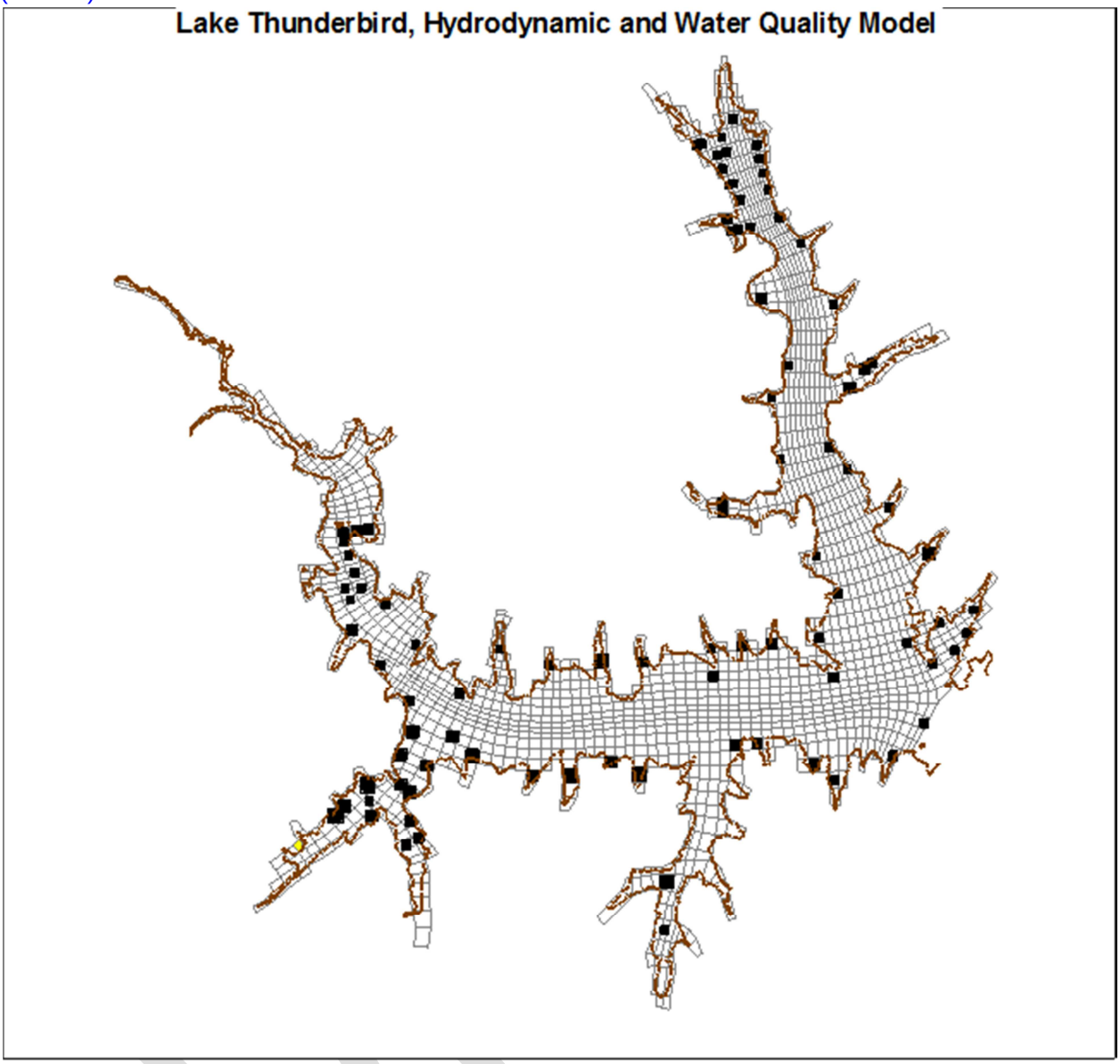

Figure 6 – Lake Thunderbird EFDC model boundary location map. Black contour line shows normal pool elevation of 316.8 m.

2.5 HSPF-EFDC Linkage

Boundary conditions for EFDC must be specified for flow boundary conditions to define external inflows of water and mass loading into the model domain. Flow boundary data sets required for input to EFDC include time series of flow, water temperature, suspended solids and water quality constituents to define mass loading inputs to a waterbody. Data sources for flow boundary condition time series data sets can include (a) USGS streamflow and water quality monitoring station locations; (b) simulated streamflow and water quality from watershed models; and (c) NPDES program discharge monitoring records (DMR) for effluent flow and pollutants for wastewater facilities and stormwater outflows. For the Lake Thunderbird model, streamflow and pollutant loading data obtained from the HSPF model developed to represent runoff over the drainage area to the reservoir. Sub-watersheds of the HSPF model defined by reaches where flow and pollutant loads are routed through a one-dimensional reach network simulate flow and water quality concentrations at fixed downstream outlet locations. Sub-watersheds not defined by an in stream reach simulates water volume and constituent loads as distributed NPS runoff over the drainage area of the sub-watershed. The HSPF sub-watersheds defined as in-stream reaches (TRIB) and distributed catchments (NPS) that provide external flow loads to the lake are listed in **Table 2** and mapped as boundary locations in **Figure 5** and **Figure 6**.

State variables of the HSPF watershed model developed for the Lake Thunderbird project are listed in Table 2**.** State variable units are identified for in-stream reaches (TRIB) and distributed catchments (NPS).

Table 2. HSPF State Variables and Units for Lake Thunderbird Model

HSPF State Variable	**Name**	**Units**	**Units**
HYDROLOGY		**TRIB**	**NPS**
Streamflow; NPS Runoff	FLOW	cfs	cf/hr
Water Temperature	WTEM	Deg-F	Deg-F
SEDIMENT TRANSPORT			
Inorganic Total Suspended Solids	TSS	mg/L	tons/hr
WATER QUALITY			
Algae biomass (as Chl-a)	PHYT	mg/L	lbs/hr
CBOD	CBOD	mg/L	lbs/hr
Refractory Organic Carbon	TORC	mg/L	lbs/hr
Refractory Organic Phosphorus	TORP	mg/L	lbs/hr
Total Phosphate	PO4	mg/L	lbs/hr
Total Phosphorus	TP	mg/L	lbs/hr
Refractory Organic Nitrogen	TORN	mg/L	lbs/hr
Ammonia+Ammonium-Nitrogen	NH3+NH4	mg/L	lbs/hr
Nitrate+Nitrite-Nitrogen	NO2+NO3	mg/L	lbs/hr
Total Nitrogen	TN	mg/L	lbs/hr
Dissolved Oxygen	DOX	mg/L	lbs/hr

The functional relationships used to link the HSPF results for input to the EFDC model are listed in Table 3. The HSPF-EFDC linkage of flow, water temperature, suspended solids, phosphate, ammonia, nitrate and dissolved oxygen is straightforward and only requires conversion of some of the HSPF units to EFDC units. HSPF-EFDC linkage of algae and organic matter requires transformations as described below.

Table 3. HSPF-EFDC Linkage

EFDC HYDRODYNAMICS & SEDIMENT TRANSPORT	**Units**	**HSPF-EFDC Linkage**
Flow	cms	HSPF Streamflow; Runoff
Water Temperature	C	HSPF Water Temperature (WTEM)
Inorganic Cohesive Solids	mg/L	HSPF TSS
EFDC WATER QUALITY		
Bluegreen Algae	mg/L	HSPF PHYT Biomass * C/Chl * F_BG
Diatoms Algae	mg/L	HSPF PHYT Biomass * C/Chl * F_D
Green Algae	mg/L	HSPF PHYT Biomass * C/Chl * F_G
Refractory Particulate Org Carbon	mg/L	HSPF (CBOD * C/O2 + TORC)* F_R
Labile Particulate Org Carbon	mg/L	HSPF (CBOD * C/O2 + TORC)* F_L
Diss Org Carbon	mg/L	HSPF (CBOD * C/O2 + TORC)* F_D
Refractory Particulate Org Phosphorus	mg/L	HSPF (CBOD * C/O2 *P/C + TORP)* F_R
Labile Particulate Org Phosphorus	mg/L	HSPF (CBOD * C/O2 *P/C + TORP)* F_L
Diss Org Phosphorus	mg/L	HSPF (CBOD * C/O2 *P/C + TORP)* F_D
Total Phosphate	mg/L	HSPF PO4
Refractory Particulate Org Nitrogen	mg/L	HSPF (CBOD * C/O2 *N/C + TORN)* F_R
Labile Particulate Org Nitrogen	mg/L	HSPF (CBOD * C/O2 *N/C + TORN)* F_L
Diss Org Nitrogen	mg/L	HSPF (CBOD * C/O2 *N/C + TORN)* F_D
Ammonium Nitrogen	mg/L	HSPF NH3+NH4
Nitrate+Nitrite Nitrogen	mg/L	HSPF NO2+NO3
Chemical Oxygen Demand	mg/L	HSPF n/a COD=0
Dissolved Oxygen	mg/L	HSPF DOX

HSPF represents algae as a single assemblage with output units for the Thunderbird project as mg Chla/L. HSPF algae is assigned to the EFDC functional groups based on the C/Chl ratio of each algae group and an equal split of biomass with the Blue Green (F_BG) and Green (F_G) groups. The Blue Green C/Chl ratio is assigned as 0.010 mg C/ug Chl and the Green C/Chl is assigned as 0.060 mg C/ug Chl.

Labile HSPF CBOD and refractory HSPF organic carbon (TORC), organic phosphorus (TORP), and organic nitrogen (TORN) are added as shown in the HSPF-EFDC linkage in Table 3 to derive TOC, TOP and TON for input to the EFDC model. HSPF derived TOC, TOP and TON is then split for input to EFDC as refractory, labile and dissolved components of total organic

matter using the fractions given in Table 4. CBOD is represented as ultimate CBOD in the HSPF model. The stoichiometric ratio for carbon to oxygen has a value of C/O2 = 12/32 = 0.375 mg C/mg-O2. The stoichiometric ratios for Phosphorus to Carbon and Nitrogen to Carbon are based on Redfield ratios where C/P = 41.1 mg C/mg-P and C/N = 5.7 mg C/mg-N (Di Toro 2001). Parameter values for assignment of the splits of TOC, TOP and TON (**Table 4**) are taken from tributary fall line data compiled for the Chesapeake Bay model (Cerco and Cole, 1994).

Table 4. Refractory, Labile and Dissolved Splits for Organic Matter (Source: Cerco and Cole, 1994)

	Refractory F_R	Labile F_L	Dissolved F_D
	RPOM	LPOM	DOM
TOC	0.16	0.04	0.80
TOP	0.72	0.18	0.10
TON	0.16	0.24	0.60

Section 3 WATER QUALITY AND SEDIMENT FLUX MODEL

3.1 Water Quality Model

For the Lake Thunderbird EFDC model, the water quality model is internally coupled with the hydrodynamic model, a sediment transport model and a sediment diagenesis model. The hydrodynamic model describes circulation and physical transport processes including turbulent mixing and water column stratification during the summer months. The sediment transport model describes the water column distribution of inorganic cohesive particles resulting from deposition and resuspension processes. The sediment diagenesis model describes the coupling of particulate organic matter deposition from the water column to the sediment bed, decomposition of organic matter in the bed, and the exchange of nutrients and dissolved oxygen across the sediment-water interface.

State variables of the EFDC hydrodynamic model (water temperature) and sediment transport model (inorganic suspended solids) are internally coupled with the EFDC water quality model. State variables of the EFDC water quality model include algae; organic carbon, inorganic phosphorus (orthophosphate), organic phosphorus; inorganic nitrogen (ammonium and nitrite + nitrate), organic nitrogen; chemical oxygen demand (COD) and dissolved oxygen. The state variables represented in the Lake Thunderbird hydrodynamic and water quality model are listed in Table 5. The EFDC water quality model is based on the kinetic processes developed for the Chesapeake Bay model (Cerco and Cole, 1995; Cerco et al., 2002). An overview of the source and sink terms for each state variable is presented in this section. The details of the state variable equations and kinetic terms for each state variable are presented in Park et al. (1995), Hamrick (2007) and Ji (2008). Tables listing the calibrated values of selected water quality model parameters and coefficients are presented in **Appendix A**.

Table 5. EFDC State Variables

	EFDC State Variable		**EFDC UNITS**	**Used in Model**
	Flow	FLOW	cms	Yes
	Water_Temperature	TEM	Deg-C	Yes
	Salinity	SAL	ppt	No
	Cohesive Suspended Solids	COH	mg/L	Yes
	Nocohesive Suspended Solids	NONCOH	mg/L	No
1	BlueGreen_Algae	CHC	mgC/L	Yes
2	Diatoms_Algae	CHD	mgC/L	No
3	Green_Algae	CHG	mgC/L	Yes
4	Refractory_Particulate_Org_C	RPOC	mgC/L	Yes
5	Labile_Particulate_Org_C	LPOC	mgC/L	Yes
6	Diss_Org_C	DOC	mgC/L	Yes

	EFDC State Variable		EFDC UNITS	Used in Model
7	Refractory_Particulate_Org_P	RPOP	mgP/L	Yes
8	Labile_Particulate_Org_P	LPOP	mgP/L	Yes
9	Diss_Org_P	DOP	mgP/L	Yes
10	Total_PhosphatePO4	TPO4	mgP/L	Yes
11	Refractory_Particulate_Org_N	RPON	mgN/L	Yes
12	Labile_Particulate_Org_N	LPON	mgN/L	Yes
13	Diss_Org_N	DON	mgN/L	Yes
14	Ammonium_N	NH4	mgN/L	Yes
15	Nitrate+Nitrite_N	NO3	mgN/L	Yes
16	Particulate-Biogenic_Silica	PBSI	mgSi/L	No
17	Available_Silica	SI	mgSi/L	No
18	Chemical_Oxy_Demand	COD	mg/L	Yes
19	Dissolved_Oxygen	OXY	mgO2/L	Yes
20	Total_Active_Metal	TAM	mg/L	No
21	Fecal_Coliform_Bacteria	FCB	# /100mL	No

Suspended Solids

Suspended solids in the EFDC model can be differentiated by size classes of cohesive and non-cohesive solids. For the Lake Thunderbird model, suspended solids are represented as a single size class of cohesive particles. Cohesive suspended solids are included in the model to account for the inorganic solids component of light attenuation in the water column. Since cohesive particles derived from silts and clays are characterized by a small particle diameter (< 62 microns) and a low settling velocity, cohesive particles can remain suspended in the water column for long periods of time and contribute to light attenuation that can influence algae production. Non-cohesive particles, consisting of fine to coarse size sands, by contrast, are characterized by much larger particles (> 62 microns) with rapid settling velocities that quickly remove any resuspended non-cohesive particles from the water column.

The key processes that control the distribution of cohesive particles are transport in the water column, flocculation and settling, deposition to the sediment bed, consolidation within the bed, and resuspension or erosion of the sediment bed. In the EFDC model for Lake Thunderbird, cohesive settling is defined by a constant settling velocity that is determined by model calibration. Deposition and erosion are controlled by the assignment of critical stresses for deposition and erosion and the bottom layer velocity and shear stress computed by the hydrodynamic model. The critical stress for erosion is typically defined with a factor of 1.2 times the critical deposition stress (Ji, 2008). Critical stresses for deposition and erosion of cohesive particles are taken from parameter values defined by Ji (2008) for a sediment transport model of Lake Okeechobee.

With a bed thickness of 0.5 meters, the sediment bed initial conditions for cohesive solids (520,000 g/m**2) are derived using a solids density of 2.6 g/cm**3, a porosity of 0.6 and a dry bulk density of 1.04 g/cm**3. These parameter values are considered typical for fine grained cohesive particles and a sediment bed characterized as silty-clay (Lick, 2009). Parameter values for deposition and erosion assigned for the calibration of cohesive solids are summarized in Table 6.

Table 6. EFDC model parameter values for cohesive solids

Variable	Value	Description	Units
SDEN	3.84615E-07	Sediment Specific Volume	m^3/g
SSG	2.6	Sediment Specific Gravity	--
WSEDO	1.75E-06	Constant Sediment Settling Velocity	m/s
TAUD	1.30E-05	Critical Stress for Deposition	$(m/s)^2$
WRSPO	5.00E-04	Reference Surface Erosion Rate	$g/m^2/s$
TAUR	1.60E-05	Critical Stress for Erosion	$(m/s)^2$

The units of $(m/s)^2$ shown in Table 6 for critical shear stress for deposition and erosion are not typical for sediment transport literature. The units assigned for the EFDC model are derived by normalizing the units typically measured for shear stress (e.g., dynes/cm^2) by a water density of 1000 kg/m^3. A critical shear stress for erosion of 0.16 dynes/cm^2 is thus assigned for input to EFDC with a value of 1.6e-05 $(m/s)^2$ by multiplying the shear stress of 0.16 dynes/cm^2 by a factor of 1.0e-04 since 1 dyne is defined as 1 g-cm/sec^2.

Algae

Phytoplankton in the EFDC model can be represented by three different functional groups of algae as (1) blue-green cyanobacteria; (2) diatoms and (3) green chlorophytes. For Lake Thunderbird, unlike many waterbodies, species group abundance data is available from OWRB (2004) to characterize the proportion of total algae biomass that can be attributed to different species groups over the course of the sampling season in 2003 from spring through fall. As described by OWRB (2004), blue-green algae species (cyanobacteria) were dominant during the late summer months of 2001-2003. Since species group data was available from 2001-2003 to gain insight into the trends of seasonal dominance of blue-green algae and green algae, the EFDC model of Lake Thunderbird accounted for both blue-green cyanobacteria and green algae as functional groups for the water quality model.

Kinetic processes represented for algae include photosynthetic production, basal metabolism (respiration and excretion), settling and predation. Photosynthetic production is described by a growth rate that is functionally dependent on a maximum growth rate, water temperature, the availability of sunlight at the surface, light extinction in the water column, the optimum light level for growth, and half-saturation dependent nutrient limitation by either nitrogen or phosphorus. Growth and basal metabolism are temperature dependent processes while settling and predation losses are assigned as constant parameter values. Key parameter values for kinetic coefficients for the algae model were based on data available from a model of Lake Washington in Seattle (Arhonditsis and Brett (2005). Maximum growth rates, for example, were assigned as

1.2 /day for blue-green cyanobacteria and as 1.8 /day for green algae. Other kinetic coefficients determined for calibration of the algae model are presented in **Appendix A**.

Light extinction in the EFDC model is dependent on the concentrations of state variables simulated for cohesive inorganic solids, detrital particulate organic matter and algal biomass (as chlorophyll-a). Although turbidity, *per se*, is not represented as a state variable in the EFDC model, the non-algal suspended matter components of turbidity, however, are included in the EFDC model as inorganic solids and detrital particulate organic carbon. The formulation used in the EFDC model to describe total light extinction (k_e) based on background light extinction and the state variable concentrations for InorgSS, Chla and POC is given as:

$$k_e = k_e(o) + k_e(InorgSS) + k_e(POC) + k_e(Chla)$$

Background light extinction [$k_e(o)$] is used to account for light attenuation of optically clear water (0.04 /meter) plus any light attenuation that is not controlled by inorganic suspended solids, detrital particulate organic matter and algal biomass. Color, for example, is not represented in the EFDC model but color can account for a portion of light attenuation. The coefficients used in EFDC for calculating the components of light extinction from inorganic solids, algae Chla and detrital particulate organic matter are based on coefficients reported by Di Toro (1978). For the application of the EFDC model to Lake Thunderbird, background light extinction [$k_e(o)$] is estimated using the equation given above with averaged secchi depth, chlorophyll, POC and TSS observations for stations with paired data sets. Based on the locations of the monitoring stations, 10 water quality zones were defined (**Figure 7**). Background light extinction coefficients were estimated and assigned for each zone as summarized in **Table** 7. Where station data was not available for Zone 1 and Zone 6, background coefficients of 1.0 /m and 0.5 /m were based on best judgment for these shallow areas. The background light extinction coefficients derived from paired chlorophyll, TSS, and secchi depth station data for 2008-2009 are in good agreement with the non-algal turbidity data compiled by OWRB (2011) using a longer time period of water quality records for the lake.

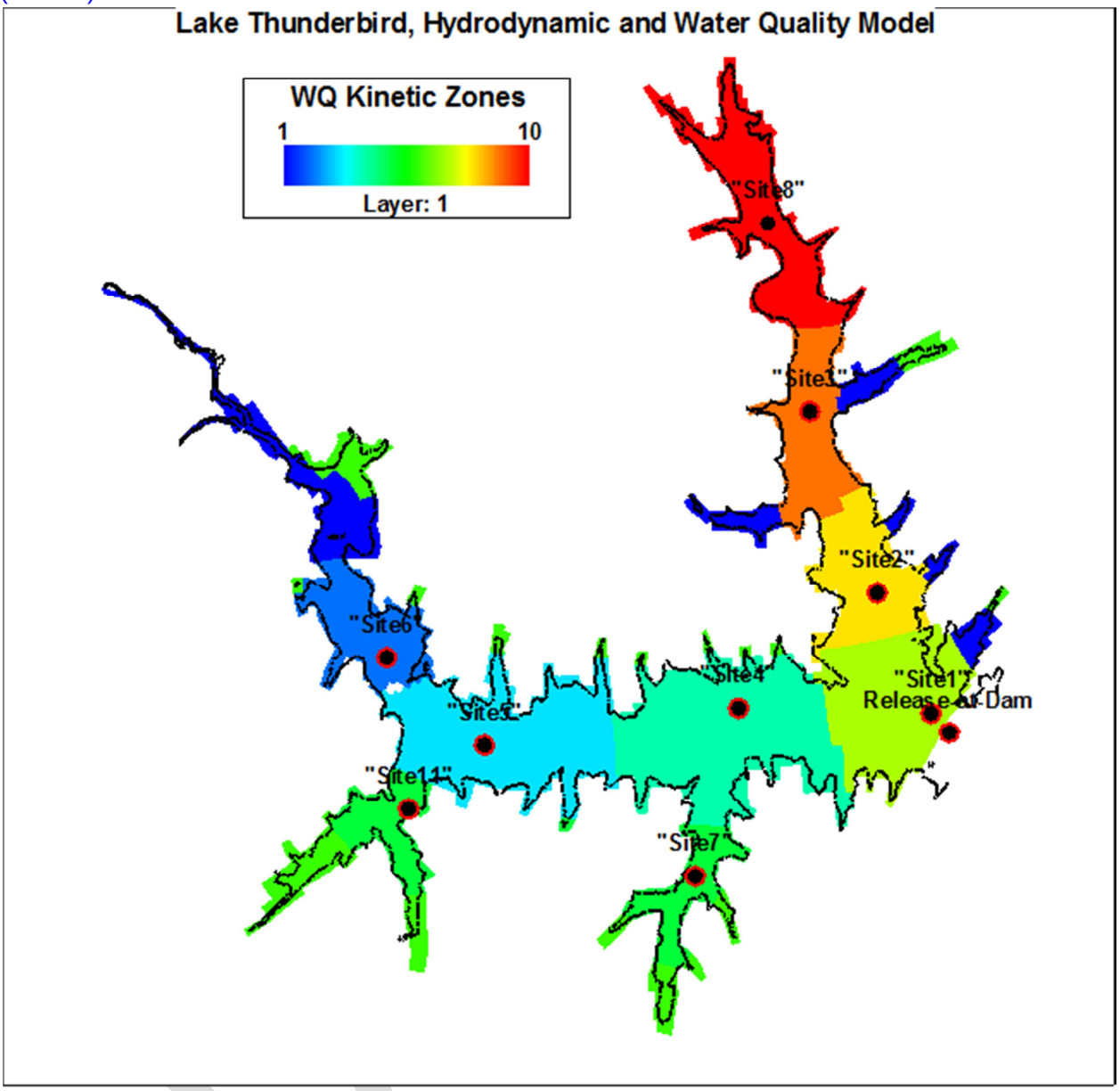

Figure 7 – Spatial water quality kinetic zones defined for Lake Thunderbird

Table 7. Water Quality Zones and Background Light Extinction Ke(o)

WQ Zone	OWRB Site	WQ Zone Characteristics	WQ Zone Location	Ke(o) 1/m
1	none	small streams	Little River	1.0
2	Site-6	riverine	Little River	5.0
3	Site-5	transition	Little River	2.2
4	Site-4	lacustrine	Little River	1.8
5	Site-7	wide tributary	Clear Creek	2.3
	Site-11	wide tributary	Dave Blue Creek	
6	none	headwaters; wet/dry		0.5
7	Site-1	lacustrine	Forebay/dam	1.8
8	Site-2	lacustrine	Hog Creek	1.8
9	Site-3	transition	Hog Creek	2.0
10	Site-8	riverine	Hog Creek	3.0

Organic Carbon

Total organic carbon is represented in the model with three state variables as dissolved organic carbon (DOC) and refractory and labile particulate organic carbon (RPOC and LPOC). The time scale for decomposition of particulate organic matter (POM) is used to differentiate refractory and labile POM with labile matter decomposing rapidly (weeks to months) while decay of refractory POM takes much longer (years). Although DOC is not termed “labile”, DOC is considered to react with a rapid time scale for decomposition (weeks to months).

Kinetic processes represented in the model for particulate organic carbon (POC) include algal predation, dissolution of RPOC and LPOC to DOC, and settling. Kinetic processes for DOC include sources from algal excretion and predation and dissolution of POC and losses from decomposition and denitrification. With the exception of settling of POC, all the kinetic reaction processes are temperature dependent.

Phosphorus

Total organic phosphorus is represented in the model with three state variables as dissolved organic phosphorus (DOP) and refractory and labile particulate organic phosphorus (RPOP and LPOP). As with organic carbon, the time scale for decomposition of particulate organic matter (POM) is used to differentiate refractory and labile POP. Kinetic processes represented in the model for POP include algal metabolism, predation, dissolution of RPOP and LPOP to DOP, and settling. Kinetic processes for DOP include sources from algal metabolism and predation and dissolution of POP to DOP with losses of DOP from mineralization to phosphate. With the exception of settling of POP, the kinetic reaction processes are temperature dependent.

Inorganic phosphorus is represented as single state variable for total phosphate which accounts for both the dissolved and sorbed forms of phosphate. Adsorption and desorption of phosphate is defined on the basis of equilibrium partitioning using an assigned phosphate partition coefficient for suspended solids. Kinetic terms for total phosphate include sources from algal metabolism and predation and mineralization from DOP. Losses for phosphate include settling of the sorbed fraction of total phosphate and uptake by phytoplankton growth. Depending on the concentration gradient between the bottom water column and sediment bed porewater phosphate, the sediment-water interface can serve as either a source or a loss term for phosphate in the water column. With the exception of the partition coefficient and the settling of sorbed phosphate, the kinetic reaction processes for phosphate are temperature dependent.

Nitrogen

Total organic nitrogen is represented in the model with three state variables as dissolved organic nitrogen (DON) and refractory and labile particulate organic nitrogen (RPON and LPON). As with organic carbon, the time scale for decomposition of particulate organic matter (POM) is used to differentiate refractory and labile PON. Kinetic processes represented in the model for PON include algal metabolism, predation, dissolution of RPON and LPON to DON, and settling. Kinetic processes for DON include sources from algal metabolism and predation, dissolution of PON to DON and losses of DON from mineralization of PON to ammonium. With the exception of settling of PON, the kinetic reaction processes are temperature dependent.

Inorganic nitrogen (ammonia, nitrite and nitrate) is represented by two state variables as (1) ammonia and (2) nitrite+nitrate. Kinetic terms for ammonia include sources from algal metabolism and predation and mineralization from DON. Losses for ammonia include bacterially mediated transformation to nitrite and nitrate by nitrification and uptake by phytoplankton growth. Depending on the concentration gradient between the bottom water column and sediment bed porewater ammonia, the sediment-water interface can serve as either a source or a loss term for ammonia in the water column. The kinetic reaction processes for ammonia are temperature dependent. Since the time scale for conversion of nitrite to nitrate is very rapid, nitrite and nitrate are combined as a single state variable representing the sum of these two forms of nitrogen. Kinetic terms for nitrite/nitrate include sources from nitrification from ammonia to nitrite and nitrate. Losses include uptake by phytoplankton growth and denitrification to nitrogen gas. Depending on the concentration gradient between the bottom water column and sediment bed porewater nitrite/nitrate, the sediment-water interface can serve as either a source or a loss term for nitrite/nitrate in the water column. The kinetic reaction processes for nitrite/nitrate are temperature dependent.

Chemical Oxygen Demand (COD)

In the EFDC water quality model, chemical oxygen demand (COD) represents the concentration of reduced substances that can be oxidized through inorganic processes. The principal source of COD in freshwater is methane released from oxidation of organic carbon in the sediment bed across the sediment-water interface. Since sediment bed decomposition is accounted for in the coupled sediment diagenesis model, the only source of COD to the water column is the flux of methane across the sediment-water interface. Sources from the open water boundaries and upstream flow boundaries are set to zero for COD. The loss term in the water column is defined by a temperature dependent first order oxidation rate.

Dissolved Oxygen

Dissolved oxygen is a key state variable in the water quality model since several kinetic processes interact with, and can be controlled by, dissolved oxygen. Kinetic processes represented in the oxygen model include sources from atmospheric reaeration in the surface layer and algal photosynthetic production. Kinetic loss terms include algal respiration, nitrification, decomposition of DOC, oxidation of COD, and bottom layer consumption of oxygen from sediment oxygen demand. Sediment oxygen demand is coupled with particulate organic carbon deposition from the water column and is computed internally in the sediment flux model. The kinetic reaction processes for dissolved oxygen are all temperature dependent.

Kinetic Coefficients

Most of the water quality parameters and coefficients needed by the EFDC water quality model were initialized with default values as indicated in the user's manual (Park, et.al., 1995; Hamrick, 2007). These default values are, in general, the same as the parameter values determined for the Chesapeake Bay model (Cerco and Cole, 1995). Models developed for Lake Washington (Arhonditsis and Brett, 2005) and the tributaries of Chesapeake Bay (Cerco et al., 2002) also provided several of the kinetic coefficients needed for the EFDC water quality model. Kinetic coefficients and model parameters were adjusted, as needed, within ranges reported in the literature, during model calibration to obtain the most reasonable agreement between observed and simulated water quality concentrations such as suspended solids, algal biomass, organic carbon, dissolved oxygen and nutrients. A large body of literature is available from numerous advanced modeling studies developed over the past decade to provide information on reported ranges of parameter values that can be assigned for site-specific modeling projects (see Ji, 2008; Park et al, 1995; Hamrick, 2007). Kinetic coefficients and model parameters assigned for the water quality model as either global or spatial zone dependent parameters for the Lake Thunderbird model are listed in **Appendix A**.

Initial Conditions for Water Quality Model

Spatially constant initial water quality conditions were assigned for input to the lake model. The initial values of the water quality constituents were derived based on observed data from the 8 monitoring stations used for model calibration. The composite average values of water quality constituents from April 2008 were calculated and assigned as the initial water quality condition. Table 8 presents the initial condition concentrations of water quality constituents assigned as a spatially uniform data set over each layer of the water column.

Table 8. Initial Conditions for EFDC Model

	EFDC State Variable		**EFDC UNITS**	**Initial Condition**
	Flow	FLOW	cms	n/a
	Water_Temperature	TEM	Deg-C	15
	Salinity	SAL	ppt	0
	Cohesive Suspended Solids	COH	mg/L	15
	Nocohesive Suspended Solids	NONCOH	mg/L	0

	EFDC State Variable		EFDC UNITS	Initial Condition
1	Blue Green_Algae	CHC	mg/L	0.012
2	Diatoms_Algae	CHD	mg/L	0.2
3	Green_Algae	CHG	mg/L	0.096
4	Refractory_Particulate_Organic_C	RPOC	mg/L	0.135
5	Labile_Particulate_Organic_C	LPOC	mg/L	0.405
6	Diss_Organic_C	DOC	mg/L	4.86
7	Refractory_Particulate_Org_P	RPOP	mg/L	0.0002
8	Labile_Particulate_Org_P	LPOP	mg/L	0.0006
9	Diss_Organic_P	DOP	mg/L	0.0072
10	Total_PhosphatePO4	TPO4	mg/L	0.021
11	Refractory_Particulate_Org_N	RPON	mg/L	0.0116
12	Labile_Particulate_Org_N	LPON	mg/L	0.0345
13	Diss_Organic_N	DON	mg/L	0.414
14	Ammonium_N	NH4	mg/L	0.05
15	Nitrate+Nitrite_N	NO3	mg/L	0.255
16	Particulate-Biogenic_Silica	PBSI	mg/L	1.5
17	Available_Silica	SI	mg/L	1.5
18	Chemical_Oxygen_Demand	COD	mg/L	0
19	Dissolved_Oxygen	OXY	mg/L	9
20	Total_Active_Metal	TAM	mg/L	0
21	Fecal_Coliform_Bacteria	FCB	# /100mL	0
	Total_Organic_Carbon	TOC	mgC/L	5.4
	Total_Organic_Phosphorus	TOP	mgN/L	0.008
	Total_Organic_Nitrogen	TON	mgP/L	0.4601
	Total_Kjedhal_Nitrogen	TKN	mgN/L	0.5101
	Total_Nitrogen	TN	mgN/L	0.7651
	Total_Phosphorus	TP	mgP/L	0.029
	Chlorophyll-a	Chla	ug/L	1.76

3.2 Sediment Flux Model

The EFDC water quality model provides three options for defining the sediment-water interface fluxes for nutrients and dissolved oxygen. The options are: (1) externally forced spatially and temporally constant fluxes; (2) externally forced spatially and temporally variable fluxes; and (3) internally coupled fluxes simulated with the sediment diagenesis model. The water quality state variables that are controlled by diffusive exchange across the sediment-water interface include phosphate, ammonia, nitrate, silica, chemical oxygen demand and dissolved oxygen. The first two options require that the sediment fluxes be assigned as spatial/temporal forcing functions based on either observed site-specific data from field surveys or best estimates based on the literature and sediment bed characteristics. The first two options, although acceptable for model calibration against historical data sets, do not provide the cause-effect predictive capability that is needed to evaluate future water quality conditions that might result from implementation of pollutant load reductions from watershed runoff. The third option, activation of the sediment diagenesis model developed by Di Toro (2001), does provide the cause-effect predictive capability to evaluate how water quality conditions might change with implementation of alternative load reduction or management scenarios. For the Lake Thunderbird model, the third option was selected to implement the sediment diagenesis model so that load allocation scenarios could be evaluated to determine an appropriate load allocation for Lake Thunderbird.

Living and non-living particulate organic carbon deposition, simulated in the EFDC water quality model, is internally coupled with the EFDC sediment diagenesis model. The sediment diagenesis model, based on the sediment flux model of Di Toro (2001), describes the decomposition of particulate organic matter in the sediment bed, the consumption of dissolved oxygen at the sediment-water interface (SOD) and the exchange of dissolved constituents (ammonia, nitrate, phosphate, silica, COD) across the sediment-water interface, State variables of the EFDC sediment flux model are sediment bed temperature, sediment bed particulate organic carbon (POC), particulate organic nitrogen (PON), particulate organic phosphorus (POP), porewater concentrations of phosphate, ammonia, nitrate, silica and sulfide/methane. The sediment diagenesis model computes sediment-water fluxes of chemical oxygen demand (COD), sediment oxygen demand (SOD), phosphate, ammonium, nitrate, and silica. The state variables modeled for the Lake Thunderbird sediment flux model listed in Table 9. An overview of the source and sink terms is presented with a description of each state variable group in this section. The details of the state variable equations, kinetic terms and numerical solution methods for the sediment diagenesis model are presented in Di Toro (2001), Park et al. (1995) and Ji (2008).

Table 9. EFDC sediment diagenesis model state variables

No.	Name	Bed Layer	Units	Activated
1	POC-G1	Layer-2	g/m^3	Yes
2	POC-G2	Layer-2	g/m^3	Yes
3	POC-G3	Layer-2	g/m^3	Yes
4	PON-G1	Layer-2	g/m^3	Yes
5	PON-G2	Layer-2	g/m^3	Yes
6	PON-G3	Layer-2	g/m^3	Yes
7	POP-G1	Layer-2	g/m^3	Yes
8	POP-G2	Layer-2	g/m^3	Yes

No.	Name	Bed Layer	Units	Activated
9	POP-G3	Layer-2	g/m^3	Yes
10	Partic-Biogenic-Silica	Layer-2	g/m^3	No
11	Sulfide/Methane	Layer-1	g/m^3	Yes
12	Sulfide/Methane	Layer-2	g/m^3	Yes
13	Ammonia-N	Layer-1	g/m^3	Yes
14	Ammonia-N	Layer-2	g/m^3	Yes
15	Nitrate-N	Layer-1	g/m^3	Yes
16	Nitrate-N	Layer-2	g/m^3	Yes
17	Phosphate-P	Layer-1	g/m^3	Yes
18	Phosphate-P	Layer-2	g/m^3	Yes
19	Available-Silica	Layer-1	g/m^3	No
20	Available-Silica	Layer-2	g/m^3	No
21	Ammonia-N-Flux		g/m^2-day	Yes
22	Nitrate-N-Flux		g/m^2-day	Yes
23	Phosphate-P-Flux		g/m^2-day	Yes
24	Silica Flux		g/m^2-day	Yes
25	SOD		g/m^2-day	Yes
26	COD Flux		g/m^2-day	Yes
27	Bed Temperature		Deg-C	Yes

Particulate Organic Matter

The sediment diagenesis model incorporates three key processes: (1) depositional flux of particulate organic matter (POM) from the water column to the sediment bed; (2) diagenesis or decomposition of POM in the sediment bed; and (3) the resulting fluxes of dissolved oxygen, chemical oxygen demand, sulfide and nutrients across the sediment-water interface. Particulate organic matter is represented as carbon (POC), nitrogen (PON), and phosphorus (POP) stoichiometric equivalents based on carbon-to-dry weight and Redfield ratios for C/N, and C/P. In the water quality model, POM deposition describes the settling flux from the water column to the bed of non-living refractory and labile detrital matter and living algal biomass. In the sediment flux model, POM is split into three classes of reactivity. The labile fraction (POM-G1) is defined by the fastest reaction rate with a half-life on the order of 20 days. The refractory fraction (POM-G2) is defined by a slower reaction rate with a half-life of about 1 year. The inert fraction (POM-G3) is non-reactive with negligible decay before ultimate burial into the deep inactive layer of the sediment bed.

The sediment flux model represents the sediment bed as a two layer system. The first layer is a thin aerobic layer and the second layer is a thicker anaerobic active layer. The thickness of the aerobic layer, which is on the order of only a millimeter, is internally computed in the sediment flux model as a function of bottom layer dissolved oxygen concentration, the sediment oxygen demand rate and the diffusivity coefficient for dissolved oxygen. The thickness of the anaerobic active layer, assigned as a model parameter, can be adjusted during model calibration. The depth of the anaerobic active layer is defined by the depth to which benthic organisms mix particles within a homogeneous bed layer. An active layer thickness of ~10 cm has been determined from both theoretical considerations and field observations in estuaries (Di Toro,

2001). Any particle mass transported out of the active layer is not recycled back into the active layer since these particles are lost to deep burial out of the sediment bed.

The thickness of the active layer controls the volume of the anaerobic layer, the amount of mass stored in the layer and the long-term response of the sediment bed to changes in organic matter deposition from the water column. A relatively thin active layer will respond quickly to changes in watershed loading and water column deposition of particulate matter. Conversely, a thick active layer will respond more slowly to changes in deposition of particulate materials. The rate at which solutes stored in the anaerobic active layer are transported between the thin aerobic and thick active layer, and potentially the overlying water column, is controlled by the mixing coefficients assigned, as model parameters for particulate and dissolved substances. Sediment bed thickness and mixing rates were calibrated to determine appropriate parameter values for each spatial zone for particulate and dissolved mixing coefficients.

Since the surface aerobic sediment layer is very thin, the depositional flux from the overlying water column is assigned to the lower anaerobic active sediment layer where decomposition then occurs. The source term for the three "G" classes of POM is the depositional flux from the overlying water column to the sediment bed. The loss terms for POM are the temperature dependent decay (i.e., diagenesis) of POM and removal by burial from the aerobic (upper) to active anaerobic (lower) layers and from the anaerobic (lower) layer to deep burial out of the sediment bed model domain.

Dissolved Constituents

The decay or mineralization of POM results in the diagenetic production of dissolved constituents. The concentration gradients of ammonia, nitrate, phosphate, and sulfide/methane within the two porewater layers and between the surficial porewater layer 1 and the bottom layer of the water column control the sediment fluxes computed in the model. Mineralization of POP produces phosphate which is then subject to adsorption/desorption by linear partitioning with solids in the sediment bed. Diffusive exchange is controlled by the concentration gradient of dissolved constituents, the diffusion velocity, and the bed layer thickness. Other processes that govern the mass balance of dissolved materials in the sediment bed include burial, particle mixing and removal by kinetic reactions.

Ammonia and Nitrate

Ammonia is produced in layer 2 by temperature dependent decomposition of the reactive G1 and G2 classes of PON. Ammonia is nitrified to nitrate with a temperature and oxygen dependent process. The only source term for nitrate is nitrification in the surficial layer. Nitrate is removed from both layers by temperature dependent denitrification with the carbon required for this process supplied by organic carbon diagenesis. Nitrogen is lost from the sediment bed by the denitrification flux out of the sediments as nitrogen gas (N2). The sediment-water fluxes of ammonia and nitrate to the overlying water column are then computed from the concentration gradients, the porewater diffusion coefficient and the thickness of the surficial bed layer.

Phosphate

Phosphate is produced by temperature dependent decomposition of the reactive G1 and G2 classes of particulate organic phosphorus in the lower layer 2 of the sediment bed. Since linear partitioning with solids is defined for phosphate, a fraction of total phosphate is computed as

particulate phosphate and a fraction remains in the dissolved form. The partition coefficient for phosphate for the surficial layer 1 is functionally dependent on (a) the oxygen concentration in the overlying bottom layer of the water column based on the assignment of 2 mg/L as a critical concentration for oxygen that triggers the oxygen dependent process, (b) the magnitude of the partition coefficient assigned for the lower layer 2, and (c) an enhancement factor multiplier. There are no removal terms for phosphate in either of the two layers. The sediment-water flux of dissolved phosphate to the overlying water column is then computed from the concentration gradient, the porewater diffusion coefficient and the thickness of the surficial bed layer.

Methane/Sulfide

Sulfide is produced by temperature decomposition of the reactive G1 and G2 classes of particulate organic carbon in the lower layer of the sediment bed. Sulfide is lost from the system by the organic carbon consumed by denitrification. Linear partitioning with solids is also defined for sulfide to account for the formation of iron sulfide. The sediment flux model accounts for three pathways for loss of sulfide from the sediment bed: (1) temperature dependent oxidation of sulfide; (2) aqueous flux of sulfide to the overlying water column; and (3) burial out of the model domain. If the overlying water column oxygen concentration is low then the sulfide that is not completely oxidized in the upper sediment layer can diffuse into the bottom layer of the water column. The aqueous flux of sulfide from the sediments is the source term for the flux of chemical oxygen demand (COD) from the sediment bed to the water column.

When sulfate is depleted, methane can be produced by carbon diagenesis and oxidation of methane then consumes oxygen. In saltwater systems, such as estuaries and coastal waters, sulfate is abundant and methane production and oxidation are not represented in the sediment flux model. In freshwater systems, such as Lake Thunderbird, sulfate is typically characterized by very low concentrations. In freshwater systems methane production and oxidation are represented in the sediment diagenesis model instead of sulfide production and oxidation.

Sediment Oxygen Demand

The sulfide/methane oxidation reactions in the surficial layer result in an oxygen flux to the sediment bed from the overlying water column. Sediment oxygen demand (SOD) includes the carbonaceous oxygen demand (CSOD) from sulfide/methane oxidation and the nitrogenous oxygen demand (NSOD) from nitrification. The total SOD is computed as the sum of the carbonaceous and nitrogenous components of the oxygen flux.

Sediment Diagenesis Model Parameters and Kinetic Coefficients

The sediment diagenesis model requires the assignment of a large number of model parameters and kinetic coefficients. Based on the results of sediment flux models developed for estuaries, coastal systems and lakes, Di Toro (2001) has summarized parameter values used for diagenesis, sediment properties, mixing and kinetic coefficients for the different projects. The comparison of data assigned for several different projects shows the robustness of the sediment flux model since many of the parameter values and kinetic coefficients were essentially unchanged for model applications unless there was a site-specific reason that supported the use of a different value. The exception to this generality, however, is the extreme variation of the kinetic coefficients required to represent partitioning of phosphate in the upper and lower layers of the sediment bed and the benthic release of dissolved phosphate under anoxic conditions in the hypolimnion. Since the sediment flux model does not explicitly represent the chemical

reactions and interactions that determine phosphate sorption, particularly under low oxygen conditions in the overlying water column when dissolved phosphate is released across the sediment-water interface, the sediment flux model coefficients that represent phosphate partitioning are parameters that were adjusted, as needed, to calibrate the model.

Ideally calibration of the sediment flux model would be supported by comparison of model results to site-specific measurements of sediment fluxes of oxygen, phosphate, ammonia and nitrate under aerobic and anoxic conditions. Since sediment flux measurements for oxygen and nutrients, however, are not available for Lake Thunderbird, measurements of phosphate fluxes from Lake Wister (Haggard and Scott, 2011); Lake Frances (Haggard and Soerens, 2006); Eucha Lake (Haggard et al., 2005); Beaver Lake in Arkansas (Sen et al., 2007; Hamdan et al., 2010), Acton Lake in Ohio (Nowlin et al., 2005) and a set of 17 lakes/reservoirs in the Central Plains (Dzialowski and Carter, undated) are used to provide a range of measured phosphate flux rates to support calibration of the sediment flux model for Lake Thunderbird.

Kinetic coefficients and parameters of the sediment flux model were initially assigned based on the Chesapeake Bay Model (Cerco and Cole, 1995; Cerco et al., 2002) and the compilation of parameter values reported in Di Toro (2001). Selected coefficients, particularly the phosphate partitioning parameters, were adjusted, as needed, to achieve calibration of the water quality and sediment flux model. Kinetic coefficients and model parameters assigned for calibration of the sediment diagenesis model as either global or spatial zone dependent parameters for the Lake Thunderbird model are listed in **Appendix B**.

Initial Conditions for Sediment Diagenesis Model

The sediment diagenesis model requires specification of initial conditions for particulate organic matter content (as C, N, P) and porewater concentrations of inorganic nutrients (as NH_4, NO_3, and PO_4). Sediment bed data was available for Lake Thunderbird from special surveys conducted in July 2008 and December 2008 to provide data needed to support the development of the lake model. Data was collected at sites to represent the lacustrine zone of the lake (Sites 1, 2, 4), the transition zone (Site 3) and the riverine zone (Site 8). Average values of the station data collected in July and December 2008 is presented in Table 10.

TKN and TP dry weight content of the sediment bed, measured as mg/kg, was converted to concentration as g/m**3 for input to the EFDC model based on solids density and porosity using the following relationship:

Bed Concentration (g/m**3) = Bed Dry Weight (mg/kg) *(1-Porosity)*Solids Density

Bed concentrations are derived using a solids density of 2.6 g/cm**3, a porosity of 0.6 and a dry bulk density of 1.04 g/cm**3. These parameter values, assigned for all zones except Zone 7, are typical for fine grained cohesive particles and a sediment bed characterized as silty-clay (Lick, 2009). A smaller value of porosity (0.4) and a larger bulk density (1.56 g/cm**3) is assigned for Zone 7 (Site 1 in the forebay area of the dam) since sediments trapped in this depositional zone presumably would be more consolidated than sediments in other zones in the reservoir. Bed parameter values used for the sediment diagenesis model are consistent with the bed parameter values used to assign initial conditions for cohesive solids in the sediment transport model.

Total phosphorus was split into TOP and TPO4 using data available from Nowlin et al. (2005) where ~50% of sediment bed TP was observed to be in the form of organic-P (Table 11). TKN

measurements were split into organic nitrogen and ammonia assuming that 99% of TKN was TON. The remaining 1% of TKN was then accounted for as ammonia. Nitrate was estimated from ammonia with the assumption that nitrate represented only a small fraction (1%) of total inorganic N (Table 12). TOC measurements were not available from the special surveys in Lake Thunderbird. In the absence of site-specific data, TOC content of the sediment bed (Table 13) was estimated from the TON data and a C:N ratio of 15 which was taken from sediment core data reported for a lake in Massachusetts (Kaushai and Binford, 1999). The G1, G2 and G3 reactive classes of TOC, TON and TOP were estimated for initial conditions using the following fractional splits:

G1: 2*[1/(1+10+100)]=0.018;

G2: 2*[10/(1+10+100)]=0.180

G3: 1*[100/(1+10+100)] =0.8018

Table 14 summarizes how sediment bed data was assigned to water quality zones (**Figure 7**) where sediment bed data was not available in Zones 1,2,3,5 and 6. Sediment bed data from Site 8 was used as a reference "river" station to estimate initial bed conditions for zones characterized by streams and tributary inflows to the lake.

Table 10. Sediment Bed Content of Nutrients and Solids (July and December 2008)

	TKN	TP	Solids
	mg/kg	mg/kg	% solids
Site 1	687.50	147.25	21.30
Site 2	581.00	123.00	22.33
Site 4	623.75	137.50	22.53
Site 6	600.25	166.50	48.00
Site 8	480.50	77.78	43.48

Table 11. Sediment Bed Phosphorus

						TOP:TP 0.5	TPO4:TP 0.5
	TP	BulkDens	SolidsDens	Porosity	TP	TOP	TPO4
	(mg/kg)	(g/cm**3)	(g/cm**3)		(g/m**3)	(g/m**3)	(g/m**3)
Site1	147.25	1.56	2.6	0.4	229.71	114.86	114.86
Site2	123.00	1.04	2.6	0.6	127.92	63.96	63.96
Site3	137.50	1.04	2.6	0.6	143.00	71.50	71.50
Site4	166.50	1.04	2.6	0.6	173.16	86.58	86.58
Site8	77.78	1.04	2.6	0.6	80.89	40.44	40.44

Table 12. Sediment Bed Nitrogen

					TN~TKN	TON:TN	NH4:DIN	NO3:DIN	DIN:TN
						0.99	0.99	0.01	0.01
	TKN	BulkDens	SolidsDens	Porosity	TKN	TON	NH4	NO3	NH4+NO3
	(mg/kg)	(g/cm**3)	(g/cm**3)		(g/m**3)	(g/m**3)	(g/m**3)	(g/m**3)	(g/m**3)
Site1	687.50	1.56	2.6	0.4	1072.50	1061.78	10.6178	0.1073	10.7250
Site2	581.00	1.04	2.6	0.6	604.24	598.20	5.9820	0.0604	6.0424
Site3	623.75	1.04	2.6	0.6	648.70	642.21	6.4221	0.0649	6.4870
Site4	600.25	1.04	2.6	0.6	624.26	618.02	6.1802	0.0624	6.2426
Site8	480.50	1.04	2.6	0.6	499.72	494.72	4.9472	0.0500	4.9972

Table 13. Sediment Bed Organic Carbon

					TKN~TN	TON:TN	C:N
						0.99	15.0
	TKN	BulkDens	SolidsDens	Porosity	TKN	TON	TOC
	(mg/kg)	(g/cm**3)	(g/cm**3)		(g/m**3)	(g/m**3)	(g/m**3)
Site1	687.50	1.56	2.6	0.4	1072.50	1061.78	15926.63
Site2	581.00	1.04	2.6	0.6	604.24	598.20	8972.96
Site3	623.75	1.04	2.6	0.6	648.70	642.21	9633.20
Site4	600.25	1.04	2.6	0.6	624.26	618.02	9270.26
Site8	480.50	1.04	2.6	0.6	499.72	494.72	7420.84

Table 14. Sediment Bed Data used for Water Quality Zones

WQ	OWRB	Sediment Bed Data	WQ Zone
Zone	Site	Available	Based on
1	none	none	Site 8; 50%
2	Site-6	none	Site 8; 100%
3	Site-5	none	Site 3; 100%
4	Site-4	Sediment Bed Data	Site 4
5	Site-7	none	Site 8; 50%
	Site-11	none	
6	none	none	Site 8; 25%
7	Site-1	Sediment Bed Data	Site 1
8	Site-2	Sediment Bed Data	Site 2
9	Site-3	Sediment Bed Data	Site 3
10	Site-8	Sediment Bed Data	Site 8

The model setup for the initial POC content and porewater PO4 concentrations are shown in **Figure 8** and **Figure 9** as examples of sediment bed initial conditions used for calibration of the Lake Thunderbird model. As shown in the maps, the initial conditions for Zone 7 (Site 1 forebay area) are considerably higher than the adjacent lacustrine zones (Zone 4 and 8) because the porosity of 0.4 assigned for Zone 7 is smaller than the porosity of 0.6 assigned for all other zones in the lake.

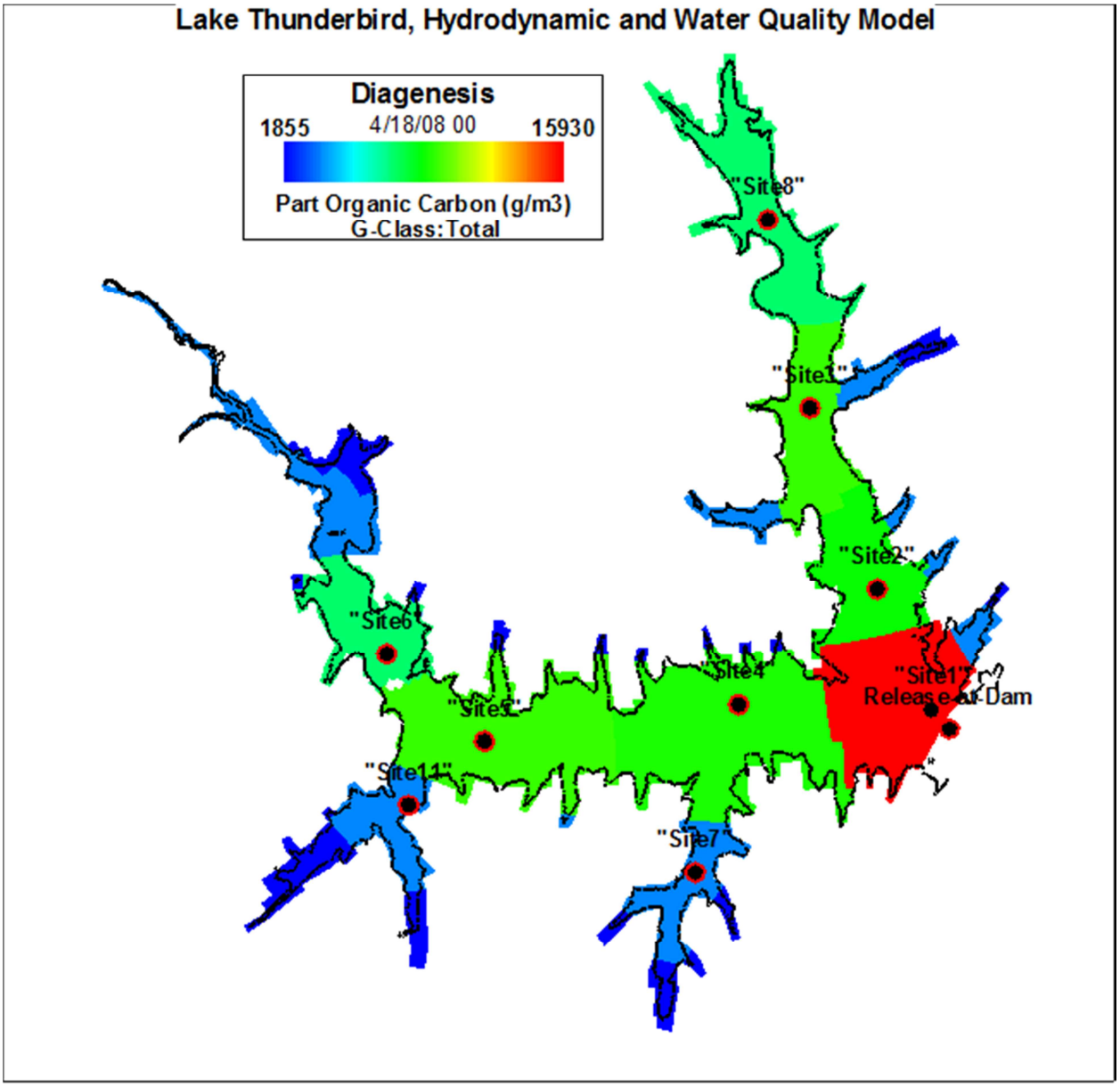

Figure 8 – Initial Conditions for Sediment Bed POC for the Sediment Diagenesis Model.

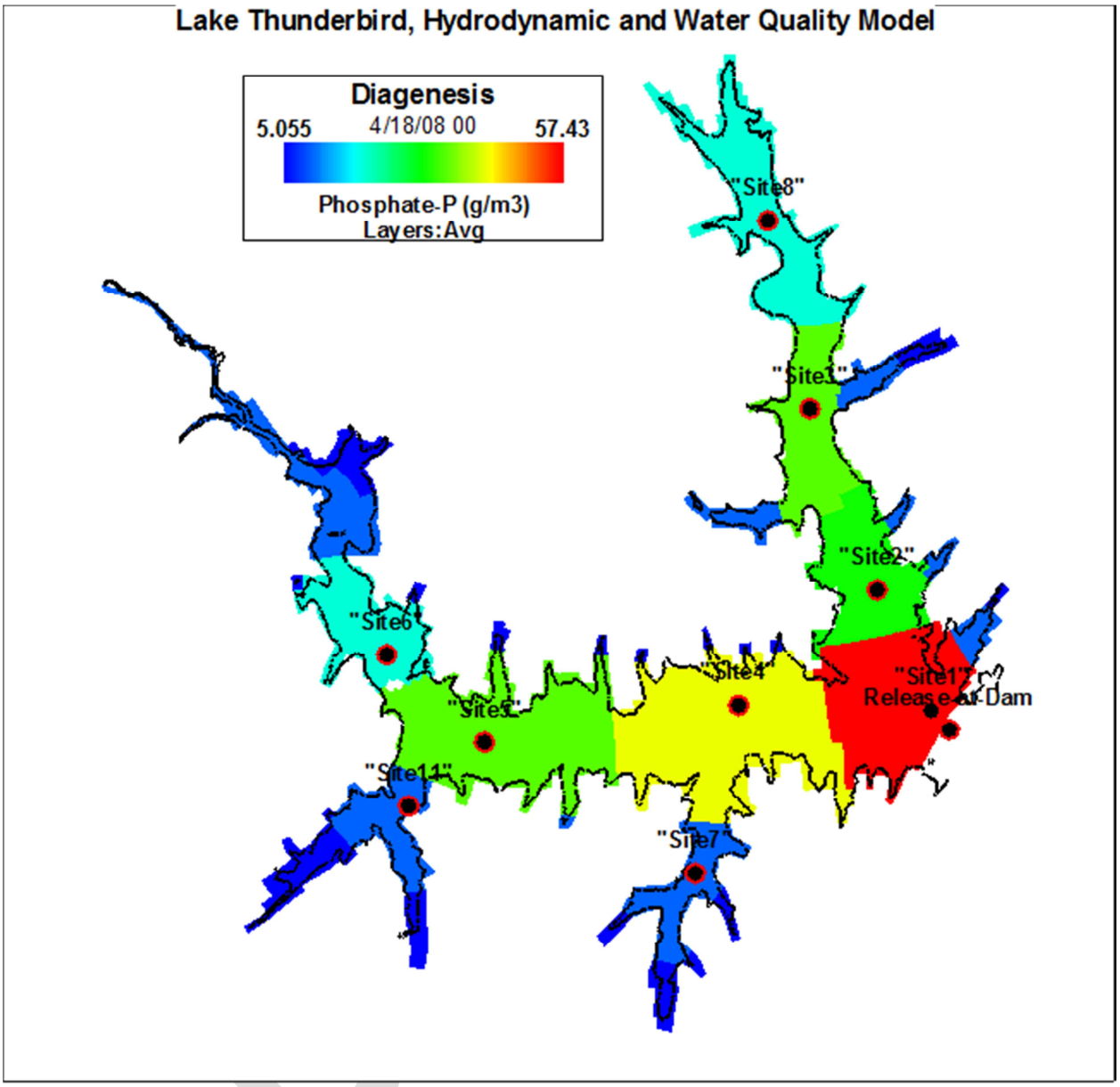

Figure 9 – Initial Conditions for Sediment Bed Porewater PO4 for the Sediment Diagenesis Model.

Section 4 WATER QUALITY MODEL CALIBRATION

4.1 Introduction

The period selected for water quality model calibration was 18 April 2008 through 27 April 2009. During this 374 day period ODEQ conducted a special monitoring program to obtain data for the development of the watershed and lake model for Lake Thunderbird.

Results of the water quality model are compiled for model-data comparison at eight stations (Sites 1 2, 3, 4, 5, 6, 7, 8). OWRB station-ID, geographic position and information about the stations are given in **Table 15**. Locations of these station sites are shown in **Figure 10**.

Table 15. Calibration Stations for Lake Thunderbird Model

Site	Station Number	Latitude	Longitude	Represents
1	520810000020-1sX	35.223333	-97.220833	Dam Site; Lacustrine
	520810000020-1-4X			
	520810000020-1-8X			
	520810000020-1-12X			
	520810000020-1bX			
2	520810000020-2X	35.238889	-97.228889	Lacustrine
	520810000020-2bX			
3	520810000020-3X	35.262222	-97.238889	Transition
4	520810000020-4X	35.224444	-97.250833	Lacustrine
	520810000020-4bX			
5	520810000020-5X	35.220278	-97.290556	Transition
6	520810000020-6X	35.231667	-97.305556	Riverine
7	520810000020-7X	35.203056	-97.258056	Riverine
8	520810000020-8X	35.286409	-97.244887	Riverine
11	520810000020-11X	35.212292	-97.302545	Riverine

Calibration of the model is demonstrated with model-data comparisons for water temperature, suspended solids, turbidity, dissolved oxygen, nutrients, organic carbon, water clarity and algae biomass as station time series. Vertical profiles are presented for water temperature and dissolved oxygen. In the station time series plots the model results are shown by a red line for the surface layer and a blue line for the bottom layer. Surface layer observed data points are shown as solid circles and bottom layer observations are shown as solid triangles. In the vertical profile plots of water temperature and dissolved oxygen, model results are shown as a solid line and observed measurements are shown as solid circles. Based on fixed bottom elevation data for each station and the time series of observed lake elevation, total water column depth was estimated for each individual survey. Using sample depths recorded for the grab samples and vertical profiles collected at each station, observed water quality records were assigned to one of the six vertical layers represented in the lake model. Observed data collected near the surface is compared to model results for the surface layer (k=6) and data collected near the bottom is compared to model results for the bottom layer (k=1). Station results are presented in the main body of the report in this section to show model calibration for selected stations located in the lacustrine (Site 1,2,4), transition (Site 3,5) and riverine (Site 6,7,8) zones of the reservoir.

Station data was not available at Site 11 for the model calibration period from April 2008 through April 2009. Water temperature, dissolved oxygen, chlorophyll a, turbidity and secchi depth records were available for all eight station locations. TSS, organic carbon and nutrient data was available at five stations (Site 1,2,4,6 and 8). A complete set of time series plots for the eight station locations and water quality variables are presented in **Appendix C**. Vertical profile plots for water temperature and dissolved oxygen are presented in **Appendix D**.

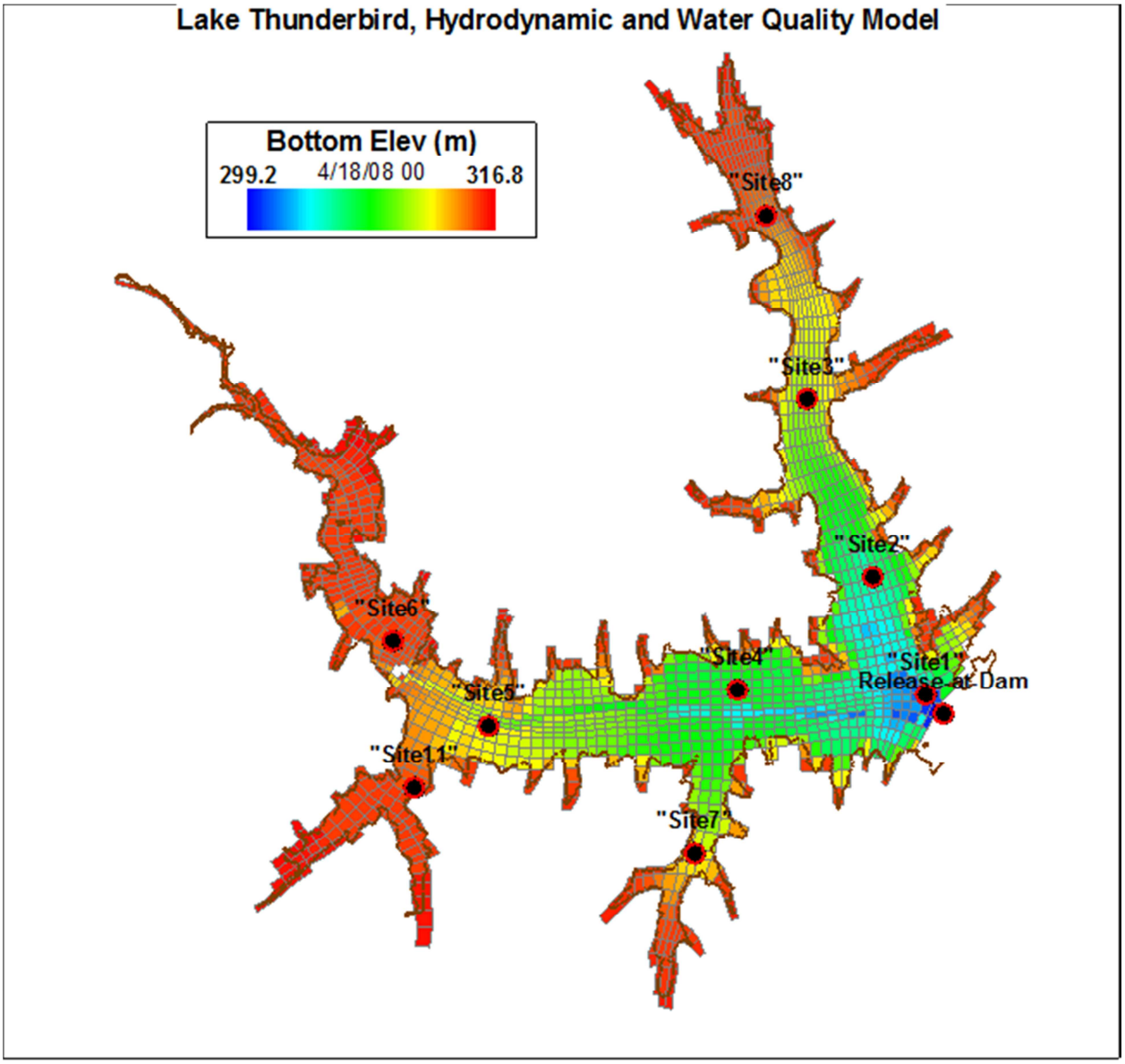

Figure 10 – Hydrodynamic and Water Quality model calibration stations.

4.2 Model Performance Statistics

Model performance is evaluated to determine the endpoint for model calibration using a “weight of evidence” approach that has been adopted for many modeling studies. The “weight of evidence” approach includes the following steps: (a) visual inspection of plots of model results

compared to observed data sets (e.g., station time series); and (b) analysis of model-data performance statistics as (a) Root Mean Square (RMS) Error and (b) Relative RMS Error as described below. The "weight of evidence" approach recognizes that, as an approximation of a waterbody, perfect agreement between observed data and model results is not expected and is not specified as a performance criterion for the success of model calibration. Model performance statistics are used, not as absolute criteria for acceptance of the model, but rather, as guidelines to supplement the visual evaluation of model-data time series plots to determine the endpoint for calibration of the model. The "weight of evidence" approach used for this study thus acknowledges the approximate nature of the model and the inherent uncertainty in both input data and observed data.

The model-data model performance statistic selected for the calibration of the hydrodynamic and water quality model are the (a) Root Mean Square Error (RMSE) and the (b) Relative RMS Error. The RMSE has units defined by the units of each state variable of the model. The Relative RMS error, computed as the ratio of the RMSE to the observed range of each water quality constituent and expressed as a percentage, is also used as a statistic to characterize model performance (Blumberg et al., 1999; Ji, 2008). Since the Relative RMS error is expressed as a percentage, this performance measure provides a straightforward statistic to evaluate the agreement between model results and observations.

The equations for the RMSE and the Relative RMS Error are,

$$\text{RMSE} = \sqrt{\frac{1}{N}\Sigma(O-P)^2}$$

$$\text{Relative RMS Error} = \frac{\text{RMSE}}{(O_{range})} x100$$

where

N is the number of paired records of observed measurements and EFDC model results,

O is the observed water quality measurement,

P is the predicted EFDC model result, and

O_{range} is the range of observed data computed from the maximum and minimum values.

In evaluating the results obtained with the EFDC model, a Relative RMS Error performance measure of $\pm 20\%$ is adopted for evaluation of the comparison of the model predicted results and observed measurements of water surface elevation of the lake. For the hydrographic state variables simulated with the EFDC hydrodynamic model, a Relative RMS Error performance measure of $\pm 50\%$ is adopted for evaluation of the comparison of the predicted results and observed measurements for water temperature. For the water quality state variables simulated with the EFDC water quality model, a Relative RMS Error performance measure of $\pm 20\%$ is

adopted for dissolved oxygen; $\pm 50\%$ for nutrients and suspended solids; and $\pm 100\%$ for algal biomass for the evaluation of the comparison of the predicted results and observed water quality measurements for model calibration. These targets for hydrodynamic, sediment transport and water quality model performance are consistent with the range of model performance targets recommended for the HSPF watershed model (Donigian, 2000).

Given the lack of a general consensus for defining quantitative model performance criteria, the inherent errors in input and observed data, and the approximate nature of model formulations, *absolute* criteria for model acceptance or rejection are not appropriate for studies such as the development of the lake model for Lake Thunderbird. The relative RMS errors presented above will be used as targets, but not as rigid criteria for rejection or acceptance of model results, for the performance evaluation of the calibration of the EFDC hydrodynamic and water quality model of Lake Thunderbird.

4.3 Water Temperature

Water temperature results are presented for comparison to observed data for the surface layer (k=6) and bottom layer (k=1) for the lacustrine zone (Site 1 and Site 4), the transition zone (Site 3) and the riverine zone (Site 6) (**Figure 11 - 14**)**.** As can be seen in these model-data plots, the model results for the surface and bottom layer are in good agreement with measured water temperature. Model results for the bottom layer in the lacustrine zone are somewhat cooler than the observed data collected at Site 1 and Site 4 during the summer months. Water temperature results are presented for comparison to observed data as vertical profiles in **Figure15** and **Figure 16** for Site 1 (lacustrine zone) and the much shallower Site 3 (transition zone)**.** Model results are extracted as "snapshots' for a time interval of the simulation that matches the observed date/time records for the survey profile**.** As can be seen in these model-data vertical profile plots, the model results are reasonably consistent with observed water temperature for both summer stratified conditions and well mixed winter conditions. The composite surface and bottom layer model performance statistics for all 8 stations show an RMS Error of 2.0 ^{0}C with a Relative RMS Error of 9.3%. The model results are well within the defined model performance target of $\pm 50\%$ for water temperature. Model performance statistics for water temperature for each station are presented in **Appendix E**.

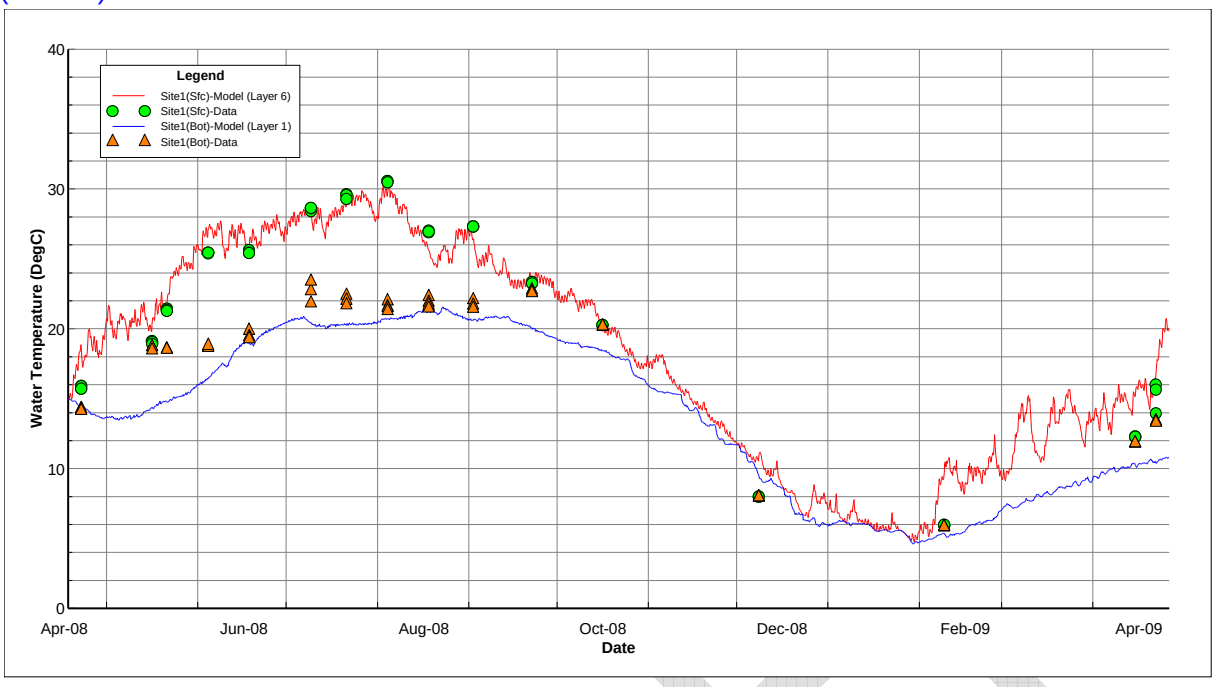

Figure 11 – Simulated and observed water temperature at Site 1.

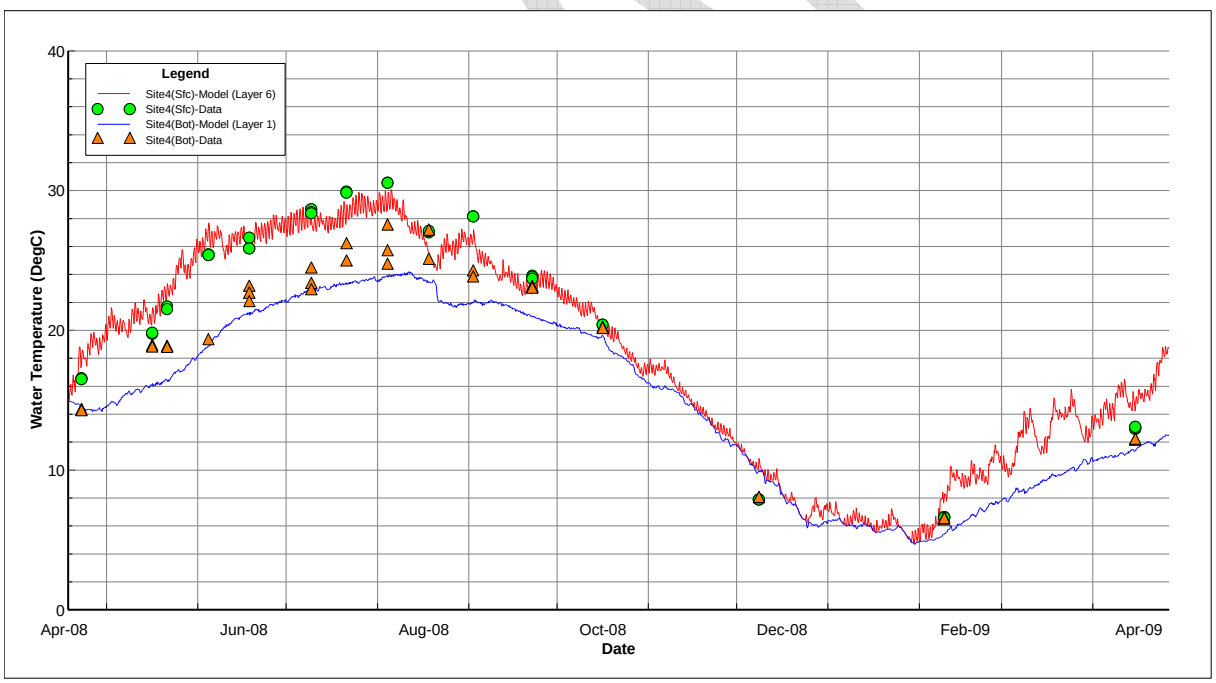

Figure 12 – Simulated and observed water temperature at Site 4.

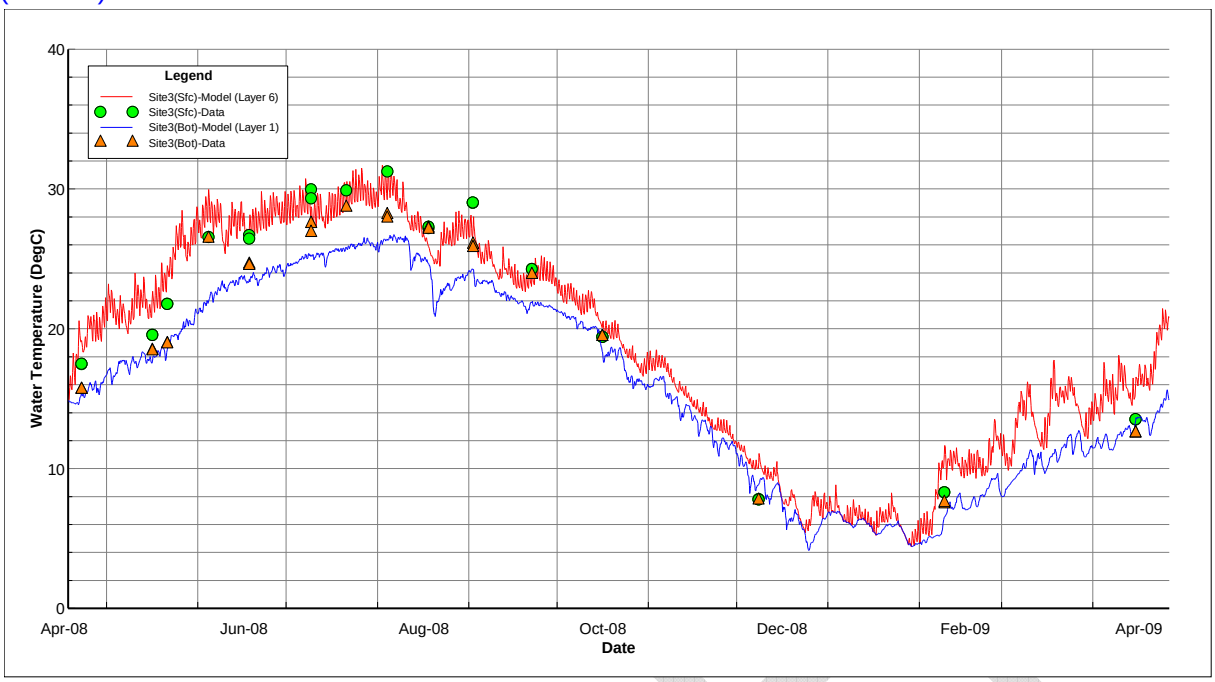

Figure13 – Simulated and observed water temperature at Site 3.

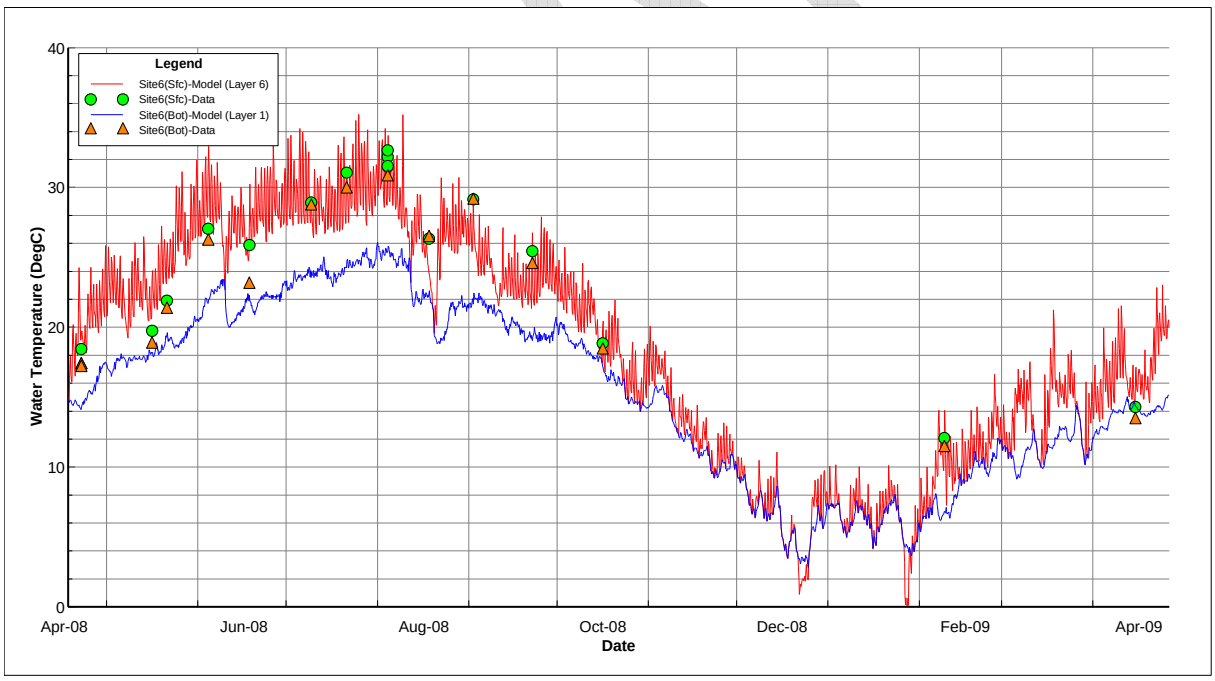

Figure 14 – Simulated and observed water temperature at Site 6.

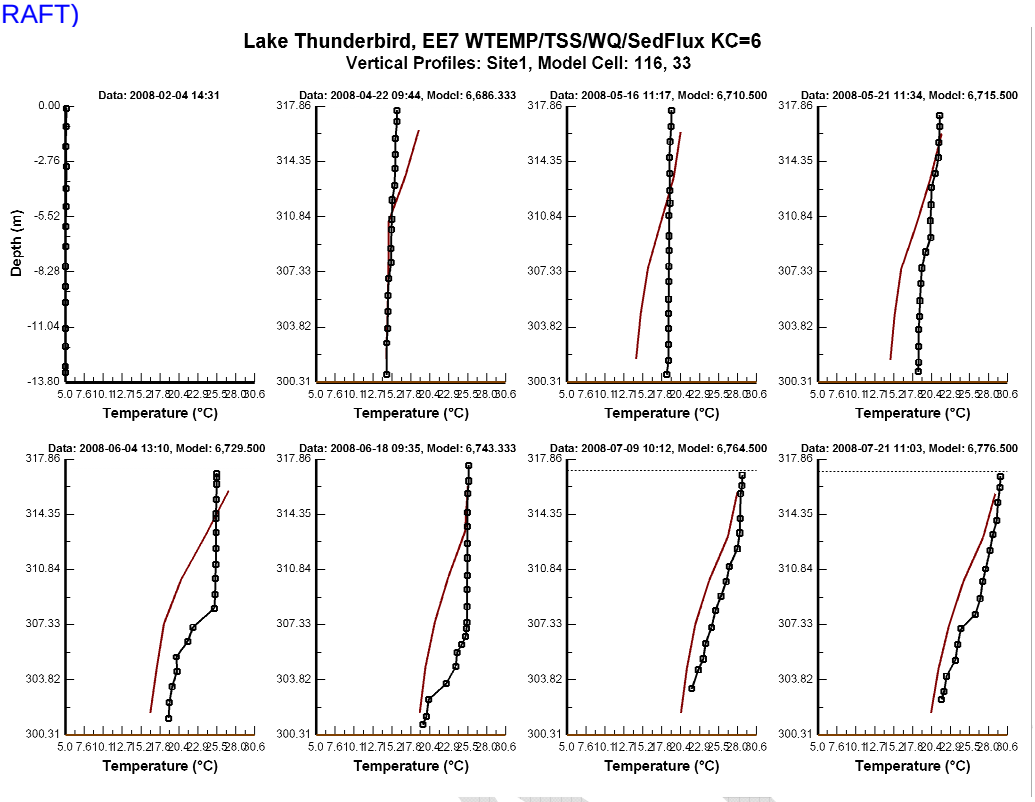

VP_Cal001_Temp_Site1_Run408_Pg01.emf

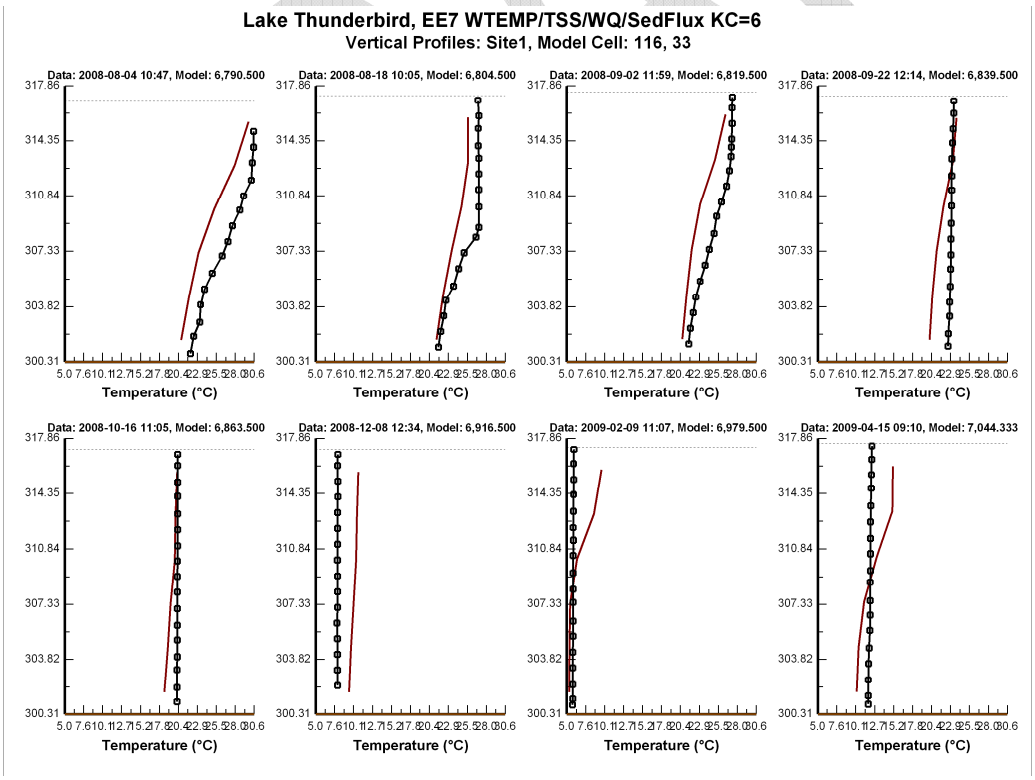

VP_Cal001_Temp_Site1_Run408_Pg02.emf

Figure15 – Simulated and observed water temperature vertical profile at Site 1.

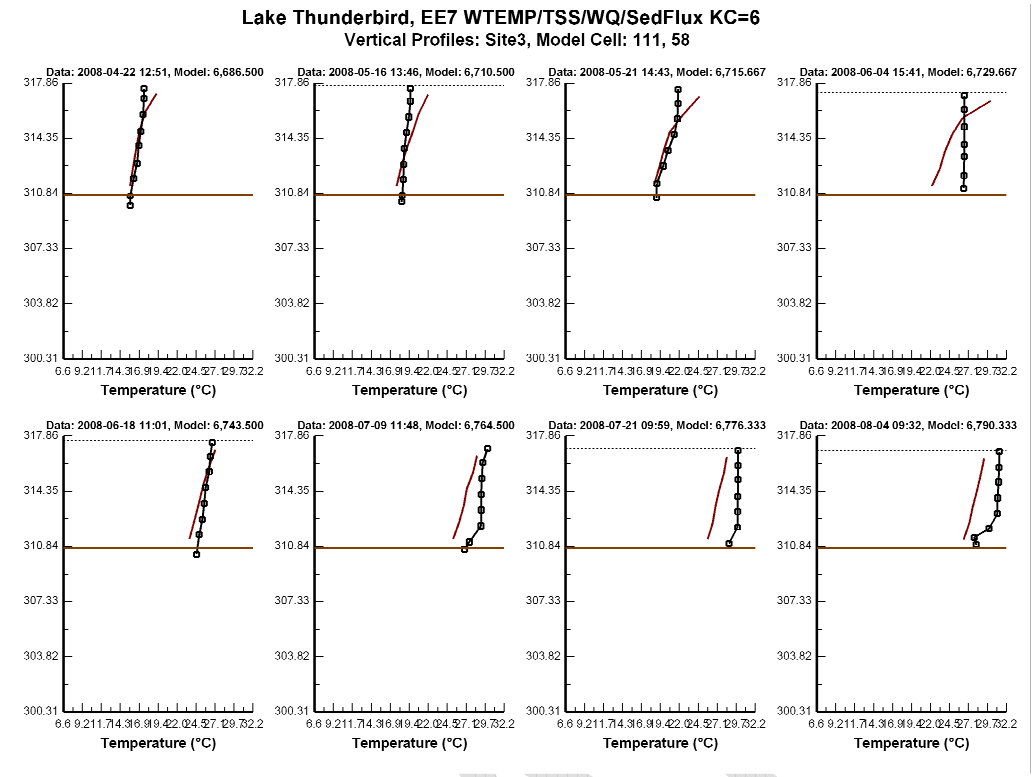

VP_Cal003_Temp_Site3_Run408_Pg01.emf

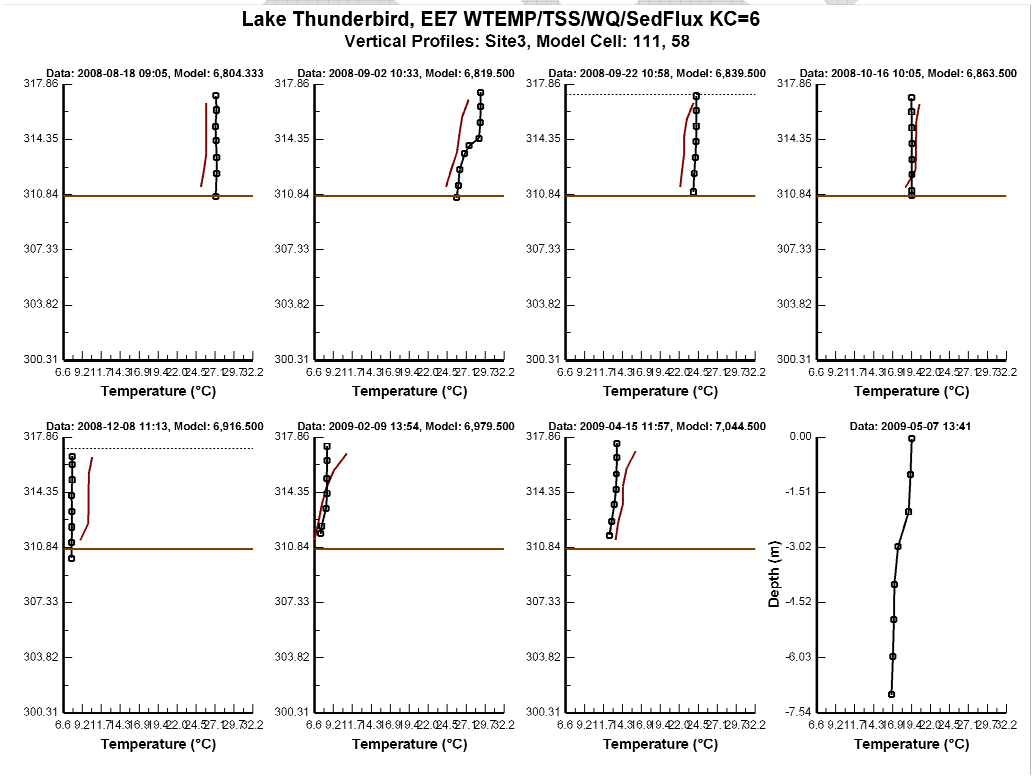

VP_Cal003_Temp_Site3_Run408_Pg02.emf

Figure 16 – Simulated and observed water temperature vertical profile at Site

4.4 Total Suspended Solids, Turbidity and Water Clarity

TSS results are presented for comparison to observed data for the surface layer (k=6) and bottom layer (k=1) for the lacustrine zone (Site 2), and the riverine zone (Site 6) (**Figure 17** and **Figure 18**)**.** As can be seen in these model-data plots, the model results for the surface and bottom layer are in reasonable agreement with measured TSS except for the time period that corresponded to the two storm large events in August 2008. Model results show a large peak in TSS of ~100-200 mg/L at Site 2 and very large peaks of ~1000 mg/L at the riverine station (Site 6). The composite surface and bottom layer model performance statistics for the TSS stations show an RMS Error of 22.9 mg/L with a Relative RMS Error of 99.6%. The model results for TSS have a larger error than the defined model performance target of $\pm 50\%$ for TSS. Model performance statistics for TSS for each station are presented in **Appendix E**.

Water clarity is an issue for impairment in Lake Thunderbird and turbidity is the parameter used to determine if the lake has fully supports the designated use. The Oklahoma water quality criteria states that no more than 10% of samples collected over a long-term period shall be greater than 25 NTU. While the EFDC model does not simulate turbidity as a state variable, the model does account for simulated light attenuation that is dependent on state variables for inorganic solids, detrital particulate organic matter and algae biomass. Since the EFDC model does not simulate turbidity as a state variable, the comparison of EFDC results with the water quality criteria for turbidity requires the development of a regression-based relationship of TSS vs. turbidity based on site-specific paired data sets for Lake Thunderbird. EFDC state variables for inorganic cohesive solids, detrital POC and algae (as chlorophyll a) are summed to compute a derived variable for total suspended solids (TSS). The TSS vs. turbidity relationship developed for Lake Thunderbird, shown in **Figure 19**, was used to transform the derived EFDC variable for TSS to turbidity. Model turbidity is then used to evaluate the comparison to water quality criteria for turbidity (25 NTU) for the calibration analysis and the load allocation evaluations. Turbidity results are presented for comparison to observed data for the surface layer (k=6) for Site 2 and Site 6 (**Figure 20** and **Figure 21**)**.** As can be seen in these model-data plots, the model results for turbidity, reflecting the results obtained for TSS, are in reasonable agreement with measured turbidity except for the time period that corresponded to the two storm large events in August 2008.

In order to compare the observed data and the model calibration results to the water quality criteria for turbidity, observed data and model calibration results were processed for each site to compile summary statistics for turbidity data collected and simulated from April 2008 through April 2009. The statistics thus describe variability of observations and model results on an annual basis. Summary statistics are shown as box-whisker plots for each monitoring site for observed turbidity (**Figure 22**) and simulated turbidity for model calibration (**Figure 23**). The box-whisker plots show the summary statistics computed from the observed data and the model results. Minimum and maximum values are shown as "outlier" data points plotted outside the tails of the box (* symbol). The lower and upper tails of the box show the 10^{th} and 90^{th} percentile values. The lower and upper horizontal lines of the box show the 25^{th} and 75^{th} percentile with the 50^{th} percentile shown as the line through the box. The mean value is shown as a data point within the box. The water quality target of 25 NTU is shown as the horizontal red line on the box-whisker plots. The 90^{th} percentile value for turbidity is used for comparison to the water quality target of 25 NTU since the water quality criteria states that no more than 10% of annual samples are allowed to be greater than 25 NTU.

The turbidity observations for Site 6 in the riverine zone of the Little River show that even the minimum observed value for turbidity of 33 NTU exceeds the water quality target of 25 NTU. The 90th percentile for turbidity at Site 5 (31 NTU) and Site 8 (38 NTU) also exceed the 25 NTU target. The 90th percentile of the turbidity observations for the remaining stations in the lacustrine zone (Site 1, 2, 4), transition zone (Site 3) and riverine zone (Site 7) are all less than 25 NTU are are in compliance with the water quality criteria for turbidity. Since the calibrated model results for turbidity are estimated from the model results for TSS, the overestimate of TSS (**Figures 17-18)** during the storm events of August 2008 results in an overestimate of turbidity (**Figures 20-21**) for the same period. As shown in **Figure 23**, the 90th percentile for the model calibration results of 82 NTU for Site 6 and 37-48 NTU for the other sites all exceed the water quality criteria of 25 NTU.

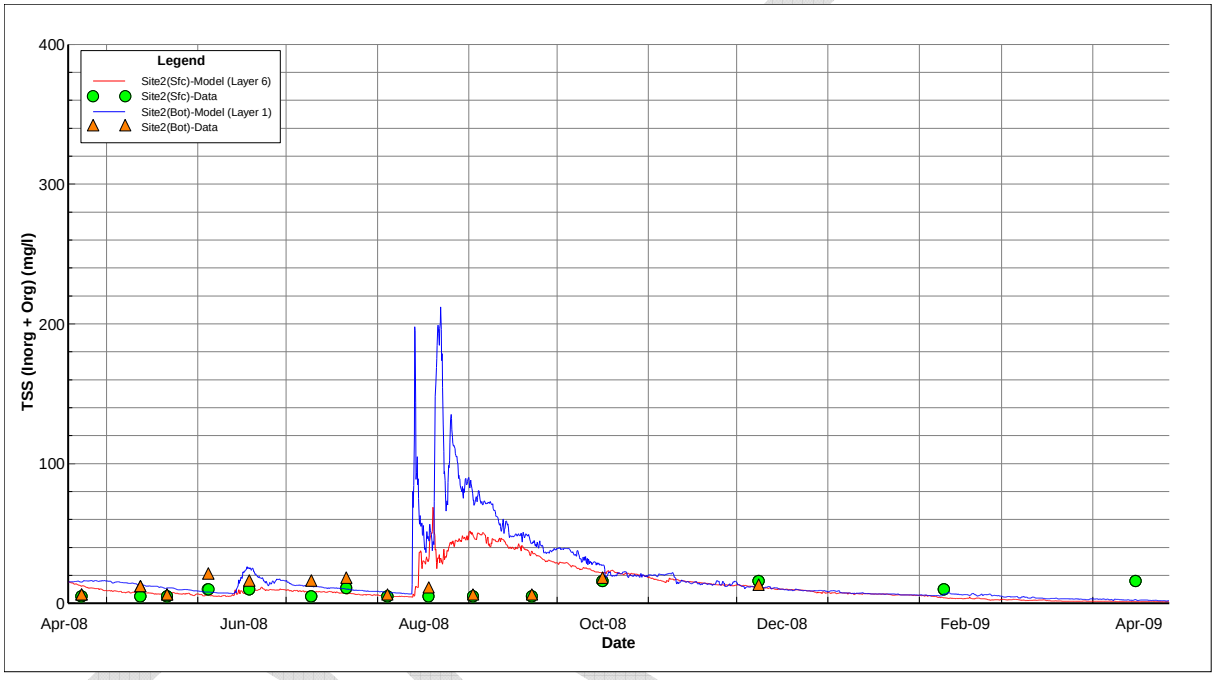

Figure 17 – TSS calibration results at Site 2

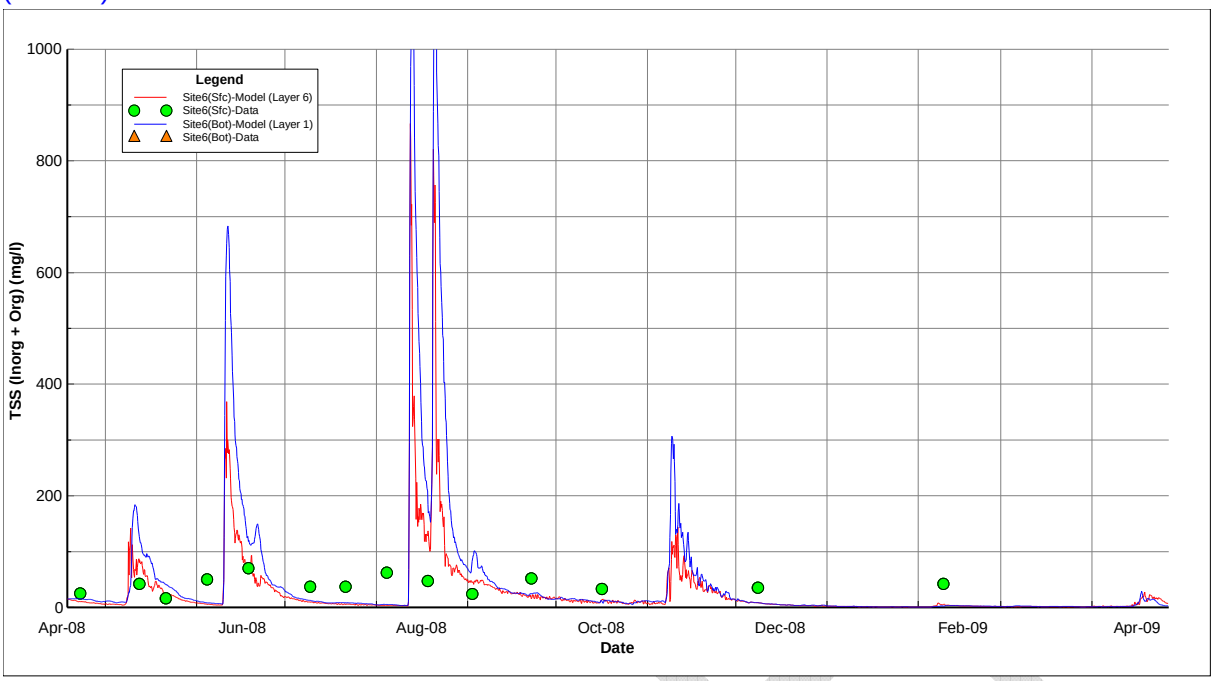

Figure 18 – TSS calibration results at Site 6

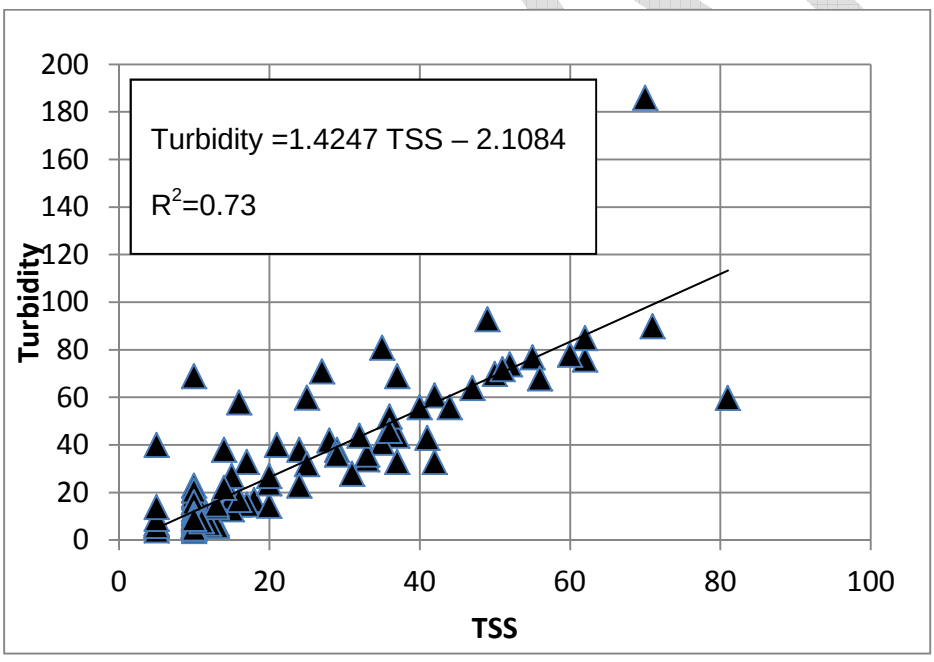

Figure 19 – TSS (mg/L) vs. Turbidity (NTU) Regression Relationship (R^2=0.73)

for Lake Thunderbird

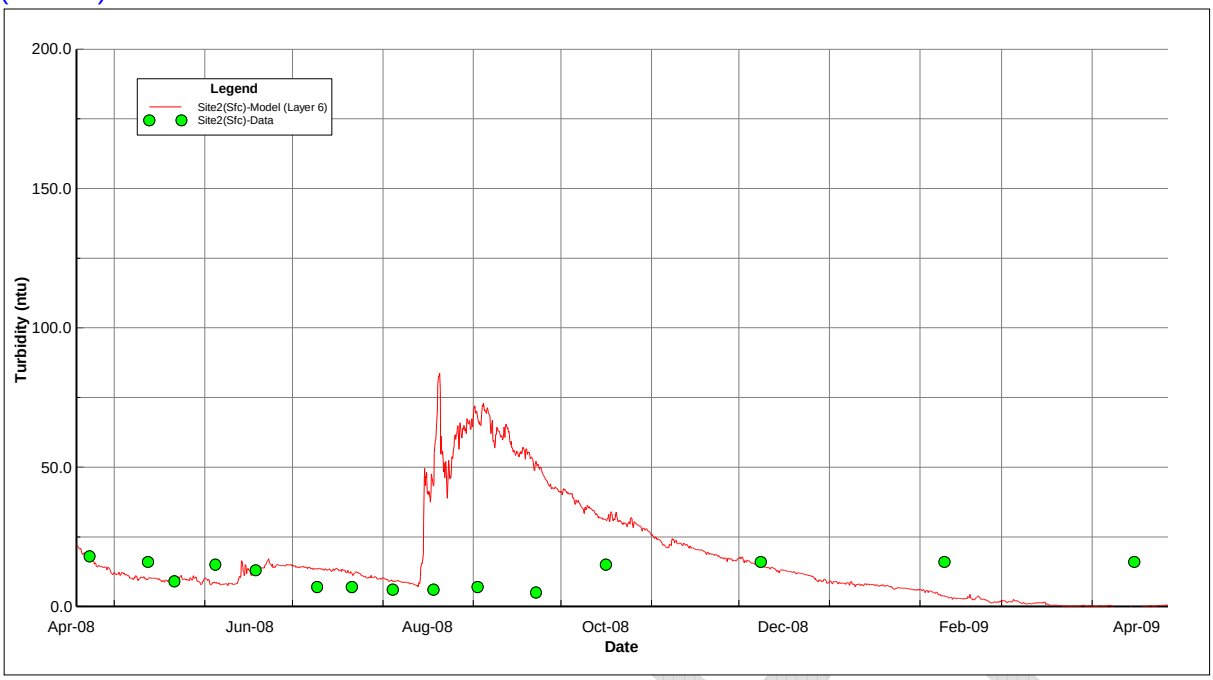

Figure 20 – Turbidity calibration results at Site 2

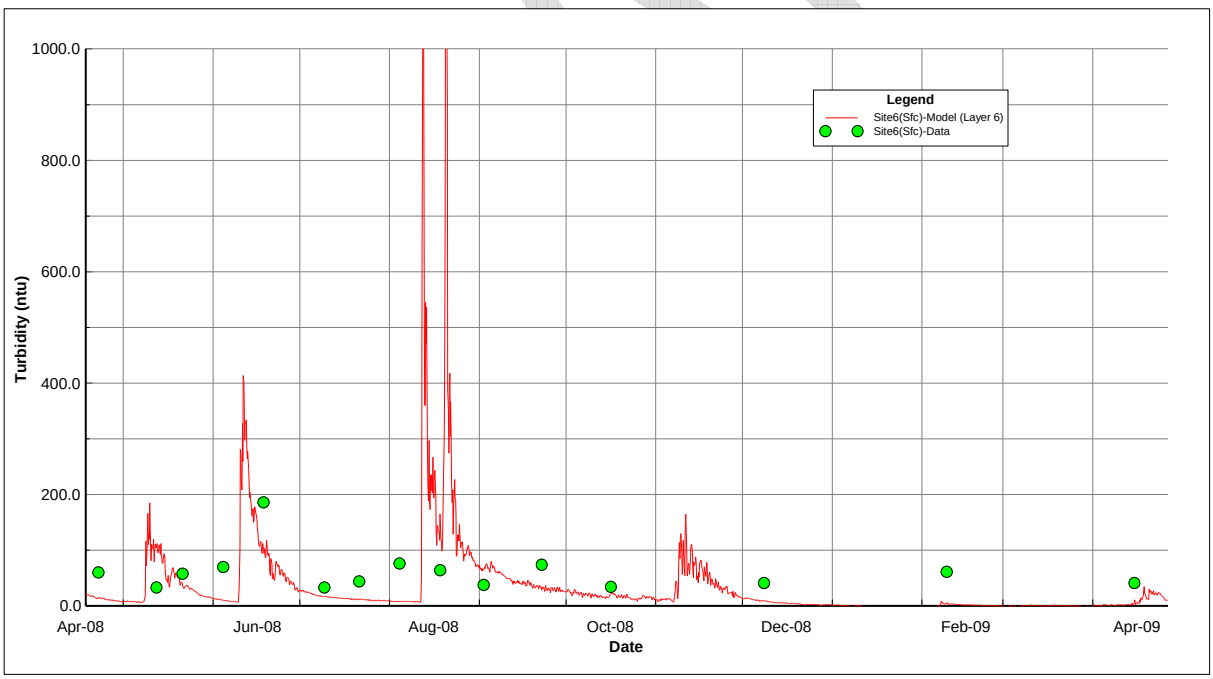

Figure 21 – Turbidity calibration results at Site 6

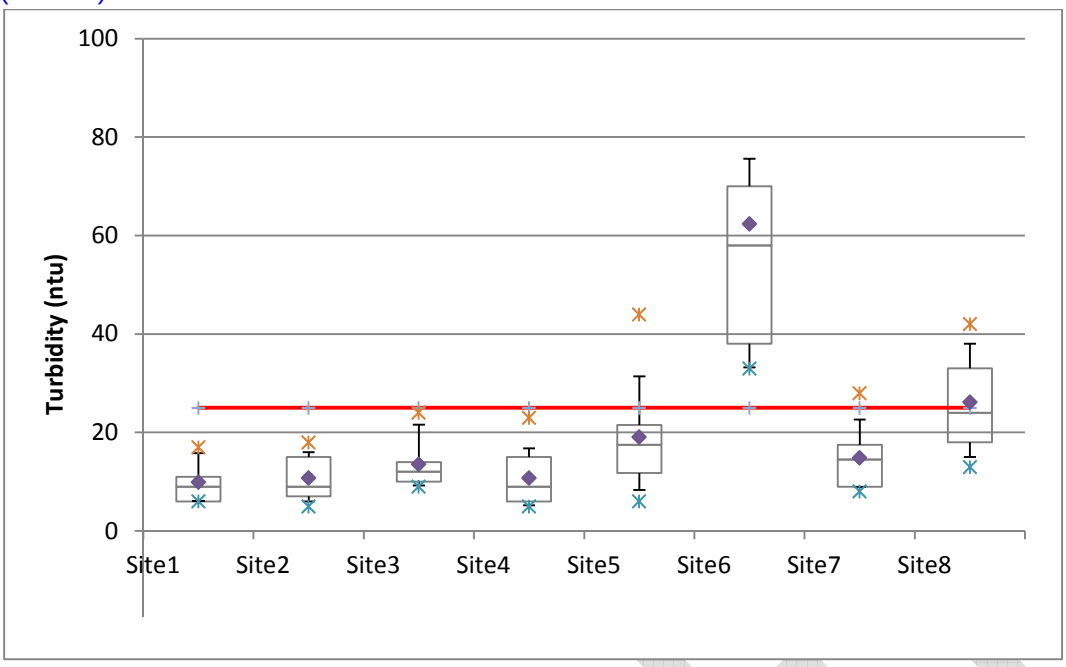

Figure 22 – Box-Whisker plots of Lake Thunderbird observed turbidity (as NTU) for annual period by monitoring site. Red line shows 25 NTU water quality criteria for turbidity. Symbols mark minimum and maximum values.

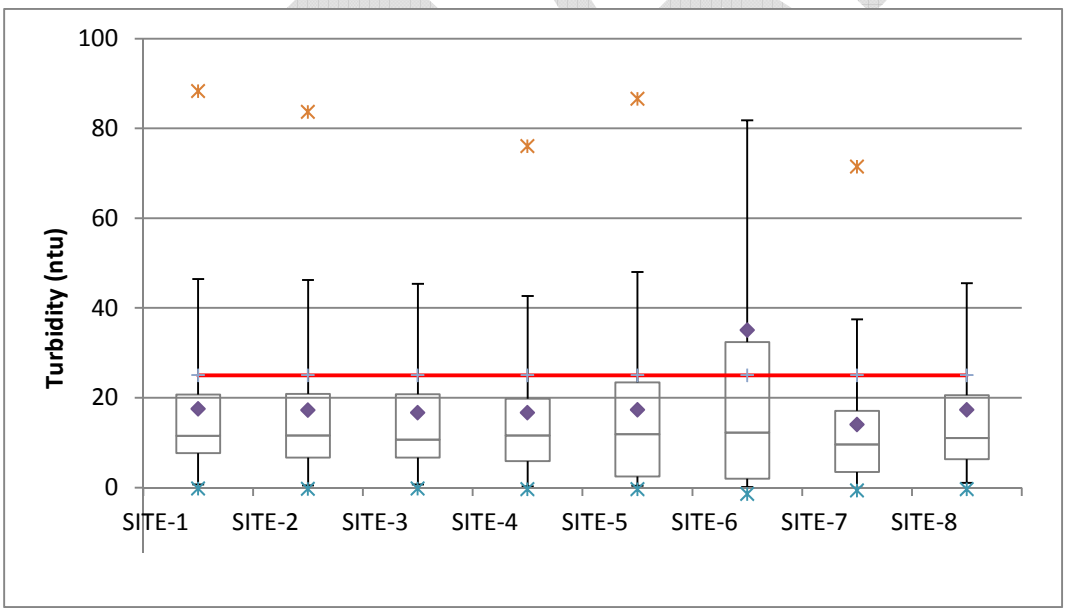

Figure 23 – Box-Whisker plots of Lake Thunderbird model calibration surface layer results for turbidity (as NTU) for annual period by monitoring site. Red line shows 25 NTU water quality criteria for turbidity. Symbols mark minimum and maximum values.

Water clarity is represented in the EFDC water quality model with an empirical relationship that computes the extinction coefficient (Ke) from state variable results for inorganic solids, detrital organic matter and algae biomass (Di Toro, 1978). A simple linear relationship for the extinction coefficient (Ke) and secchi depth (Sd) is given in Thomann and Mueller (1987) as

$$Ke = \frac{1.8}{Sd}$$

Using this relationship, the extinction coefficient (Ke) can be estimated from secchi depth (Sd) measurements. Conversely, model results for the extinction coefficient can be used to estimate secchi depths for comparison to observed data to demonstrate the ability of the model to represent this simple indicator of water clarity. Secchi depth results are presented for comparison to observed data for Site 2 (**Figure 24**) and Site 6 (**Figure 25**)**.** As can be seen in these model-data plots, the model results for water clarity are in reasonable agreement with measured secchi depths including the time period that corresponded to the two storm large events in August 2008. The reduction in water clarity that corresponds to the large increase in TSS from the August storm events is matched fairly well with the model results for secchi depth at the relatively clear lake water at Site 2 as well as at the much murkier river water at Site 6. In particular, the simulated temporal pattern of secchi depth for Site 6 is seen to track the simulated peaks in TSS at this station quite well.

Observed data and model calibration results were processed for each site to compile summary statistics for secchi depth data collected and simulated from April 2008 through April 2009. The statistics thus describe variability of observations and model results on an annual basis. Summary statistics are shown as box-whisker plots for each monitoring site for observed secchi depth (**Figure 26**) and simulated secchi depth for model calibration (**Figure 27**). The box-whisker plots show the summary statistics computed from the observed data and the model results. Minimum and maximum values are shown as "outlier" data points plotted outside the tails of the box (* symbol). The lower and upper tails of the box show the 10th and 90th percentile values. The lower and upper horizontal lines of the box show the 25th and 75th percentile with the 50th percentile shown as the line through the box. The mean value is shown as a data point within the box. Consistent with observed turbidity data, secchi depth observations for Site 6 in the riverine zone of the Little River show the poorest water clarity with the 10th percentile secchi depth less than 0.1 meter. The 10th percentile observed secchi depths at Site 5 (0.3 m) and Site 8 (0.27 m) also exhibit relatively poor water clarity that is consistent with the turbidity data. The 10th percentile of observed secchi depth for the remaining stations in the lacustrine zone (Site 1, 2, 4) and the transition zone (Site 3) are all greater than 0.45 m. As shown in the box-whisker plot for simulated secchi depth (**Figure 27**), the summary statistics for modeled secchi depth exhibit a similar spatial pattern across each of the eight monitoring sites. The major discrepancy between the observed data and the model results is seen for the 10th percentile and minimum values. The discrepancy in the model results is traced to the TSS component of light extinction and the overestimate of TSS (**Figure 17)** during the storm events of August 2008 which then results in an underestimate of secchi depth (**Figure 24**) for the same period for Site 2 and the other lacustrine stations.

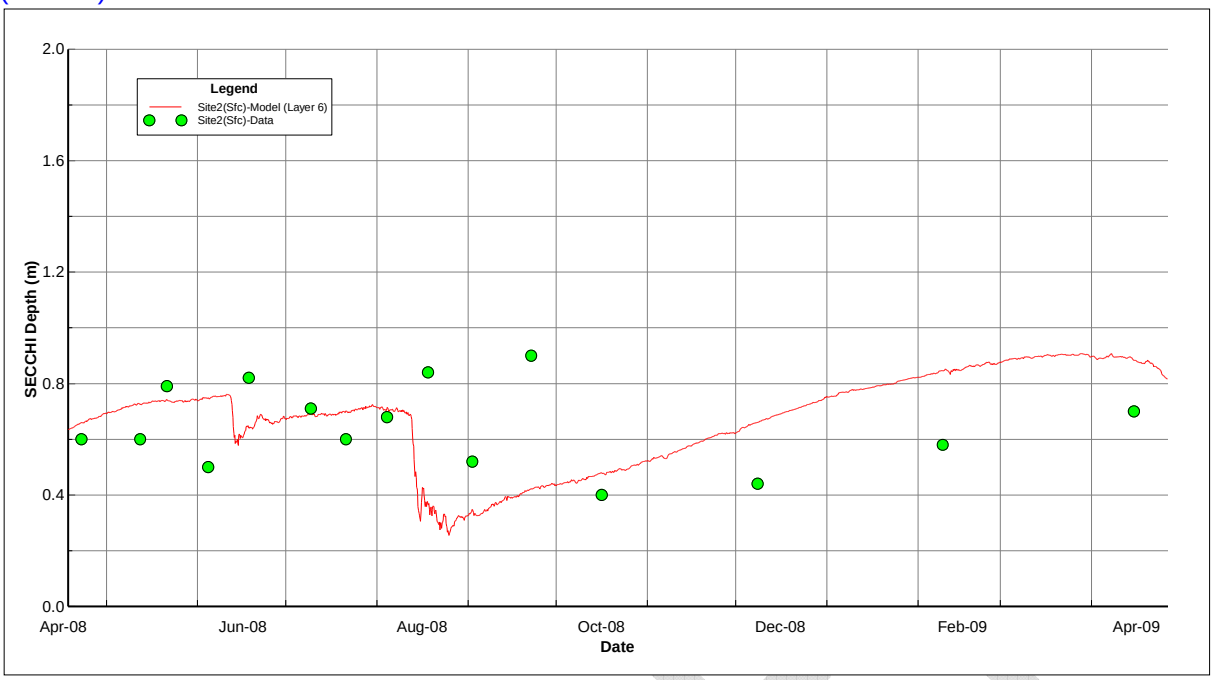

Figure 24 – Secchi depth calibration results at Site 2

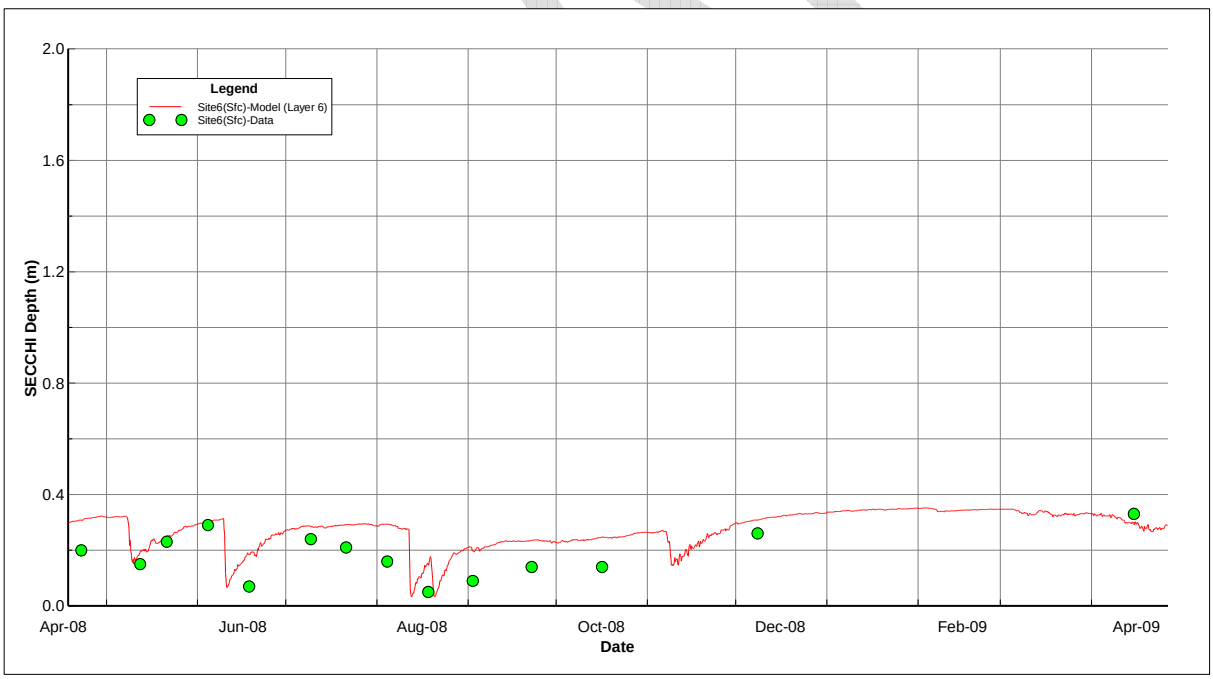

Figure 25 – Secchi depth calibration results at Site 6

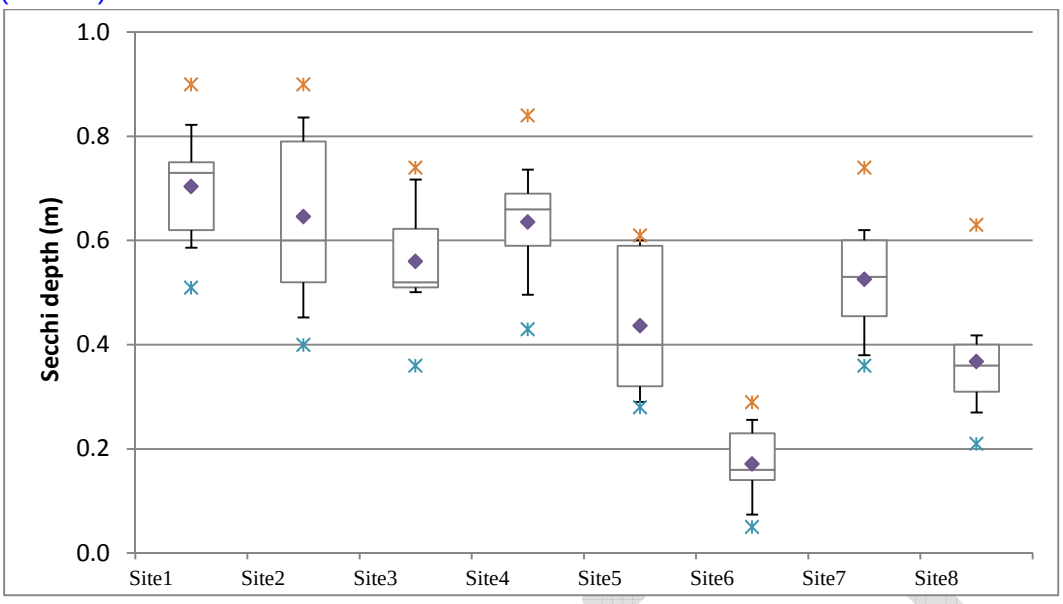

Figure 26 – Box-Whisker plots of Lake Thunderbird observed secchi depth (as meters) for annual period by monitoring site. Symbols mark minimum and maximum values.

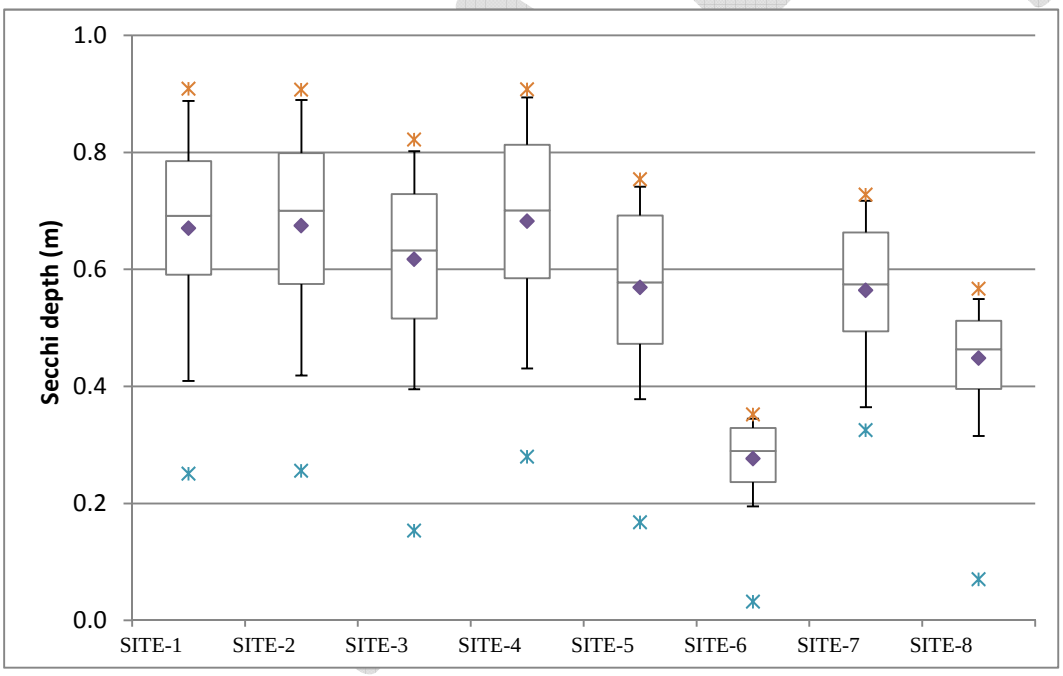

Figure 27 – Box-Whisker plots of Lake Thunderbird model calibration results for secchi depth (as meters) for annual period by monitoring site. Symbols mark minimum and maximum values.

4.5 Dissolved Oxygen

Oxygen results are presented for comparison to observed data for the surface layer (k=6) and bottom layer (k=1) for the lacustrine zone (Site 2), the transition zone (Site 3) and the riverine zone (Site 6) (**Figures 28-30**). As can be seen in these model-data plots, the model results for both the surface and bottom layer are in very good agreement with measured oxygen. The

exception is the period characterized by super saturated oxygen conditions that were observed in the surface layer during July in the lacustrine zone at Site 2. The contribution of algal photosynthetic oxygen production that is distributed over the surface layer thickness of ~ 2 m at this site is apparently "diluted" by the relatively coarse 6 layer vertical resolution of the surface layer. Similar super saturated oxygen conditions were also observed, and not matched by the model, at the other lacustrine stations (Site 1 and Site 4). What is most notable about the model results is that surface and bottom layer oxygen results at Site 2 clearly show the hydrodynamic impact of increased mixing that resulted from the storm events in August 2008. Water column stratification was eroded and the water column became well mixed with only a very small gradient between bottom layer and surface layer oxygen. When the water column restratified in September bottom oxygen was once again reduced to anoxic levels less than 2 mg/L that persisted until seasonal stratification was eroded in October.

Full supporting compliance with Oklahoma water quality criteria for dissolved oxygen for lakes in the Warm Water Aquatic Community (WWAC) subcategory of Fish and Wildlife Propagation is achieved for the following conditions: (a) 50% or less of water column station records or, if volumetric data is available, 50% or less of the volume of the lake is less than 2 mg/L during summer stratified conditions; (b) 10% or fewer of oxygen samples collected within the epilimnion during summer stratified conditions are less than 6 mg/L from April 1-June 15 and are less than 5 mg/L during the remainder of the year (from June 16-March 30); and (c) 10% or fewer of oxygen samples averaged over the entire water column during well-mixed winter conditions are less than 6 mg/L from April 1-June 15 and are less than 5 mg/L during the remainder of the year (from June 16-March 30) (Title 785. OWRB, Chapter 45. Oklahoma's Water Quality Standards).

Model calibration results for dissolved oxygen are processed using EFDC_Explorer to compute the volume of the lake that is defined as anoxic based on the criteria of 2 mg/L as a cutoff concentration. The anoxic volumes of the lacustrine zone (Site 1, Site 2, and Site 4) and the transition zone (Site 3 and Site 5) are shown as percentages of the total volume as time series in **Figure 31** and **Figure 32**. The anoxic volume in both the lacustrine and transition zone is seen to gradually increase during summer stratified conditions to a peak of just under 50% in the lacustrine zone and ~35% in the transition zone in early August 2008. The two storm events of August erode stratification, the water column becomes well mixed and the anoxic volume drops to ~10% in the lacustrine zone and <5% in the transition zone. The anoxic volume then increases with restratification of the water column to a peak of ~45% in the lacustrine zone and ~20% in the transition zone. The anoxic volume then decreases as the water column becomes well mixed in October of 2008. The anoxic volume of the lake is shown in **Figure 33** as a "snapshot" of model results on August 2, 2008 08:00. This date is selected to show the lake wide distribution of the anoxic volume at a date when the anoxic volume is seen to be the highest during the summer stratified season. The deeper area in the vicinity of the dam is characterized by the greatest anoxic volume (~66%) where 4 of 6 layers are <2 mg/L. The anoxic volume exhibits a clear spatial gradient along the lacustrine, transition and riverine zones of the Little River and Hog Creek arms of the reservoir. Model results for oxygen within the surface layer, mid-water column layer and bottom layer are shown as snapshots for August 2, 2008 08:00 in **Figures 34, 35 and 36**. A spatial section along a transect from the Little River (Site 6) to the dam (Site 1) to Hog Creek (Site 8) (**Figure 37**) is defined to extract a snapshot of dissolved oxygen results for August 2, 2008 08:00 to show the vertical gradient of oxygen conditions over the water column and the spatial gradient within the riverine, transition and lacustrine zones of the lake. Vertical profiles of oxygen for Site 1, presented in **Figure 39,** show the changes in observed and simulated vertical oxygen profiles beginning with well-mixed conditions in April 2008, the onset of stratification in May-June 2008, the seasonal progression

of hypolimnetic oxygen depletion and the return to well-mixed conditions from October 2008 through April 2009.

In order to compare the observed data and the model calibration results to the water quality criteria for surface layer dissolved oxygen, observed data and model calibration results were processed for each site to compile summary statistics for data collected and simulated from May 15, 2008 through October 1, 2008. The statistics thus describe variability of observations and model results on a seasonal basis corresponding to summer stratified conditions. Summary statistics are shown as box-whisker plots for each monitoring site for observed surface oxygen (Figure 40) and simulated surface oxygen for model calibration (Figure 41). The box-whisker plots show the summary statistics computed from the observed data and the model results. Minimum and maximum values are shown as "outlier" data points plotted outside the tails of the box (* symbol). The lower and upper tails of the box show the 10^{th} and 90^{th} percentile values. The lower and upper horizontal lines of the box show the 25^{th} and 75^{th} percentile with the 50^{th} percentile shown as the line through the box. The mean value is shown as a data point within the box. The water quality target of 5 mg/L is shown as the horizontal red line on the box-whisker plots. The 10^{th} percentile value for oxygen is used for comparison to the water quality target of 5 mg/L since the water quality criteria states that no more than 10% of seasonal samples are allowed to be less than 5 mg/L.

As shown in **Figure 40**, the 10^{th} percentile of the surface layer oxygen observations for all sites are greater than 5 mg/L and are thus in compliance with water quality criteria for the epilimnion under stratified conditions. Model calibration results for the 10^{th} percentile of surface oxygen (**Figure 41**) also exceed the water quality criteria of 5 mg/L for the epilimnion. In addition to the surface layer data, bottom oxygen observations (**Figure 42**) and bottom layer model results (**Figure 43**) were also processed to provide a model-data comparison of summary statistics across all eight monitoring sites for seasonal stratified conditions. Echoing the good agreement between the time series of model results and observed data for surface and bottom layer oxygen shown for Site 2, 3 and 6 in **Figure 28, 30** and **31,** the summary statistics of the surface layer model results for all eight sites (**Figure 41**) also show a reasonable match with the observed surface layer oxygen statistics for the sites (**Figure 40**).

The composite surface and bottom layer model performance statistics for the eight oxygen stations show an RMS Error of 1.8 mg/L with a Relative RMS Error of 20.9%. The model results for dissolved oxygen thus match the defined model performance target of $\pm 20\%$ for oxygen. Model performance statistics for dissolved oxygen for each station are presented in **Appendix E**.

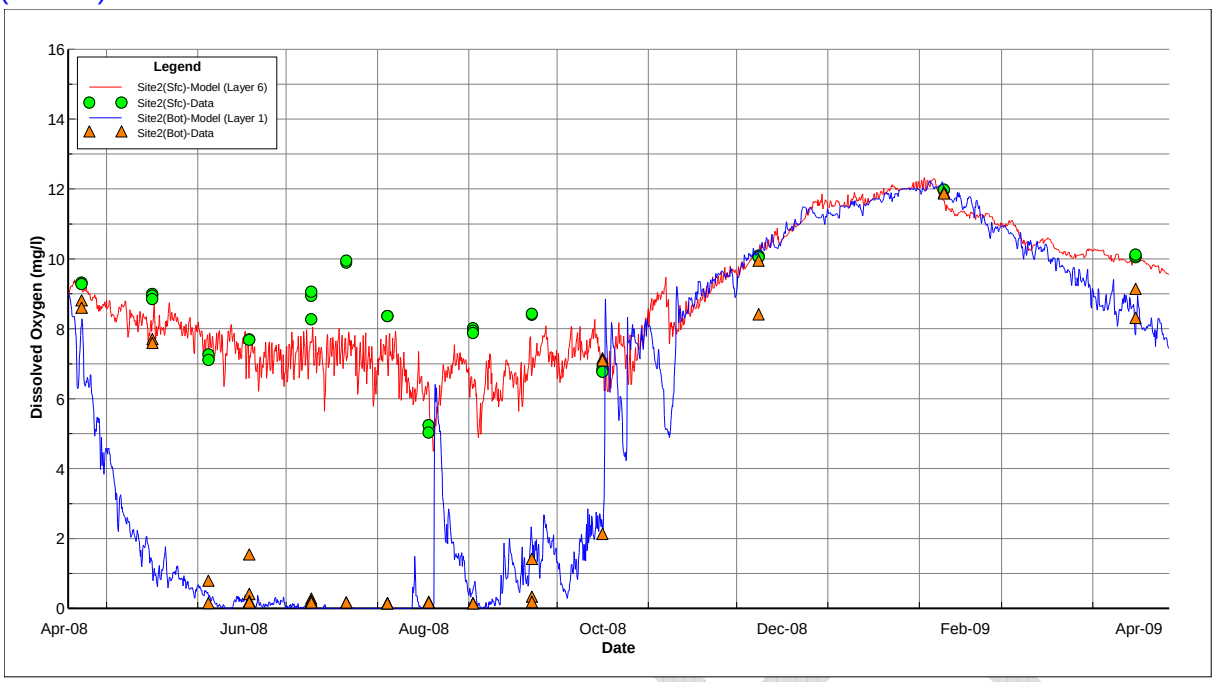

Figure 28 – Dissolved oxygen calibration results at Site 2

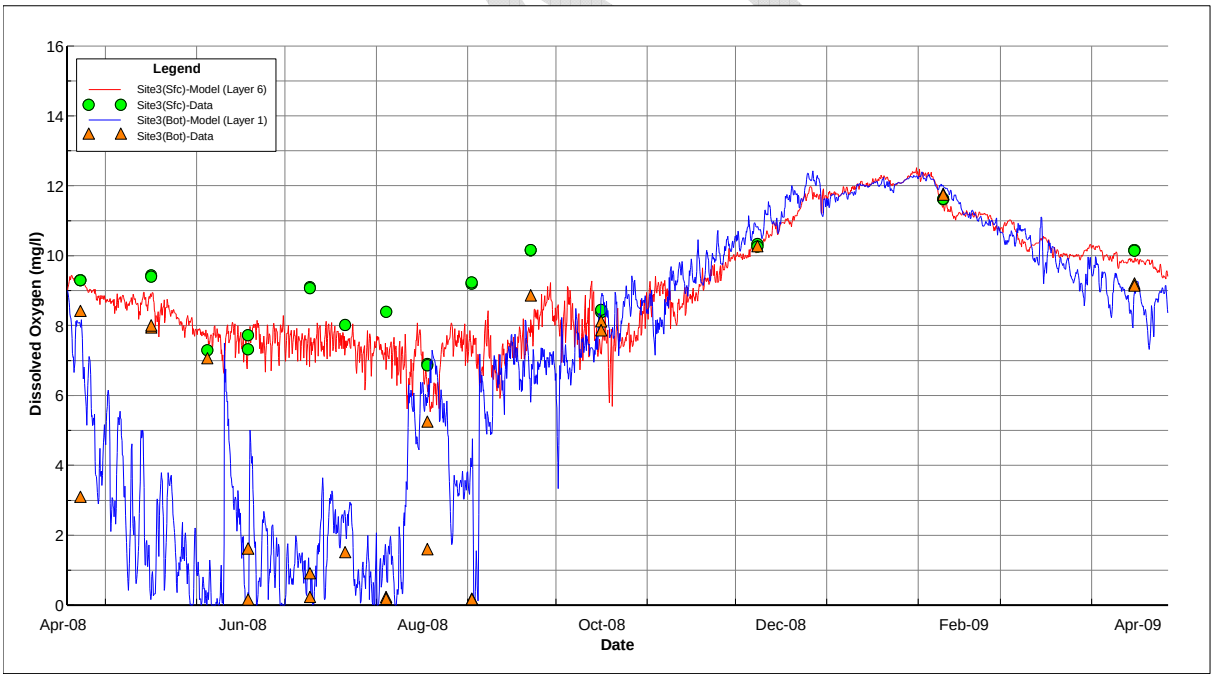

Figure 29 – Dissolved oxygen calibration results at Site 3

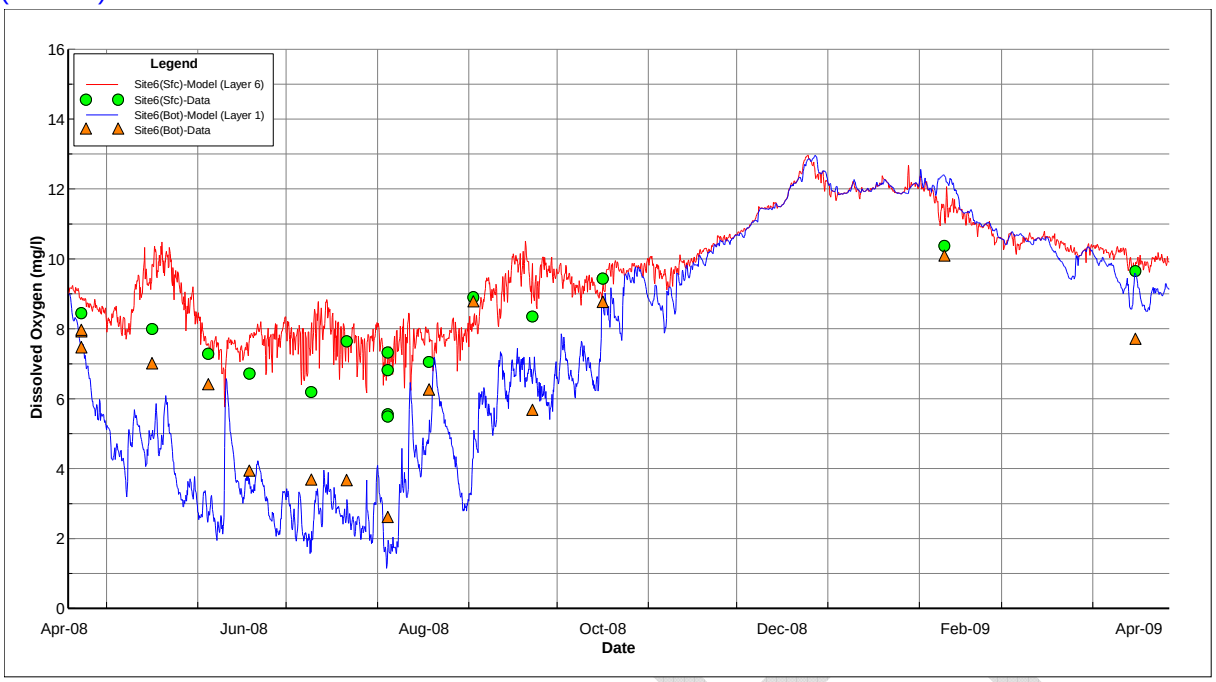

Figure 30 – Dissolved oxygen calibration results at Site 6

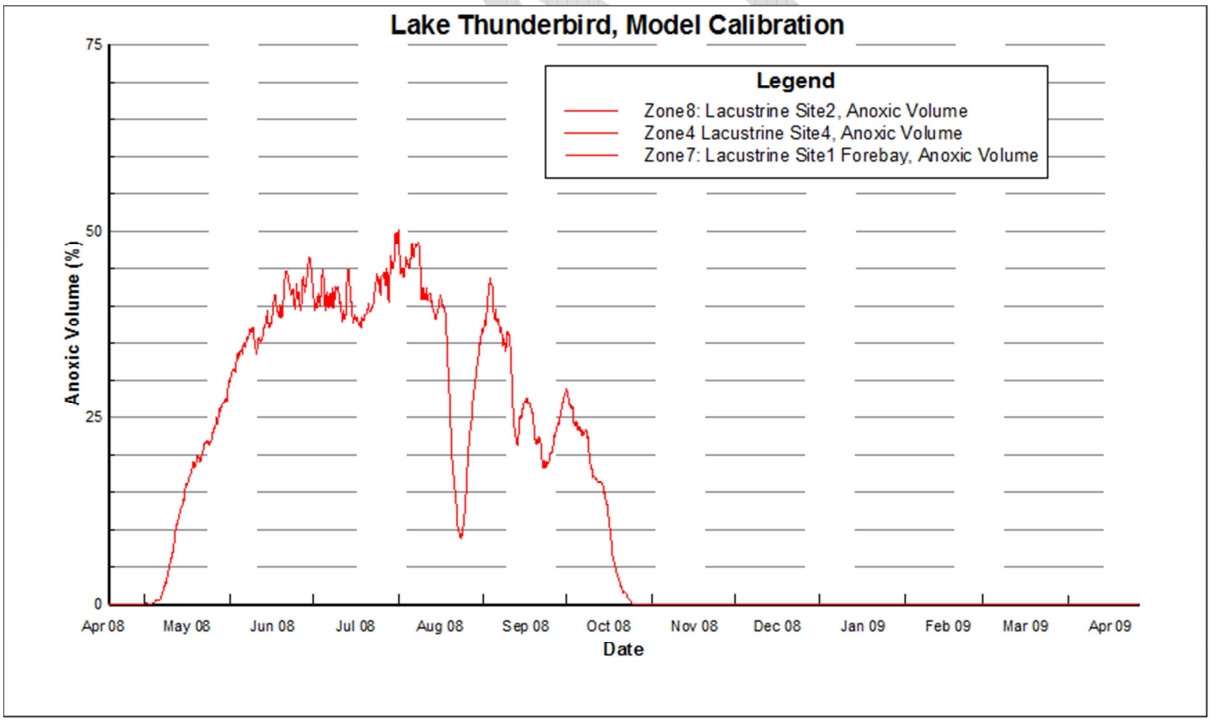

Figure 31 – Anoxic volume of the Lacustrine Zone (Site 1, Site 2 and Site 4)

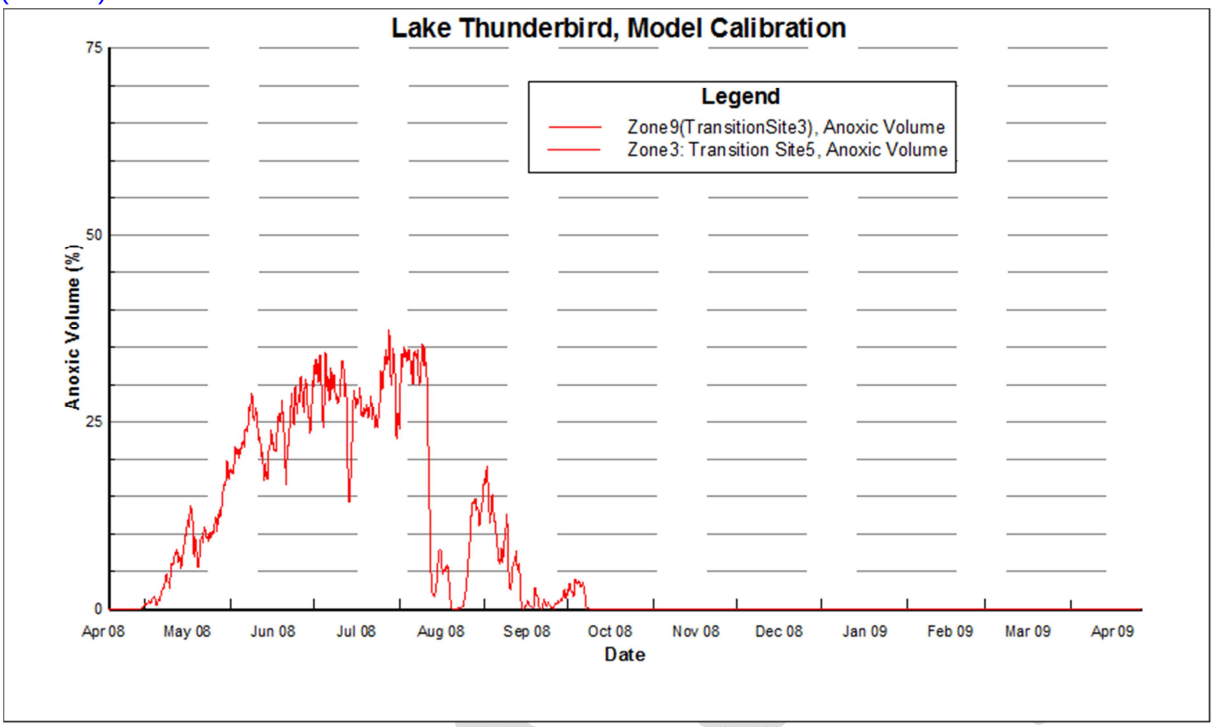

Figure 32 – Anoxic volume of the Transition Zone (Site 3 and Site 5)

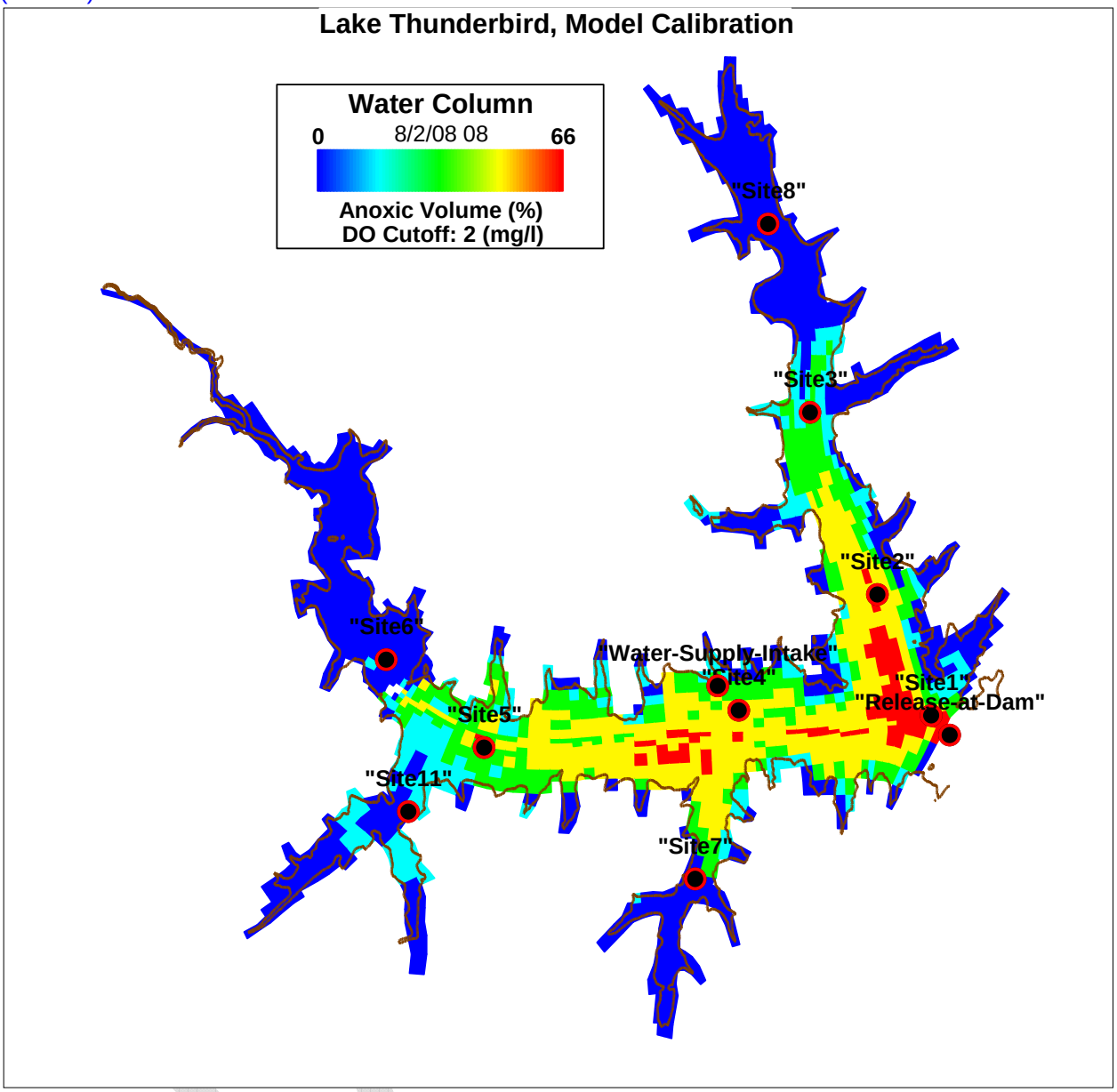

Figure 33 – Anoxic volume of Lake Thunderbird on August 2, 2008 08:00

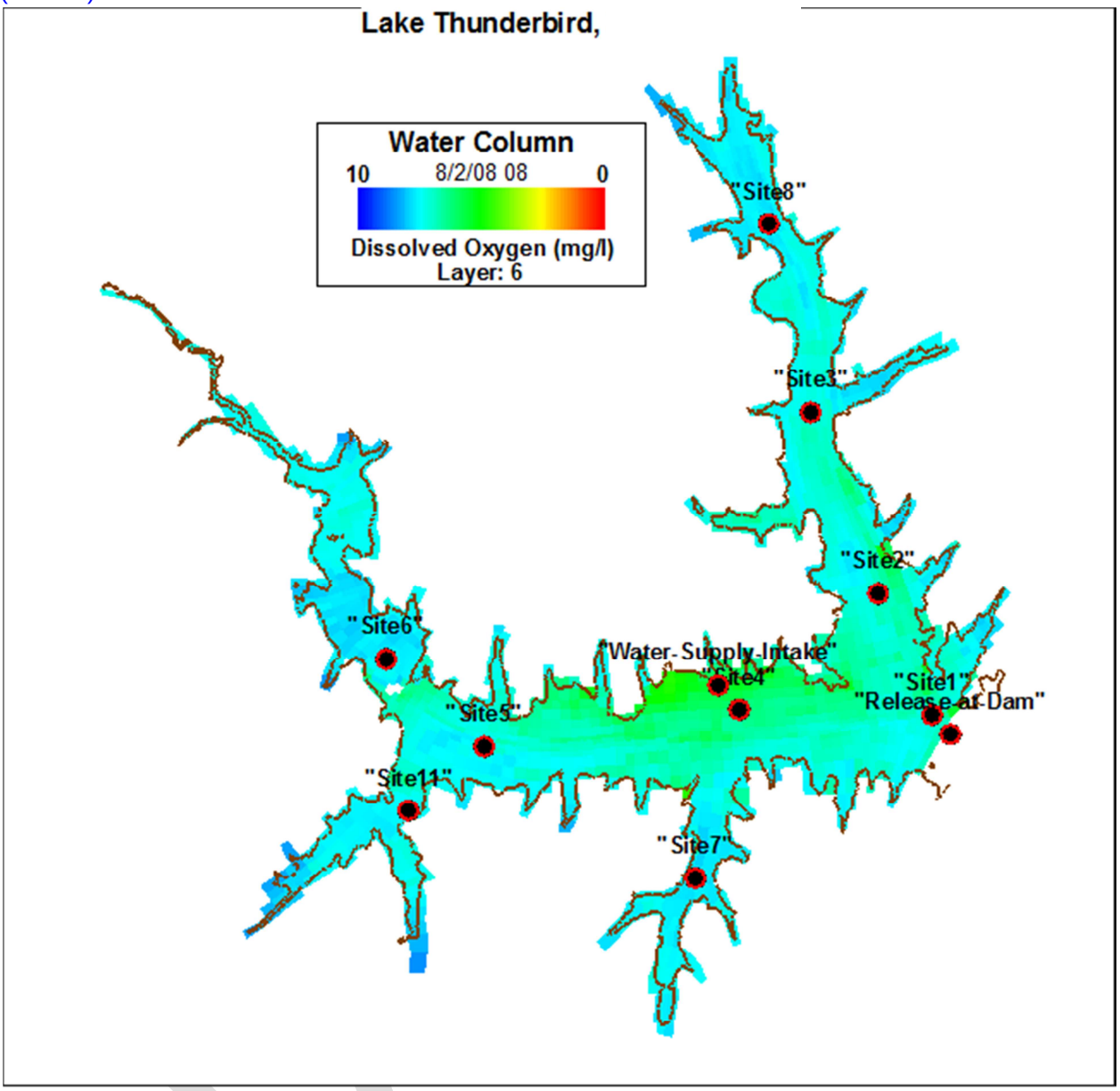

Figure 34 – Surface layer (k=6) dissolved oxygen in Lake Thunderbird on August 2, 2008 08:00

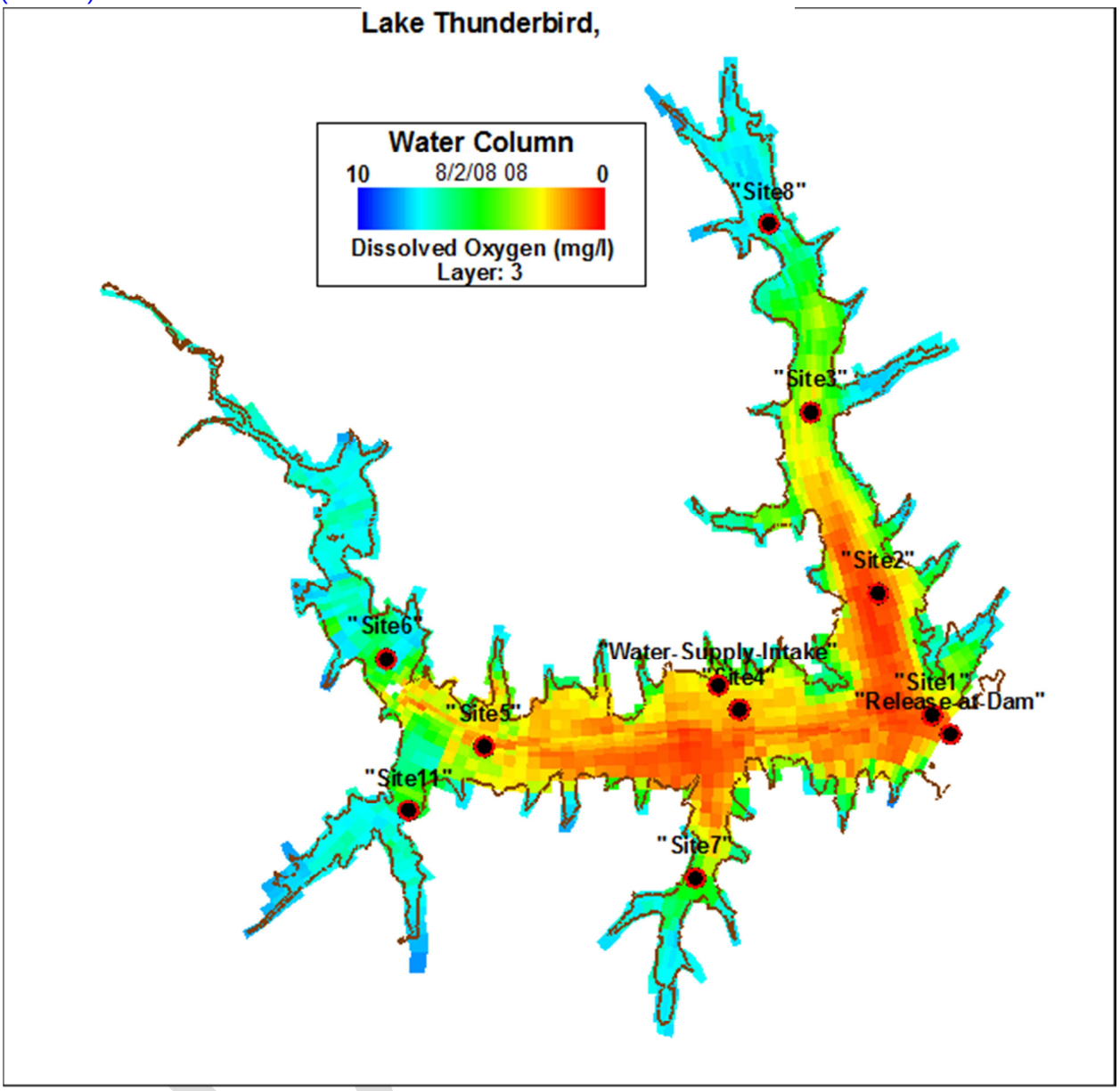

Figure 35 – Mid-water column layer (k=3) dissolved oxygen in Lake Thunderbird on August 2, 2008 08:00

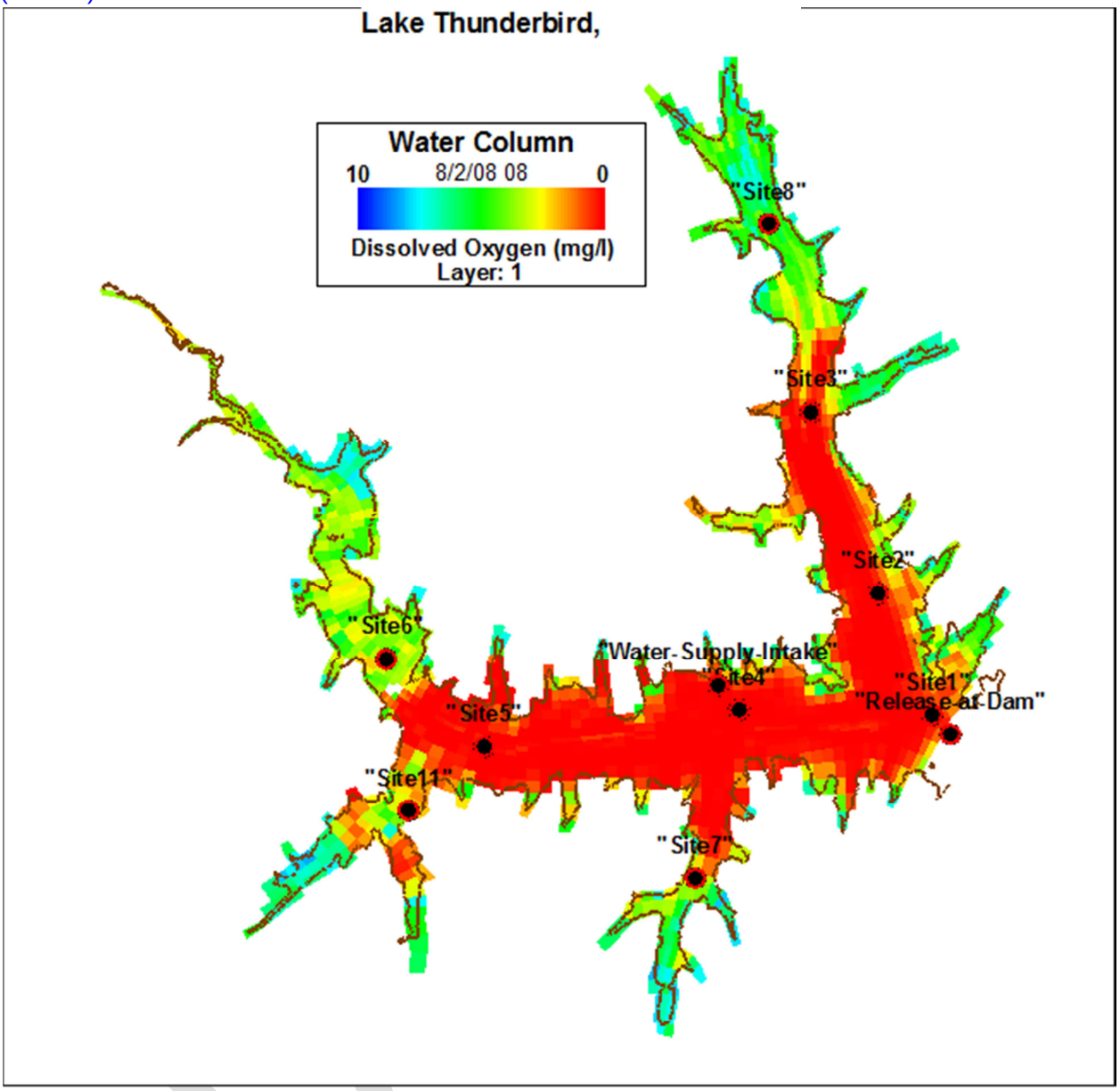

Figure 36 – Bottom layer (k=1) dissolved oxygen in Lake Thunderbird on August 2, 2008 08:00

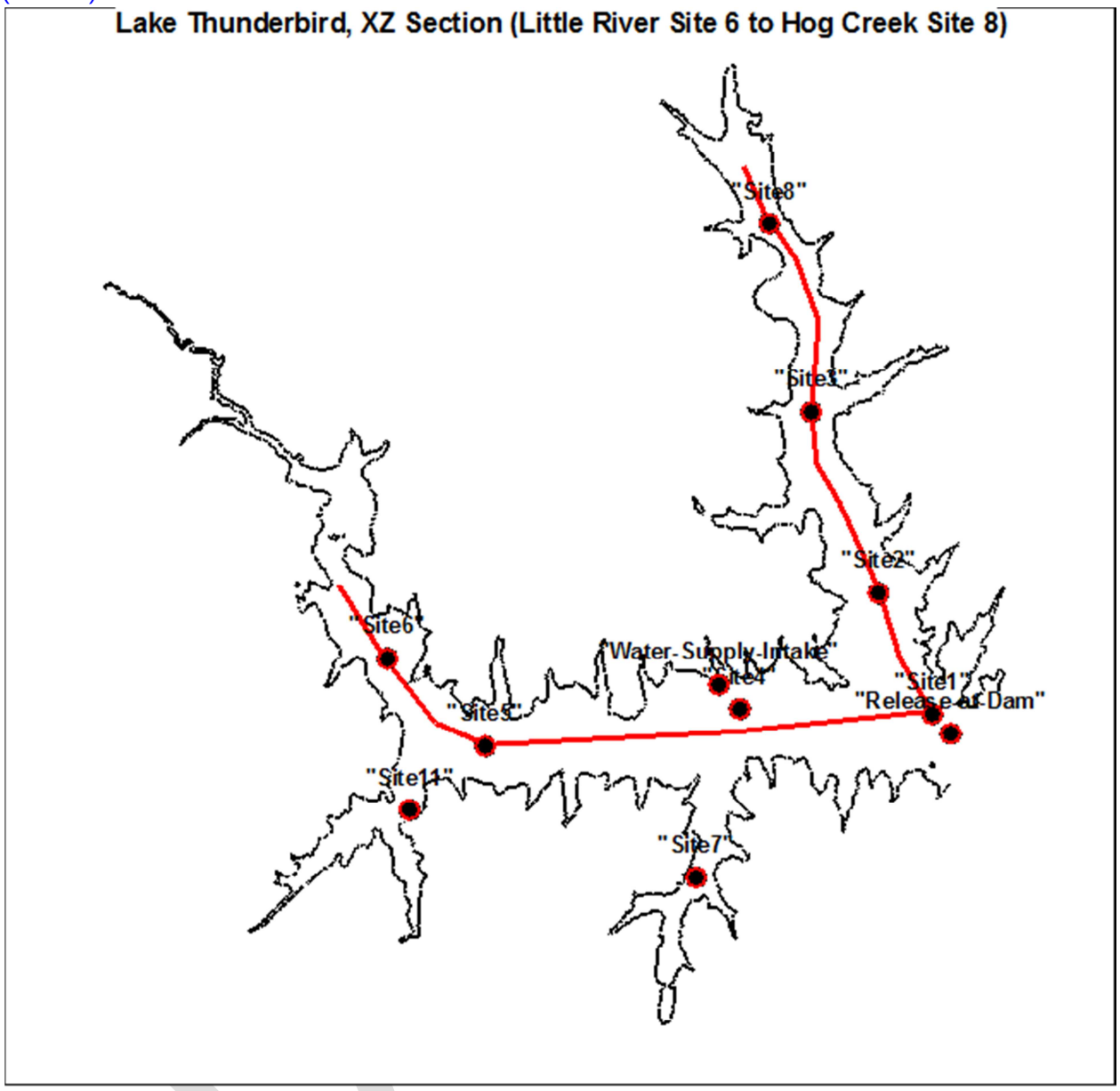

Figure 37 – XZ Section transect from the Little River (Site 6) to Hog Creek (Site 8)

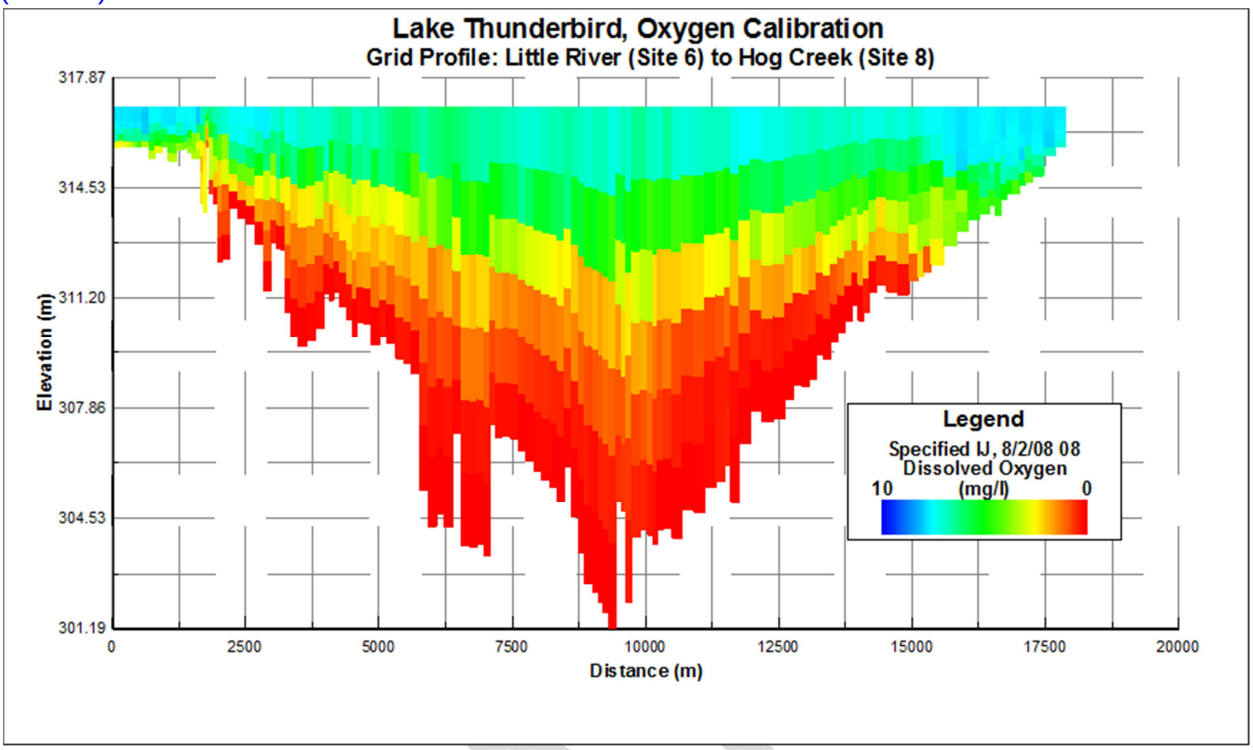

Figure 38 – XZ Section from the Little River (Site 6) to Hog Creek (Site 8) for dissolved oxygen in Lake Thunderbird on August 2, 2008 08:00

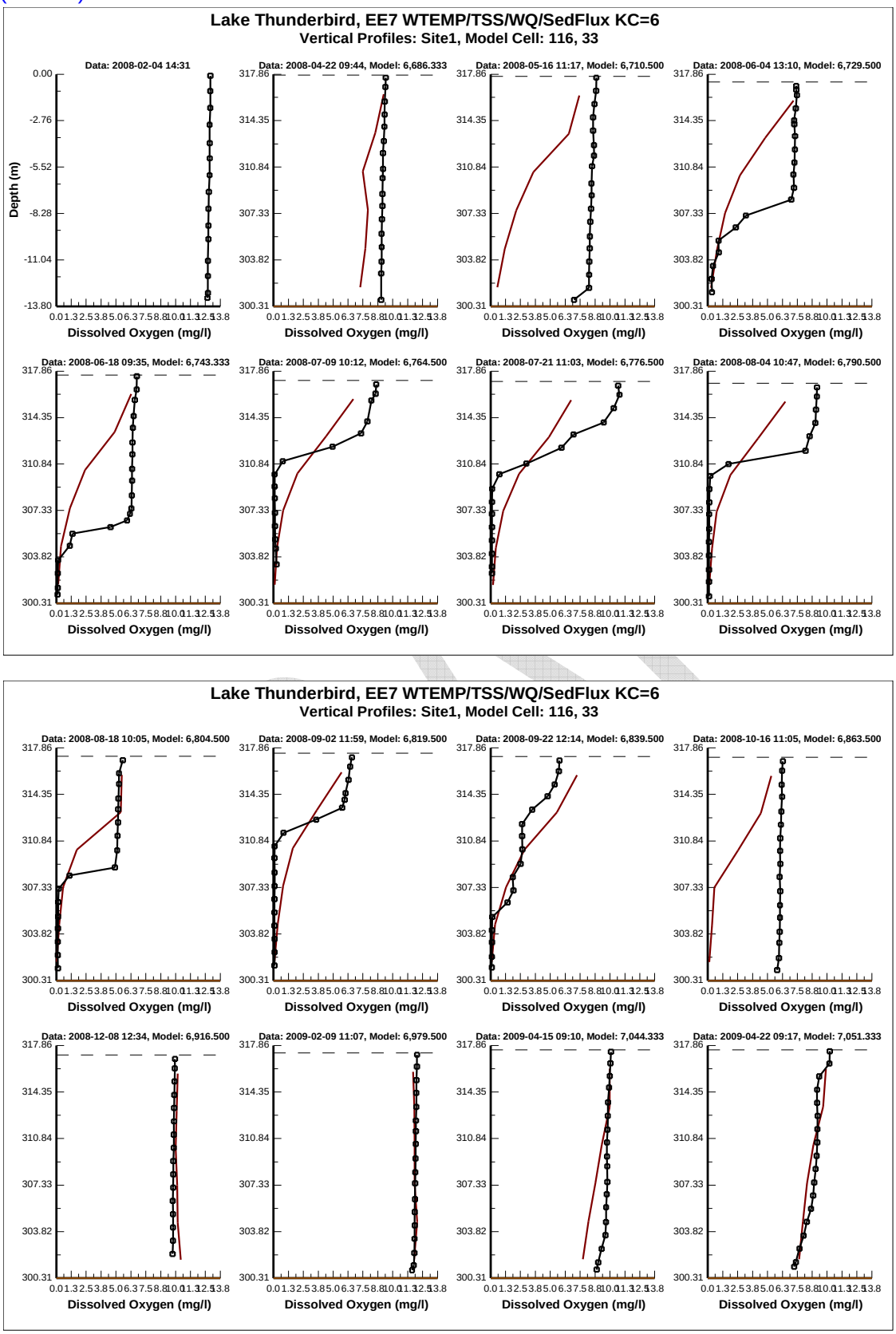

Figure 39 – Vertical profiles of dissolved oxygen in the lacustrine zone at Site 1

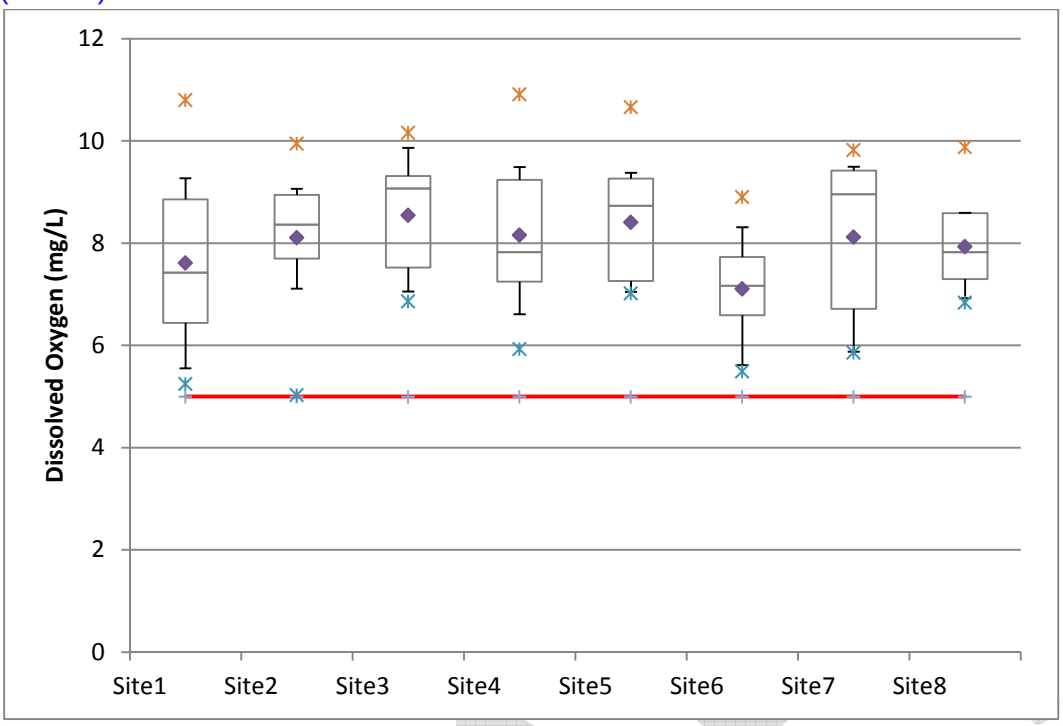

Figure 40 – Box-Whisker plots of Lake Thunderbird observed surface layer dissolved oxygen for seasonal stratified period by monitoring site. Red line shows 5 mg/L water quality criteria for oxygen in the epilimnion.

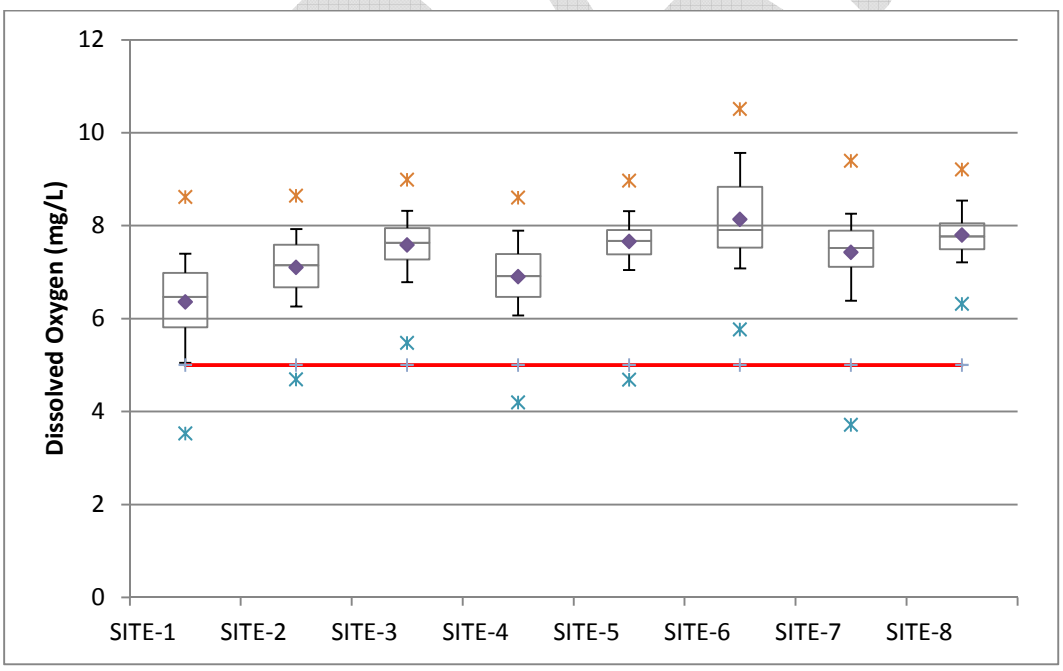

Figure 41 – Box-Whisker plots of Lake Thunderbird model calibration results for surface layer dissolved oxygen for seasonal stratified period by monitoring site. Red line shows 5 mg/L water quality criteria for oxygen in the epilimnion.

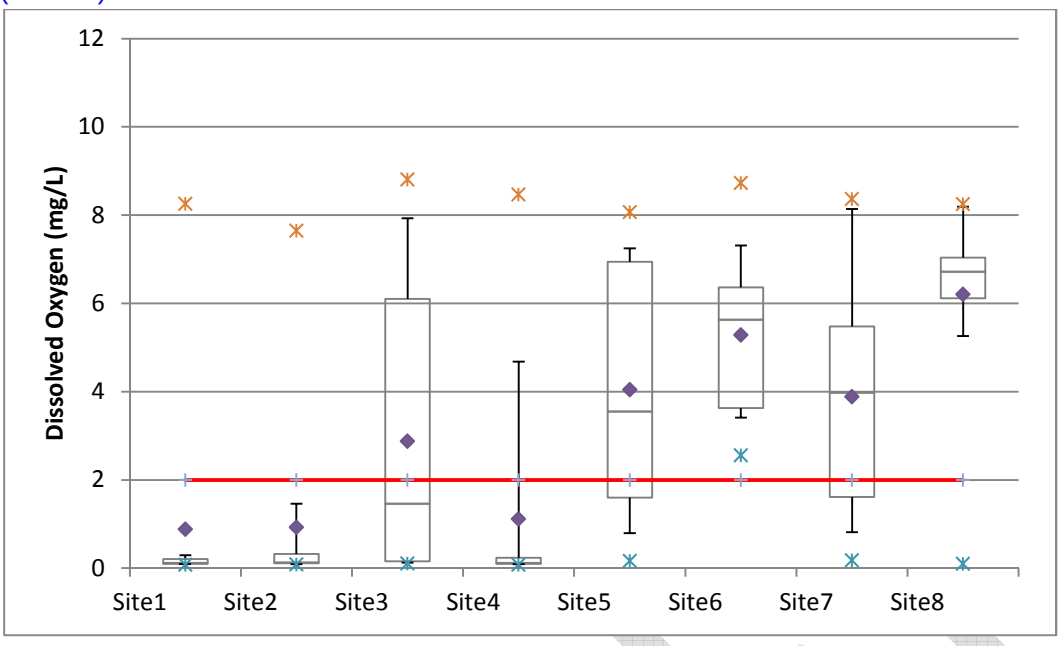

Figure 42 – Box-Whisker plots of Lake Thunderbird observed bottom layer dissolved oxygen for seasonal stratified period by monitoring site. Red line shows 2 mg/L water quality criteria for oxygen cutoff for anoxic hypolimnion.

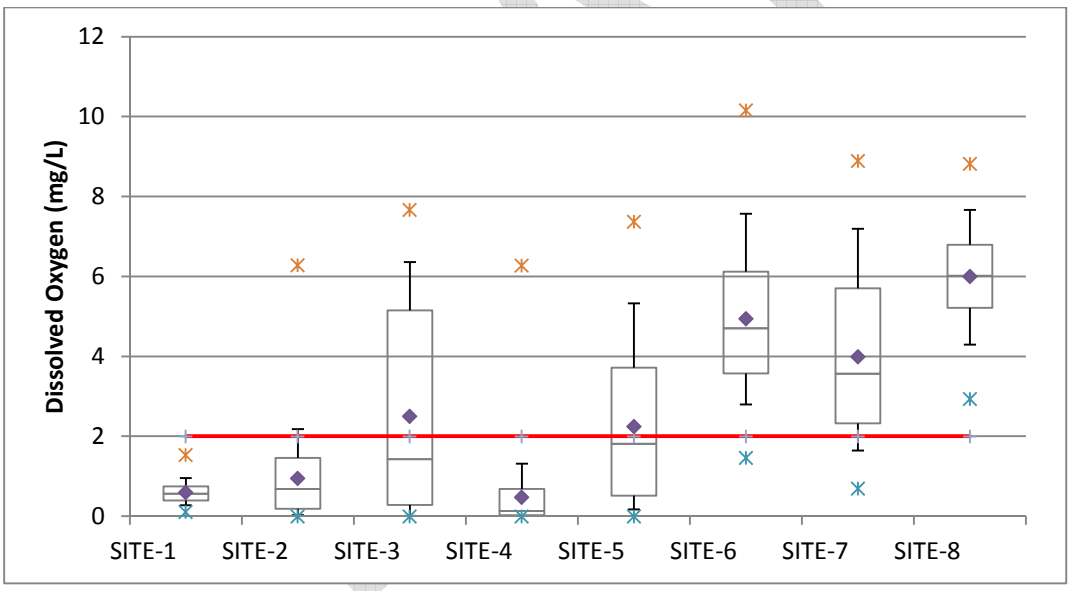

Figure 43 – Box-Whisker plots of Lake Thunderbird model calibration results for bottom layer dissolved oxygen for seasonal stratified period by monitoring site. Red line shows 2 mg/L water quality criteria for oxygen cutoff for anoxic hypolimnion.

4.6 Algae and Trophic State Index

Algae biomass results (as Chlorophyll a) are presented for comparison to observed data for the surface layer (k=6) for the lacustrine zone (Site 1), Clear Creek (Site 7) and the riverine zone in the Little River (Site 6) (**Figures 44-46**)**.** As can be seen in these model-data plots, the model results are in good agreement with measured biomass for most of the calibration period. The exception to the good agreement with the observations is the late summer period in September where the model results (~20 ug/L) underestimate the observed chlorophyll a biomass of ~40-50 ug/L in the lacustrine zone at Site 1. In patterns similar to that seen at Site 1, the model also underestimated chlorophyll at the other lacustrine stations (Site 2, Site 4) and the transition stations (Site 3 and Site 5) in comparison to higher observed peak levels of biomass. As shown in **Figure 17** for TSS at the lacustrine station Site 2, the two storm events in August 2008 resulted in large spikes in simulated TSS concentrations to ~100-200 mg/L that was much higher than the observed TSS data which was ~10-20 mg/L. The simulated peaks in TSS (**Figure 17**) resulted in an increase in light limitation for the algae groups, suppression of the growth rate and a decline in biomass that did not match the observed levels of chlorophyll (**Figure 39**).

In the Lake Thunderbird model both bluegreen and green algae groups are simulated to derive algae biomass for comparison to chlorophyll observations. As can be seen in **Figure 40**, green algae match observed chlorophyll very well from mid-April through July 2008. Green algae then decline in August in response to both the temperature dependent effect on the growth rate and the increase in light limitation that is triggered by the two storm events and large increases in the simulated levels of TSS in August 2008. As green algae decline from both light limitation and warmer water temperatures, bluegreen algae, characterized with a higher optimum temperature for growth, begin to thrive and account for most of the algae biomass in August through October 2008. The biomass of the bluegreen algae, also constrained by light limitation from the storm event driven spike in TSS, is not able to accumulate sufficient biomass to match the higher chlorophyll concentrations of ~40-60 ug/L observed in September.

Lake Thunderbird is classified as a Nutrient Limited Watershed (NLW) based on Carlson's (1977) Trophic State Index (TSI) for chlorophyll exceeding a numerical value of 62. Lake Thunderbird is also designated as a Sensitive Water Supply (SWS) because the lake serves as a public water supply for the cities of Norman, Midwest City and Del City. Full supporting compliance with Oklahoma water quality criteria for a SWS waterbody is achieved if the long-term average concentration of chlorophyll-a at a depth of 0.5 meters below the surface does not exceed 10 ug/L (OWRB, 785:45-5-10, Oklahoma's Water Quality Standards)

Model calibration results for chlorophyll are processed using EFDC_Explorer to compute Carlson's TSI based on chlorophyll (**Figure 41**). As can be seen in the model-data comparison for TSI at Site 1, the simulated TSI index is in excellent agreement with the observed TSI index with the exception of the late summer period when the model underestimated observed chlorophyll as discussed above.

In order to compare the observed data and the model calibration results to the water quality criteria for chlorophyll-a, observed data and model calibration results were processed for each site to compile summary statistics for chlorophyll data collected and simulated from April 2008 through April 2009. The statistics thus describe variability of observations and model results on an annual basis. Summary statistics are shown as box-whisker plots for each monitoring site for observed chlorophyll-a (**Figure 50**) and simulated chlorophyll-a for model calibration (**Figure 51**). The box-whisker plots show the summary statistics computed from the observed data and the model results. Minimum and maximum values are shown as "outlier" data points plotted outside the tails of the box (* symbol). The lower and upper tails of the box show the 10th and 90th percentile values. The lower and upper horizontal lines of the box show the 25th and 75th percentile with the 50th percentile shown as the line through the box. The mean value is shown as a data point within the box. The water quality target of 10 ug/L chlorophyll is shown as the horizontal red line on the box-whisker plots. The average value for chlorophyll is used for comparison to the water quality target (10 ug/L) since the water quality criteria states that the ong-term average annual samples are not allowed to be greater than 10 ug/L.

As shown in **Figure 50**, the average of the surface layer chlorophyll observations for all sites are much greater than 10 ug/L and are thus not in compliance with water quality criteria for the epilimnion under long-term annual conditions. Model calibration results for the average of surface chlorophyll (**Figure 51**) are also seen to exceed the water quality criteria of 10 ug/L for the epilimnion. Reflecting the agreement between the time series of model results and observed data for surface chlorophyll shown for Site 1, 7 and 6 in **Figures 44, 45** and **46,** the summary statistics of the surface layer model results for all eight sites (**Figure 51**) show a fair match with the observed surface layer chlorophyll statistics for the sites (**Figure 50**). As discussed above the model fails to reproduce the high biomass levels defined by the 75th and 90th percentile levels that were observed in August because of the simulated high TSS levels and corresponding reduction in light limitation from the August storm events.

The composite surface layer model performance statistics for the eight stations with chlorophyll data show an RMS Error of 12.8 ug/L with a Relative RMS Error of 18.9%. The model results for algae biomass as chlorophyll-a are thus much better than the defined model performance target of $\pm 100\%$ for chlorophyll-a. Model performance statistics for each station are presented in **Appendix E**.

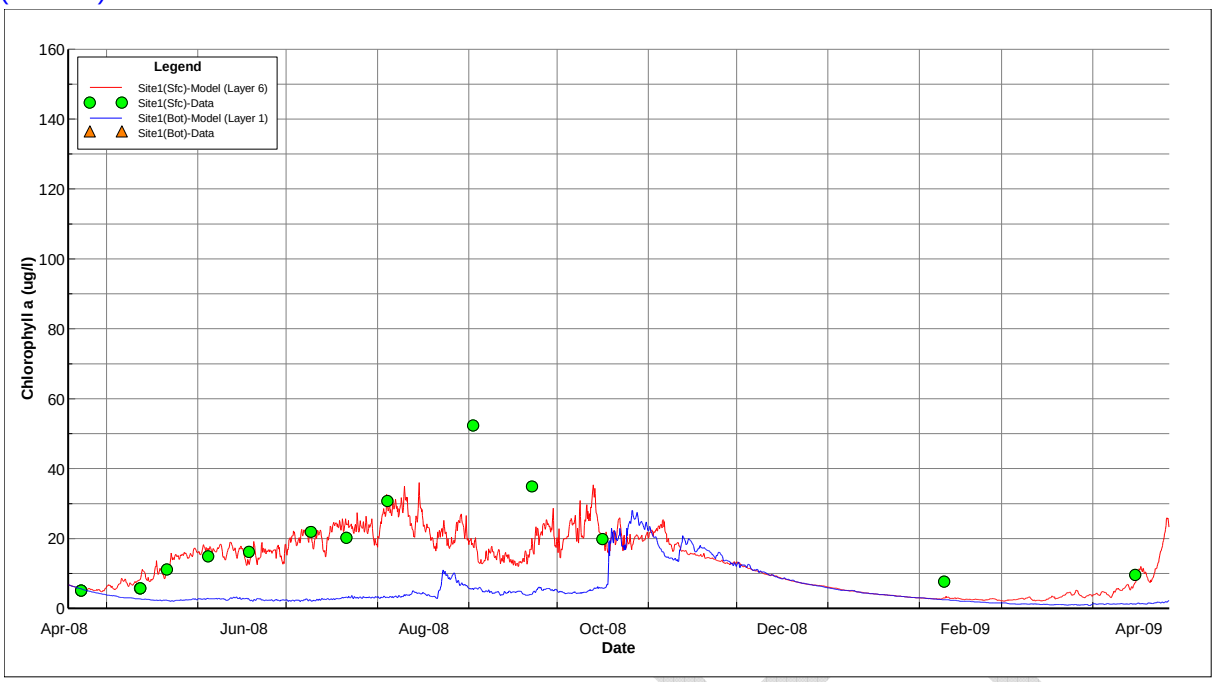

Figure 44 – Chlorophyll-a calibration results in the lacustrine zone at Site 1

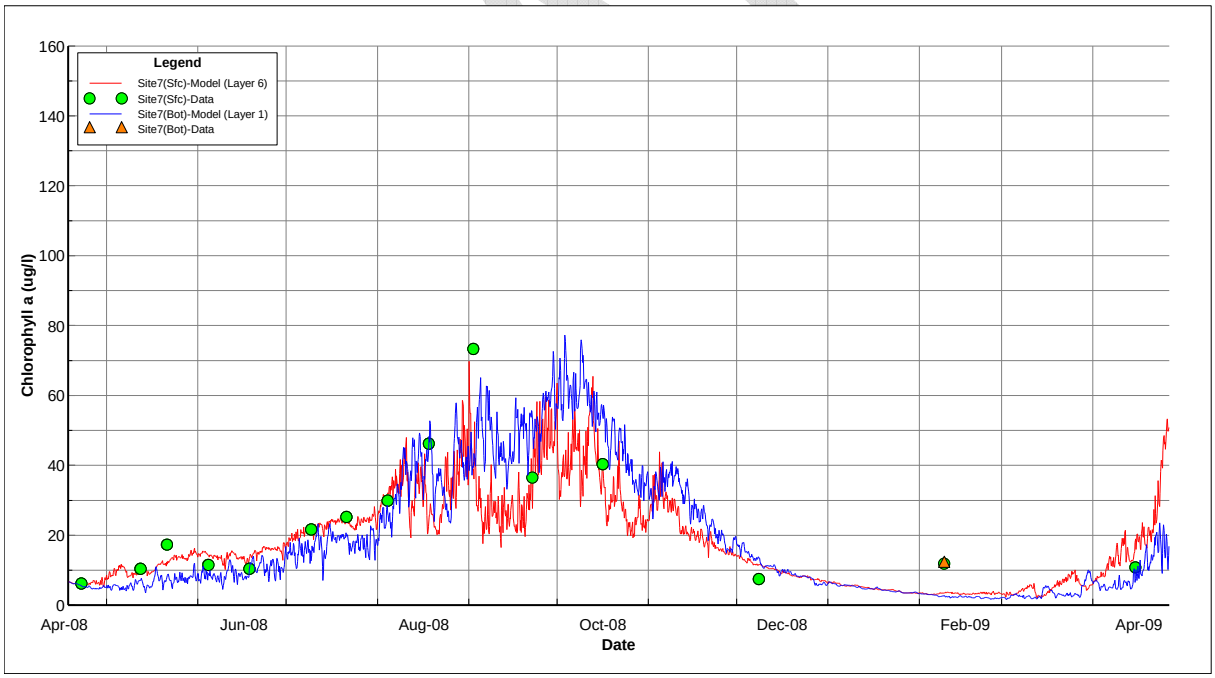

Figure 45 – Chlorophyll-a calibration results in the riverine zone at Site 7

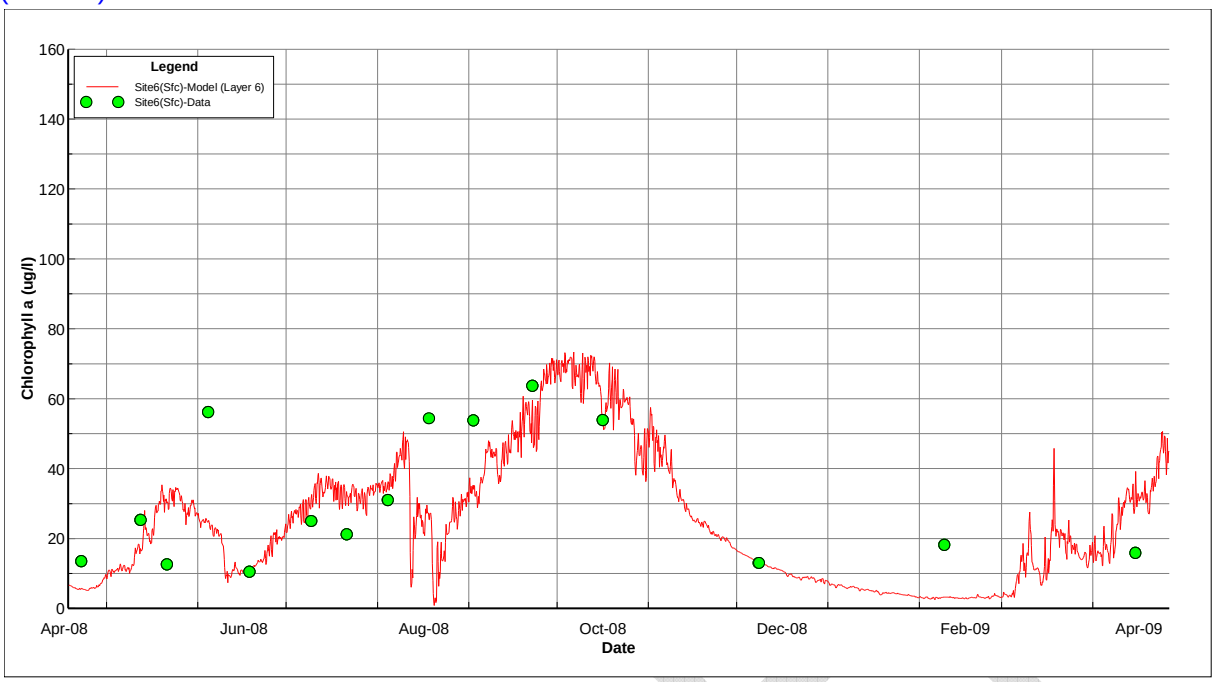

Figure 46 – Chlorophyll-a calibration results in the riverine zone at Site 6

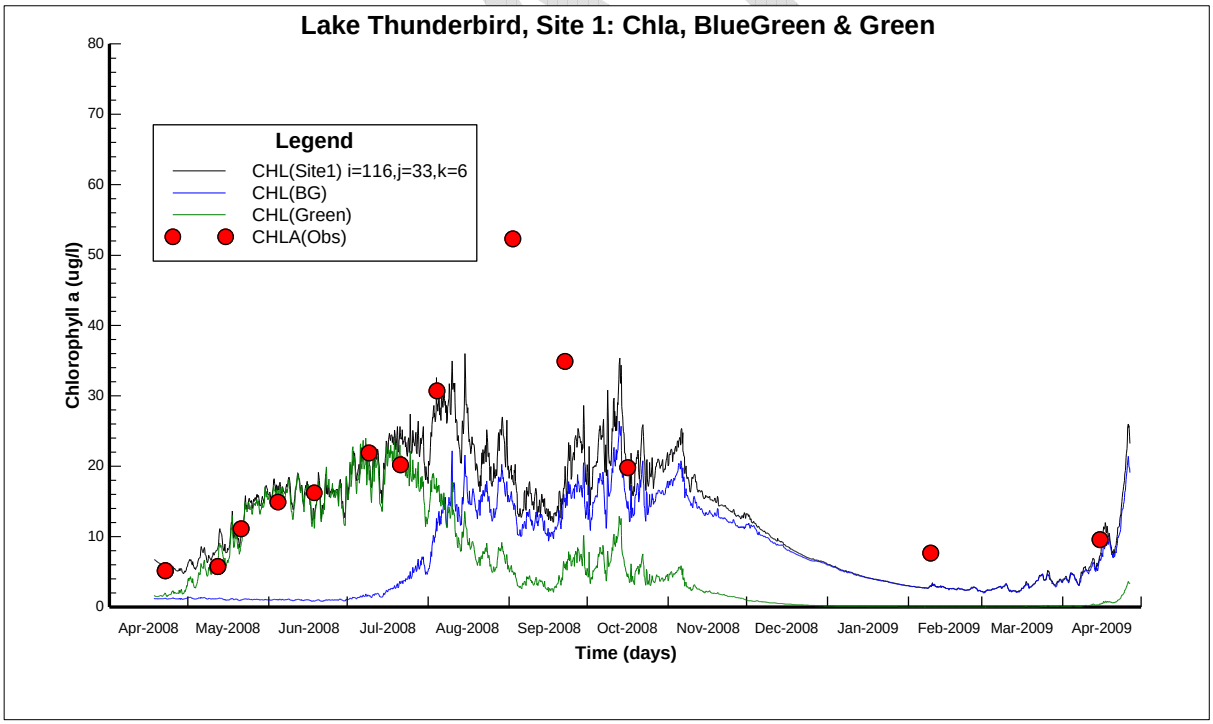

Figure 47 – Comparison of Chlorophyll a calibration results and contributions from green algae and bluegreen algae groups in the lacustrine zone at Site 1

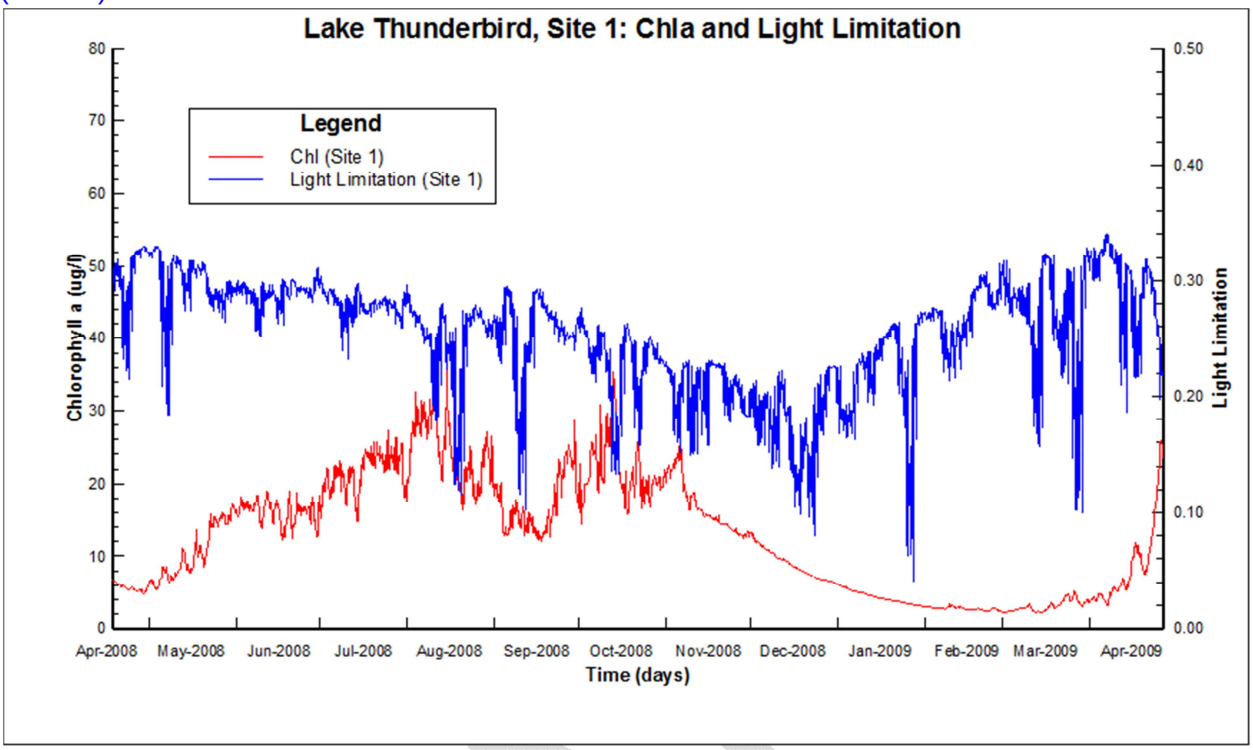

Figure 48 – Comparison of Chlorophyll a calibration results and light limitation in the lacustrine zone at Site 1

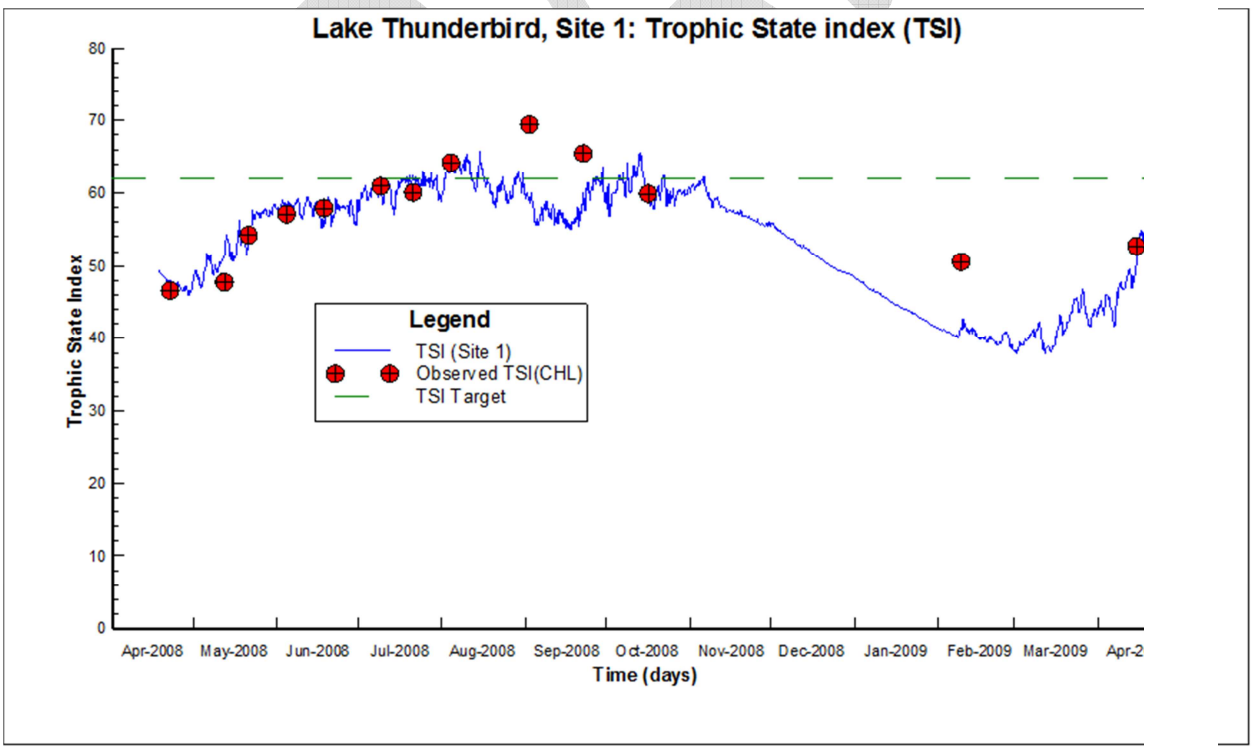

Figure 49 – Comparison of Carlson's TSI for Chlorophyll-a and Oklahoma Water Quality Criteria in the lacustrine zone at Site 1

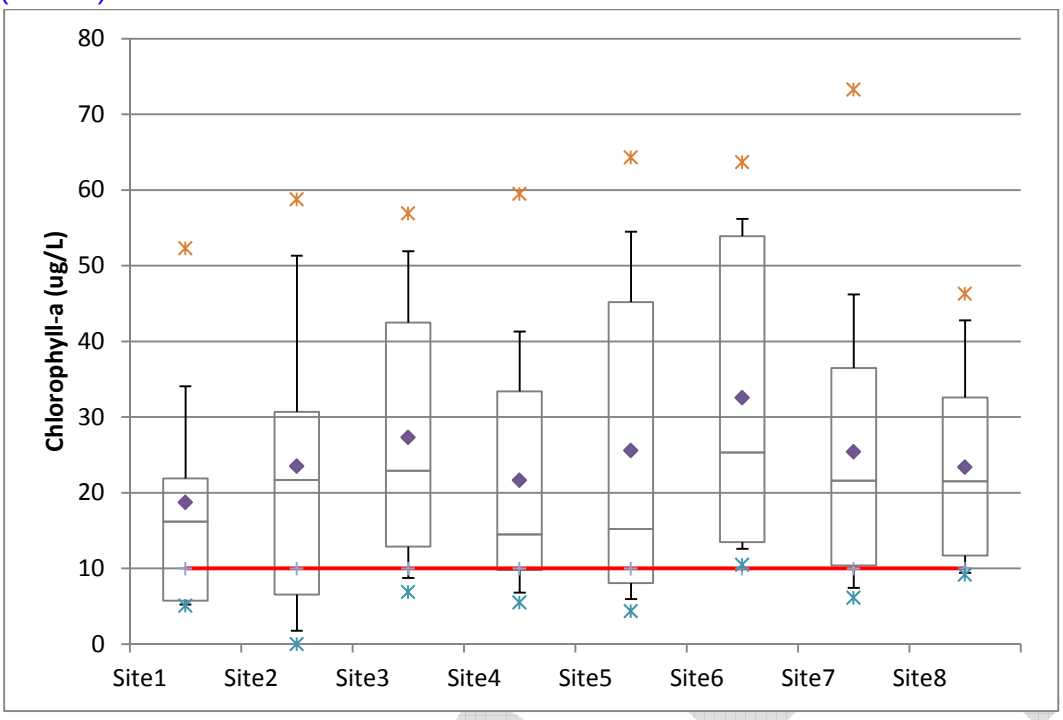

Figure 50 – Box-Whisker plots of Lake Thunderbird observed surface layer chlorophyll-a for annual period (April 2008-April 2009) by monitoring site. Red line shows 10 ug/L water quality criteria for chlorophyll in epilimnion.

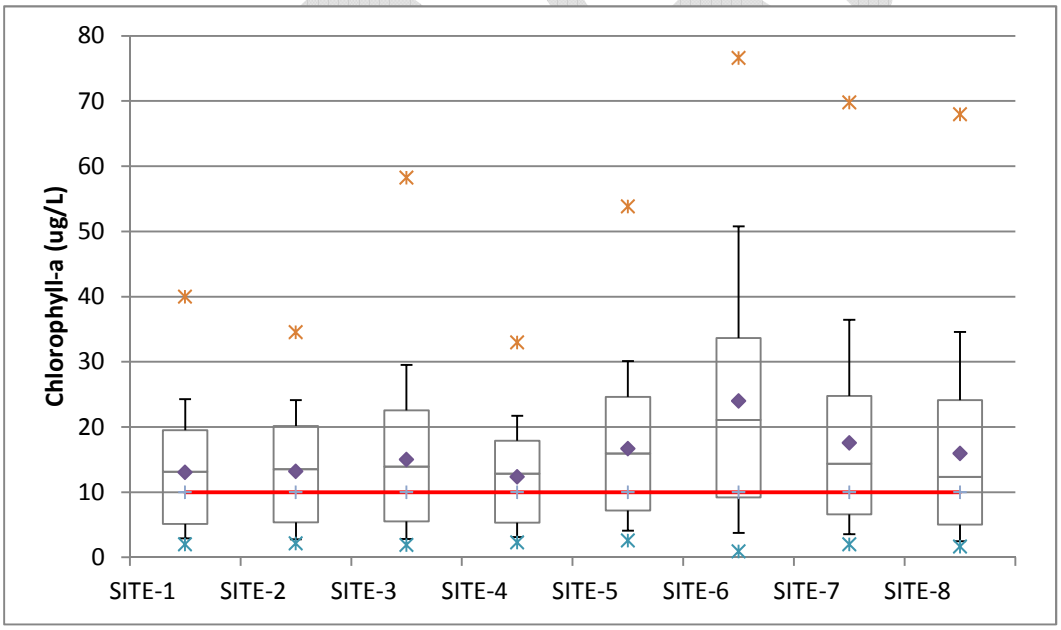

Figure 51 – Box-Whisker plots of Lake Thunderbird model calibration results for surface layer chlorophyll-a for annual period (April 2008-April 2009) by monitoring site. Red line shows 10 ug/L water quality criteria for chlorophyll in epilimnion.

4.7 Organic Carbon

Total organic carbon (TOC), particulate organic carbon (POC) and dissolved organic carbon (DOC) results are presented for comparison to observed data for the surface layer (k=6) and bottom layer (k=1) for the lacustrine zone (Site 1) (**Figures 52-54**)**.** Similar results are obtained for the other lacustrine stations at Site 2 and Site 4. As can be seen in the model-data plots for Site 1, the model results are in reasonable agreement with measured TOC from April 2008 through October 2008. The model results then underestimate TOC for the subsequent winter-spring from November 2008 through April 2009 (**Figure 52**). In the model TOC is derived as the sum of detrital POC, algal POC and DOC. The model-data comparisons for POC (**Figure 53**) and DOC (**Figure 54**) show that DOC is the larger component of TOC. The results for POC and DOC show that the model overestimates POC and underestimates DOC somewhat. In contrast to TOC observations after October 2008, POC and DOC data was not available for comparison to the winter-spring model results to gain insight into reasons for the possible discrepancy in the simulation of POC and DOC. POC results are sensitive to the C/Chl ratios assigned for the BlueGreen algae (0.010 mg C/ug Chl) and Green algae (0.060 mg C/ug Chl) and the DOC results are sensitive to the fraction of algal metabolism assigned as a source term for the DOC pool. The discrepancy in simulated and observed TOC during the winter-spring months is likely due to algae biomass from diatoms that is not represented in the model. The model results for total chlorophyll (**Figure 44**), although showing reasonable agreement with the observations, underestimate the observed biomass during this period. The winter-spring data suggests that the underestimate of algae biomass in the model may be explained by the observed biomass being comprised of diatoms rather than a small assemblage of bluegreen algae.

The composite model performance statistics for the five stations (Sites 1, 2, 4, 6, 8) with TOC data show an RMS Error of 1.0 mg/L with a Relative RMS Error of 61.6%. The model results for TOC are thus between the defined model performance target of $\pm 50\%$ for nutrients and $\pm 100\%$ for chlorophyll. Model performance targets were not specifically identified for organic carbon. Model performance statistics for each station for TOC, POC and DOC are presented in **Appendix E**.

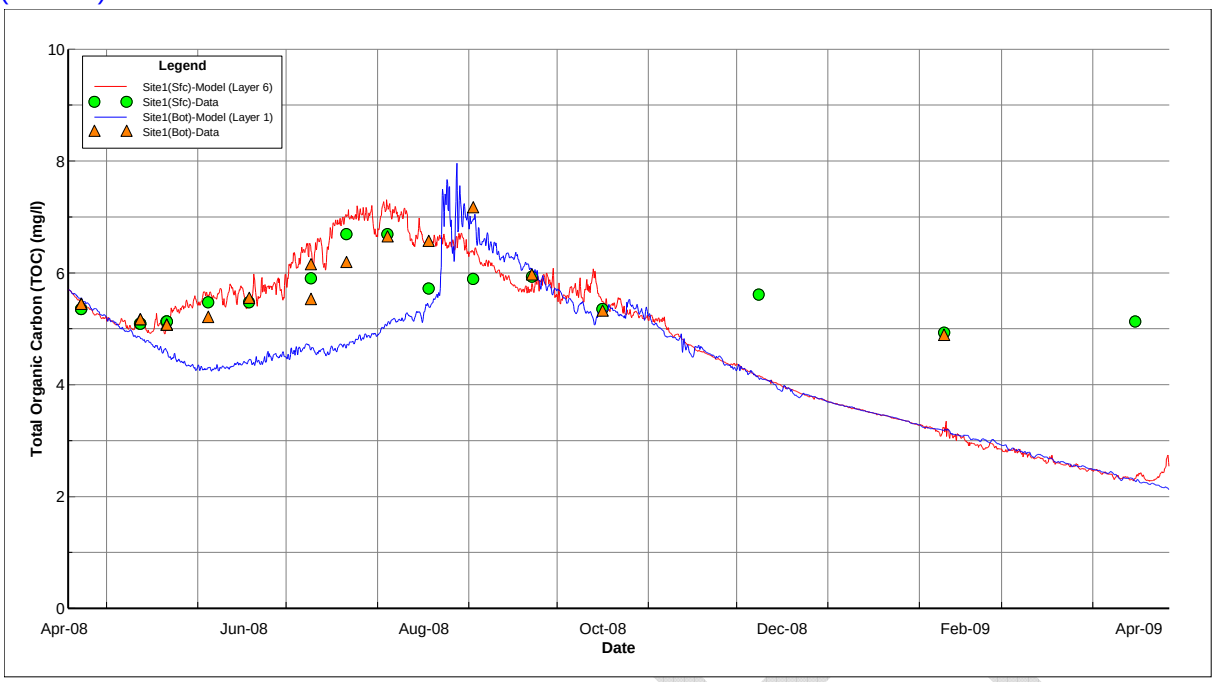

Figure 52 – TOC calibration results in the lacustrine zone at Site 1

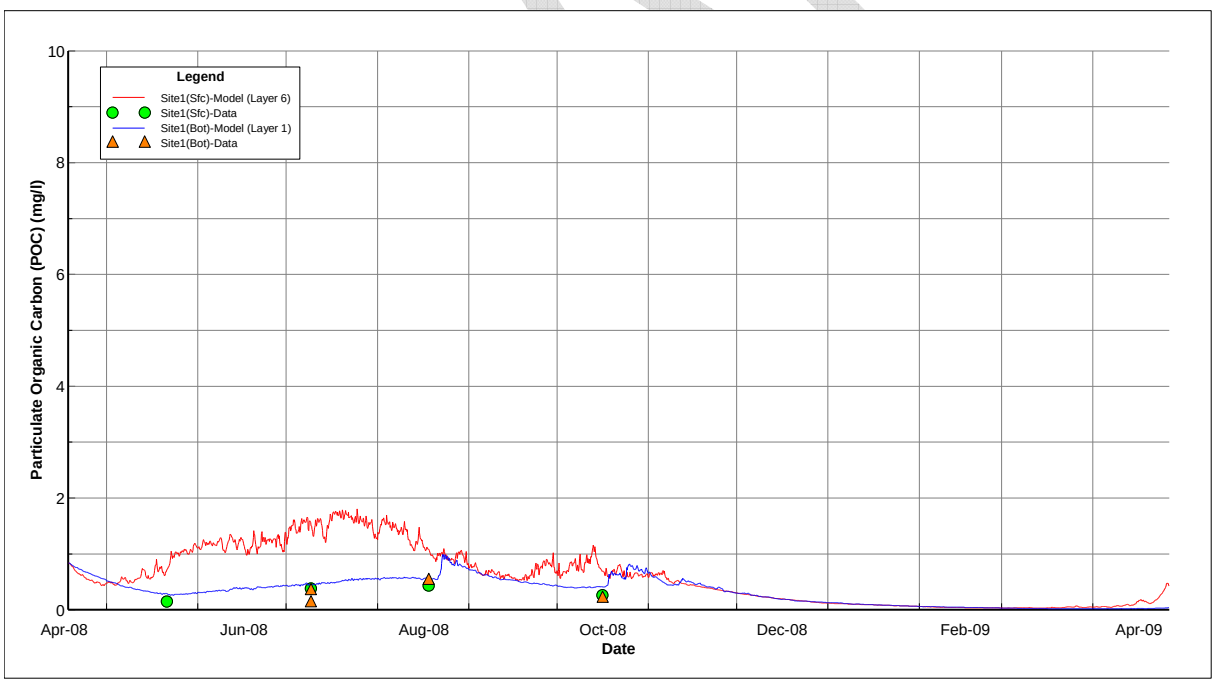

Figure 53 – POC calibration results in the lacustrine zone at Site 1

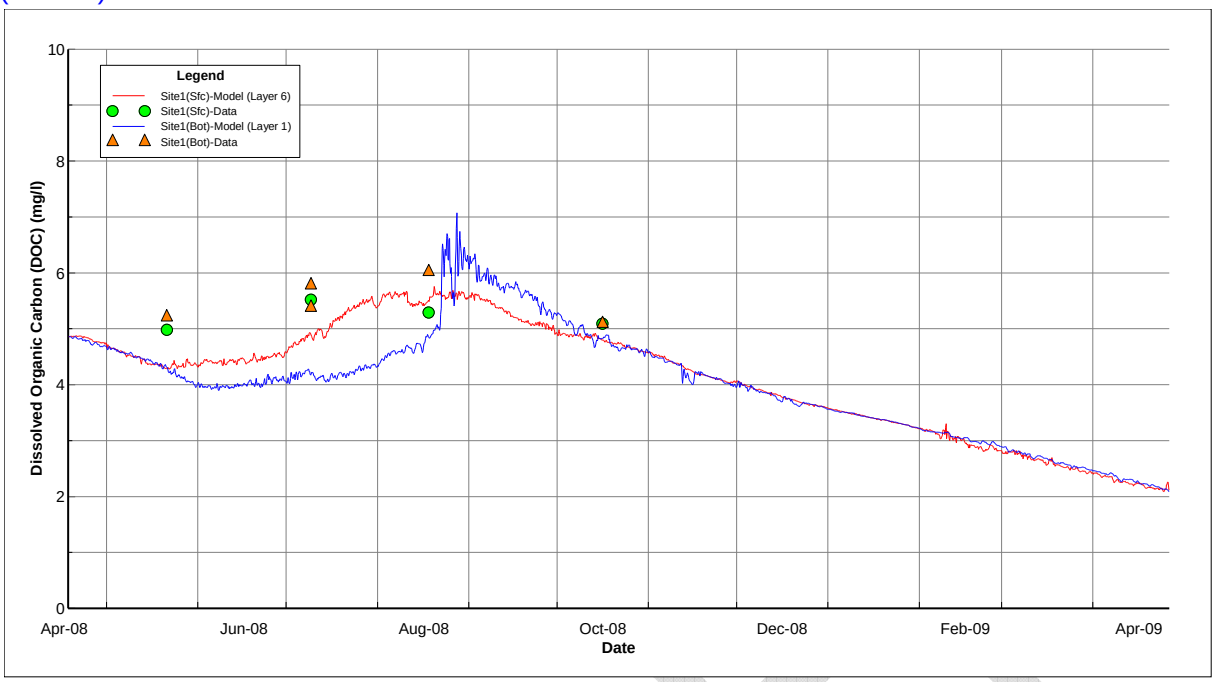

Figure 54 – DOC calibration results in the lacustrine zone at Site 1

4.8 Nitrogen

Total Nitrogen (TN), Total Organic Nitrogen (TON), ammonia-N (NH4) and nitrite+nitrate-N (NO2+NO3) results are presented for comparison to observed data for the surface layer (k=6) and bottom layer (k=1) for the lacustrine zone (Site 2) (**Figures 55-58**)**.** As can be seen in the model-data plots for Site 2, the model results are in reasonable agreement with measured TN and TON from April 2008 through July 2008. The model results then underestimate TN and TON for the late summer-fall (August-October 2008) and the subsequent winter-spring from November 2008 through April 2009 (**Figure 55** and **Figure 56**). In the model TN is the sum of TON, ammonia-N and nitrate-N and TON is derived as the sum of detrital PON, algal PON and DON. Unlike the dataset for organic carbon, observed data is not available to compare the model results to measured PON and DON. The model-data comparison for inorganic nitrogen at Site 2 is shown for ammonia-N (**Figure 57**) and nitrate-N (**Figure 58**). Observed data for bottom layer ammonia shows a sharp increase from relatively low concentrations (~0.05 mg/L) in April-June to much higher concentrations (~0.25-0.6 mg/L) in response to the onset and persistence of anoxia during July-August 2008. Bottom layer ammonia is overestimated in the model in May-June because thermal stratification is initiated in the model somewhat earlier than observed. Bottom oxygen in the model at Site 2 then decreases more rapidly than observed in May (**Figure 28**) and bottom ammonia increases as a result of the increased benthic flux of ammonia that is triggered by anoxic conditions in the overlying water column (Figure 59). The model results show good agreement with the low levels of ammonia observed during the winter-spring from October-November 2008 through April 2009 (**Figure 57**). The model-data comparison for nitrate (**Figure 58**) shows reasonable agreement with both the surface and bottom layer observations with the model tracking the initial increase and decline in nitrate through August 2008. The model, although lower than the observed data, reproduces the increase in nitrate beginning in October 2008 with the transition to a well-mixed water column in the winter-spring.

The composite model performance statistics for the five stations (Sites 1, 2, 4, 6, 8) with nitrogen data show an RMS Error of 0.88 mg/L and a Relative RMS Error of 44.2% for Total Nitrogen (TN). The model results for TN are thus somewhat better than the defined model performance target of $\pm 50\%$ for nutrients. Model performance statistics for each station for TN, TON, ammonia and nitrate are presented in **Appendix E**.

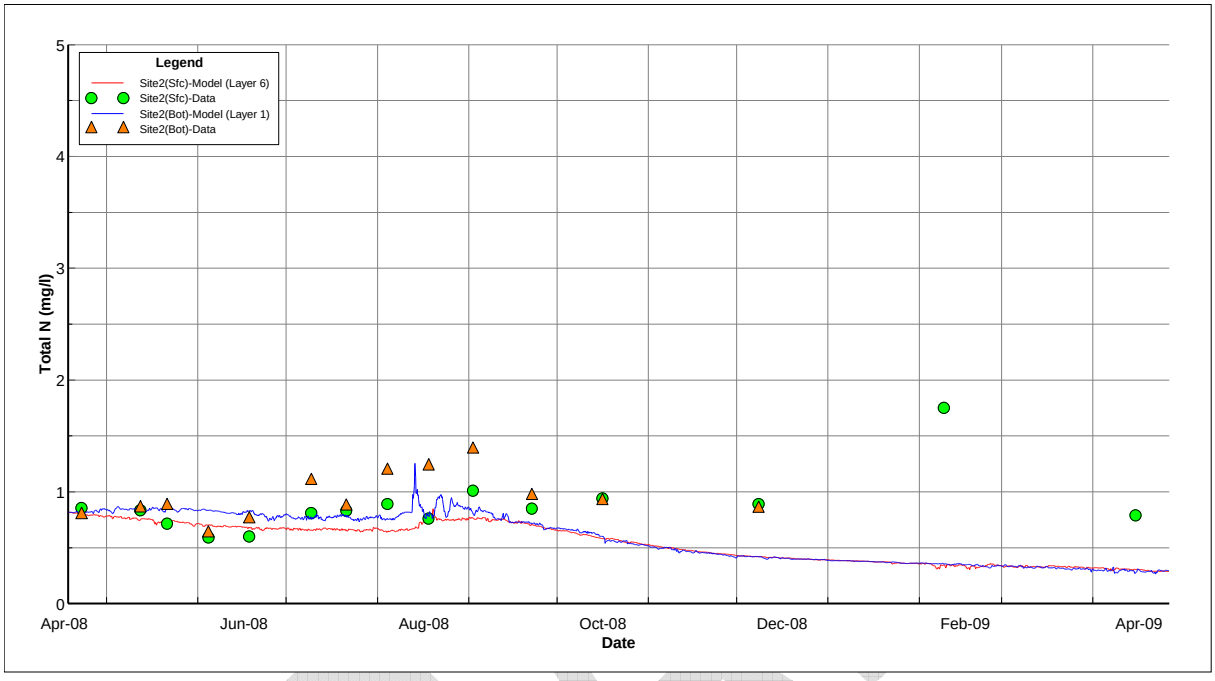

Figure 55 – Total Nitrogen (TN) calibration results in the lacustrine zone at Site 2

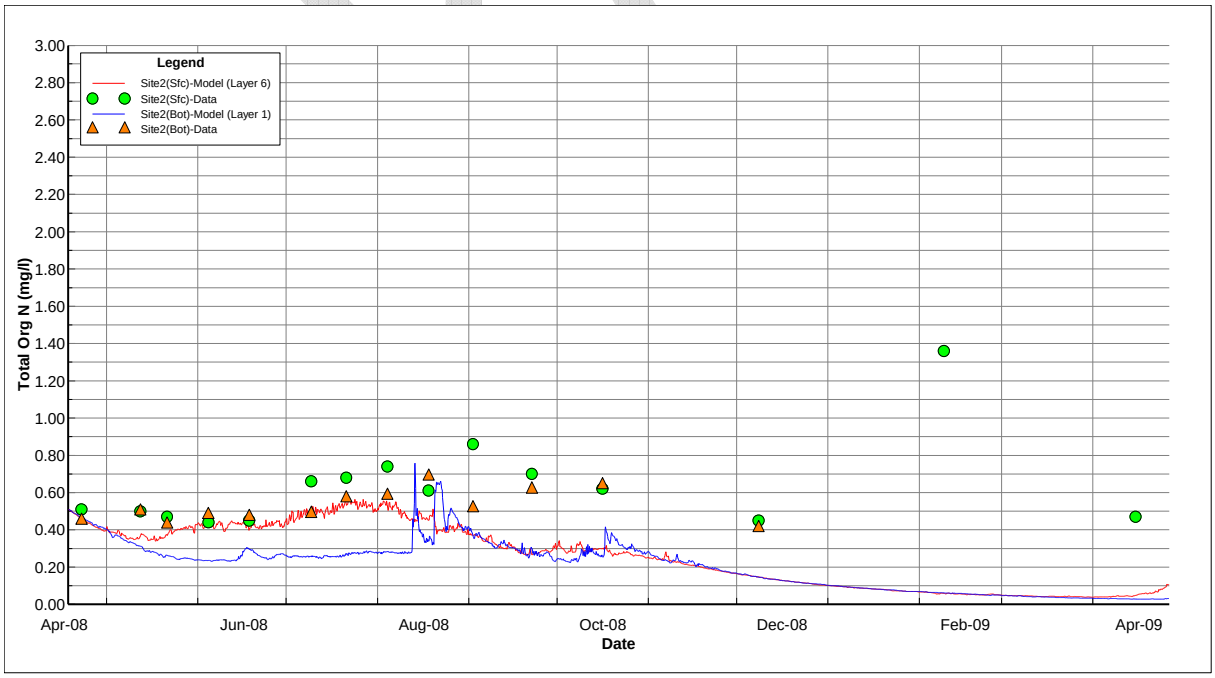

Figure 56 – Total Organic Nitrogen (TON) calibration results in the lacustrine zone at Site 2

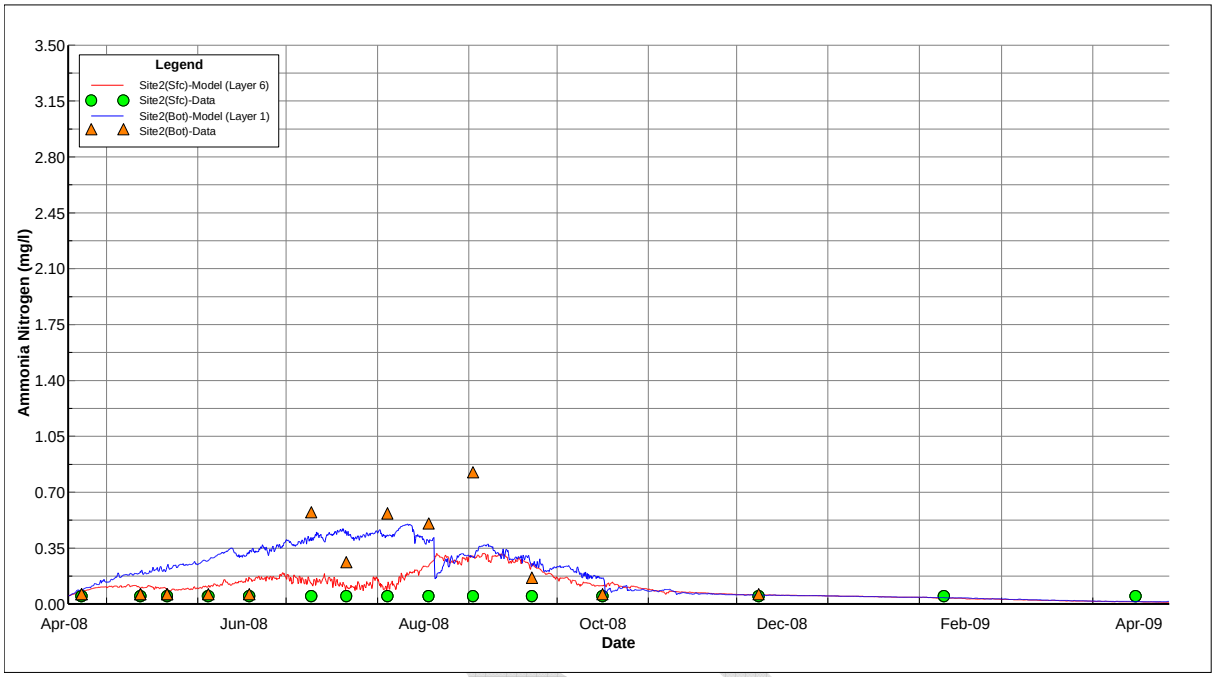

Figure 57 – Ammonia (NH4) calibration results in the lacustrine zone at Site 2

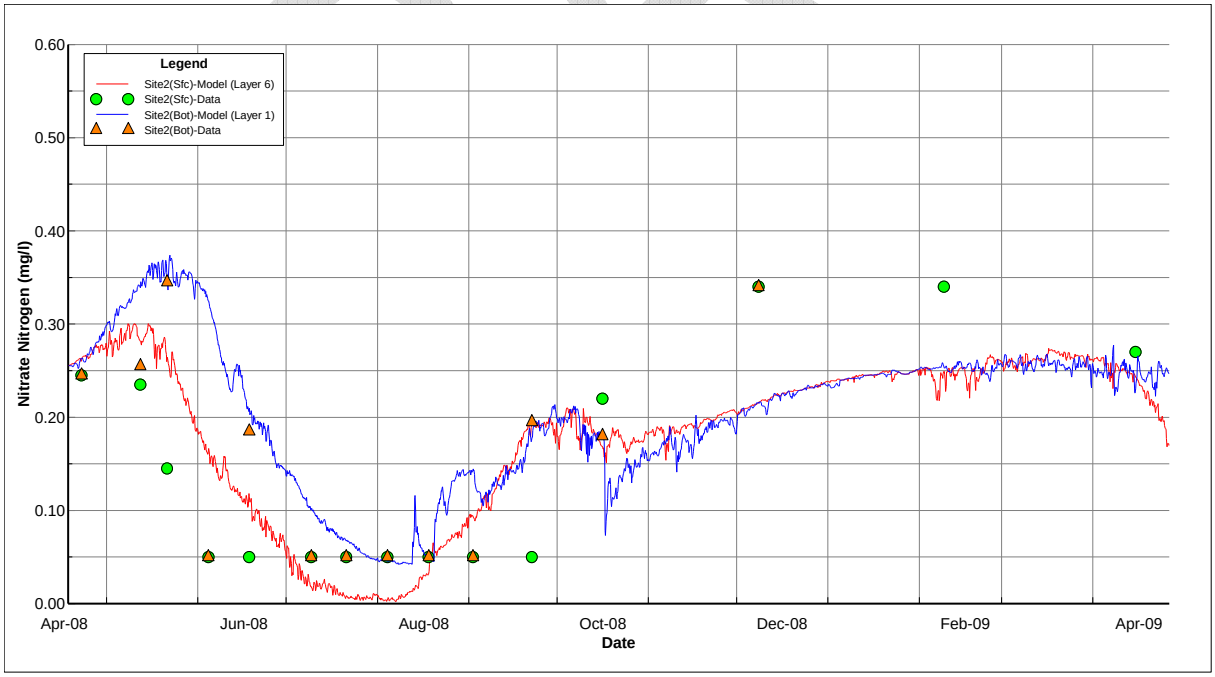

Figure 58 – Nitrite+Nitrate (NO2+NO3) calibration results in the lacustrine zone at Site 2

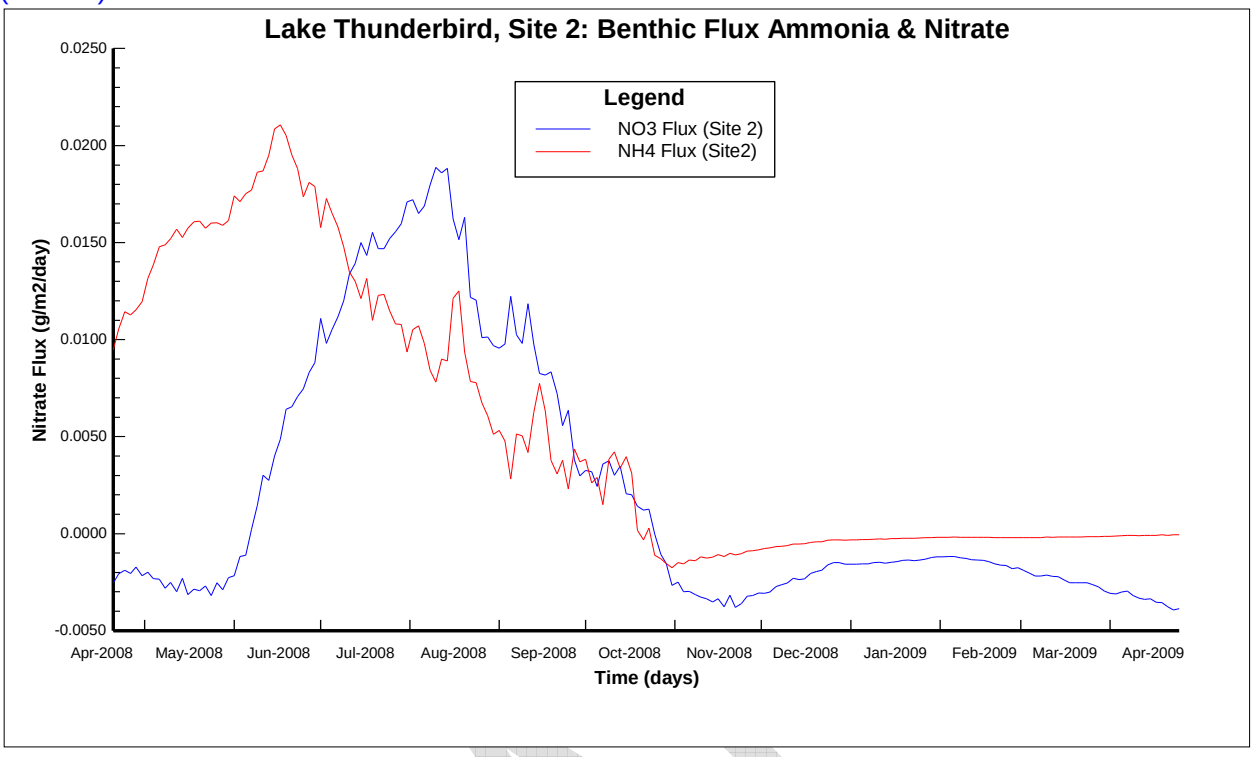

Figure 59 – Benthic flux of ammonia-N (red line) and nitrate-N (blue line) calibration results in the lacustrine zone at Site 2

4.9 Phosphorus

Total Phosphorus (TP), Total Organic Phosphorus (TOP) and total orthophosphate (TPO4) results are presented for comparison to observed data for the surface layer (k=6) and bottom layer (k=1) for the lacustrine zone (Site 2) (**Figures 60-62**)**.** As can be seen in the model-data plots shown for Site 2, the model results are in fair agreement with measured TP, TOP and TPO4 for the bottom layer from April 2008 through August 2008. The model results then overestimate surface and bottom layer TP and TPO4 beginning in September through the winter-spring into April 2009 (**Figure 60** and **Figure 62**). In contrast to TP and TPO4, the model results for TOP are in reasonable agreement with the observations from September 2008 through April 2009. In the model TP is the sum of TOP, total phosphate and TOP is derived as the sum of detrital POP, algal POP and DOP. The model-data comparison for total phosphate at Site 2 is shown in **Figure 62**. Observed data for bottom layer phosphate shows a sharp increase from relatively low concentrations (<0.05 mg/L) in April-June to much higher concentrations (~0.1-0.2 mg/L) in response to the onset and persistence of anoxia during July-August 2008. As described for ammonia, bottom layer phosphate is overestimated early in the model simulation in May-June because thermal stratification is initiated in the model somewhat earlier than observed and bottom oxygen at Site 2 in the model then decreases more rapidly than was observed in May (Figure **28**). Bottom phosphate then increases as a result of the increased benthic flux of dissolved phosphate that is triggered by anoxic conditions in the overlying water column (**Figure 63** and **Figure 64**). Following erosion of the thermocline, the model results show poor agreement with the low levels of TP and phosphate observed during the winter-spring from October-November 2008 through April 2009 (**Figure 60** and **Figure 62**).

The physical-chemical sequence of cause-effect mechanisms that control the mineralization of organic phosphorus to phosphate and the benthic release of dissolved phosphate across the sediment-water interface have been understood to be very complex for over 50 years. Pioneering experiments by Mortimer (1941, 1942) with lake sediments provided insight into the significant controlling effect of the near bottom water oxygen concentration on the release of phosphate across the sediment-water interface into a lake. As long as bottom water oxygen is above hypoxic concentrations (i.e., >2 mg/L), phosphate remains strongly sorbed to an iron oxyhydroxide precipitate and the release of dissolved phosphate via diffusion from porewater is prevented. As the near bottom oxygen concentration decreases to anoxic conditions under stratified conditions, however, the redox potential is lowered, iron oxyhydroxide is reduced to a soluble form of iron, phosphate is no longer sorbed and dissolved phosphate is released from the sediment bed to the overlying water column (Di Toro, 2001). Environmental variables that appear to control the release of dissolved phosphate from the sediment bed under stratified hypoxic conditions in a lake are (a) abiotic processes related to bottom water temperature, overlying water dissolved oxygen level, pH, sediment bed composition and the redox potential and (b) biotic processes related to microbial activity (Nowlin et al., 2005). Hupfer and Lewandowski (2008) present a thorough review of the literature related to phosphorus release from the sediment bed, including experiments related to artificial aeration of the hypolimnion. They summarize how phosphorus release is controlled by many factors other than low oxygen concentration in the overlying water column. Hupfer and Lewandowski state that “P-release is controlled by a complex coupling of sediment composition, external load, catchment hydrology, lake morphometry and biogeochemical reactions”.

In the model, bottom layer phosphate is dependent on sorption/desorption with cohesive solids and the sediment bed release of phosphate. The benthic flux of phosphate from the sediment bed, in turn, is controlled by production of phosphate from mineralization (decay) of organic phosphorus in the bed, burial loss of organic phosphorus to an inactive sediment layer and sorption/desorption of phosphate with sediment bed solids. Mineralization of organic phosphorus is temperature dependent, burial of organic matter is a constant loss and sorption is dependent on the oxygen concentration of the overlying water via a functional dependence of the partition coefficient on bottom layer oxygen. Adjustable model parameters that control the release of sediment bed phosphate are the mineralization rate for organic phosphorus, the phosphate partition coefficient, the critical oxygen concentration that triggers the release of phosphate and an “enhancement factor” for partitioning. The enhancement factor, combined with a functional term that incorporates the ratio of the overlying oxygen concentration to the critical oxygen concentration, smoothly reduces the phosphate partition coefficient as overlying oxygen approaches zero. As the partition coefficient is decreased under anoxic conditions, the proportion of dissolved phosphate in the bed is increased, the sediment-water diffusive flux of phosphate is increased and phosphate in the bottom layer of the water column is increased. The mineralization rate, the phosphate partition coefficient and the critical oxygen concentration for sorption are applied globally across all grid cells of the model domain while the “enhancement factor” is assigned to each spatial zone developed for the model framework (see **Figure 7**). As noted by Di Toro (2001), the mineralization rate and the critical oxygen concentration for sorption was typically not adjusted in several sediment flux modeling studies. A review of the calibrated values of the phosphate partition coefficient and the enhancement factor used in the different studies, however, showed that the range of values assigned for these two parameters was extreme. Combinations of the partition coefficient and the enhancement factor were systematically adjusted during calibration of the Lake Thunderbird model to obtain as good a match to the observed data as was possible If the phosphate partition parameters were assigned large values to trap phosphate in the bed and suppress benthic phosphate release to match the low bottom water phosphate observed after stratification ended in October,

then the simulated bottom phosphate levels during the anoxic period were much lower than the observed high phosphate concentrations during the summer. Conversely, if the parameters were assigned smaller values to increase benthic phosphate release to match the high bottom water phosphate observed during the anoxic period then modeled phosphate concentrations were higher than observed during the fall-winter.

In the absence of site-specific measurements of phosphate release from the sediment bed under anoxic conditions in Lake Thunderbird, the model results for benthic phosphate flux shown in **Figures 63, 64** and **65** are compared to observed data sets available from Lake Wister (Haggard and Scott, 2011); Lake Frances (Haggard and Soerens, 2006); Eucha Lake (Haggard et al., 2005); Beaver Lake in Arkansas (Sen et al., 2007; Hamdan et al., 2010), Acton Lake in Ohio (Nowlin et al., 2005) and a set of 17 lakes/reservoirs in the Central Plains (Dzialowski and Carter, undated) to support calibration of the sediment flux model for Lake Thunderbird. Model results were extracted for each station and processed to compile summary statistics to present box-whisker plots for benthic phosphate fluxes simulated during stratified conditions from May 15 through October 1 (Figure 65). Stratified conditions correspond to the period of anoxia so that model results can be compared to measurements of phosphate release made under anoxic conditions. The box-whisker plots show the summary statistics computed from the model results. Minimum and maximum values are shown as "outlier" data points plotted outside the tails of the box (* symbol). The lower and upper tails of the box show the 10^{th} and 90^{th} percentile values. The lower and upper horizontal lines of the box show the 25^{th} and 75^{th} percentile with the 50^{th} percentile shown as the line through the box. The mean value is shown as a data point within the box.

Model results for the lacustrine (Site 1,2,4) and transition (Site 3,5) stations (**Figure 65**) show a mean anoxic release rate ranging from 0.015-0.025 g P/m**2-day (15-25 mg P/m**2-day) with the largest range of phosphate flux simulated at Site 1. The model results are seen to be consistent with the ranges of anoxic phosphate fluxes measured in eutrophic and hypereutrophic reservoirs in the Central Plains states as shown in

Figure 66 from Dzialowski and Carter (undated). Additional data is presented in Table 16 to support the model results for SOD and phosphate release by comparison to data collected at lakes in Oklahoma, Arkansas, Texas and Ohio.

Table 16. Comparison of Measured Sediment Flux Rates for Oxygen and Phosphate in Central Plains

Reservoir		Site		Aerobic	Anoxic	Reference
Name		Description	SOD	P-Flux	P-Flux	
			g/m2-d	mgP/m2-d	mgP/m2-d	
Beaver Lake	AR	Riverine Zone		0.13	0.85	Sen et al. (2007)
		Transition Zone		0.15	1.77	
		Lacustrine Zone		0.04	< 0.01	
Lake Eucha	OK	Riverine Zone		1.14	4.7	Haggard et al. (2005)
		Transition Zone		1.01	2.46	
		Transition Zone		0.95	6.05	

Lake Frances	AR	Headwaters		0.37	14.53	Haggard & Soerens (2006)
	OK					
Wister Lake	OK	Site 1 (deep channel, dam)	0.54	0.75	1.52	Haggard & Scott (2010)
		Site 2(deep cove)	0.54	1.13	3.3	
		Site 3(shallow,headwaters)	0.24	0.94	-0.23	
Acton Lake	OH	Dam site (summer mean)		n/a	9.2	Nowlin et al. (2005)
Central Plains	KS,MO	Mesotrophic (10%-90%ile)			(1.72-7.43)	Dzialowski & Carter,
	KS,IA	Eutrophic (10%-90%ile)			(2.64-18.5)	(undated)
	KS,NE	Hypereutrophic(10%-90%ile)			(15.0-37.4)	
Broken Bow	OK	Oligotrophic	1.49			Veenstra & Nolen (1991)
Texoma	TX,OK	Eutrophic	1.69			
Birch	OK	Eutrophic	3.2			
Pine Creek	OK	Mesotrophic	3.39			
Pat Mayse	TX	Eutrophic	4.08			

The composite model performance statistics for the five stations (Sites 1, 2, 4, 6, 8) with phosphorus data show an RMS Error of 0.12 mg/L and a Relative RMS Error of 263% for Total Phosphorus (TP). The model results for TP are thus not as good as the defined model performance target of $\pm 50\%$ for nutrients. Model performance statistics for each station for TP, TOP and TPO4 are presented in **Appendix E**.

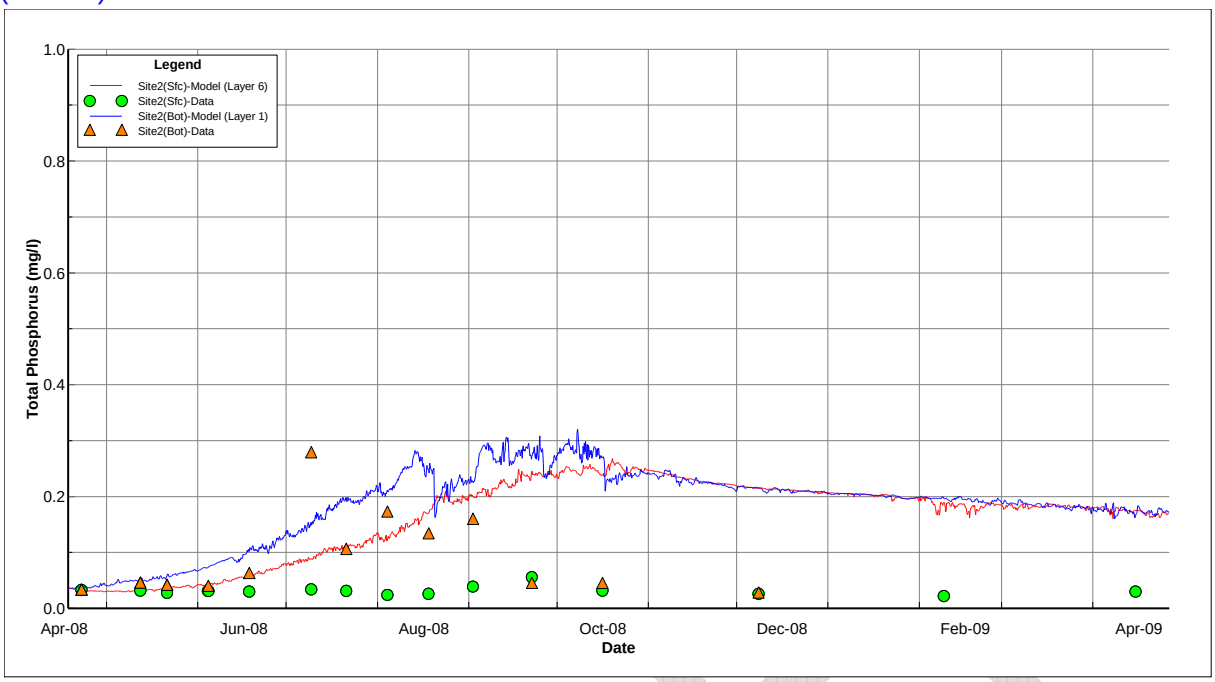

Figure 60 – Total Phosphorus (TP) calibration results in the lacustrine zone at Site 2

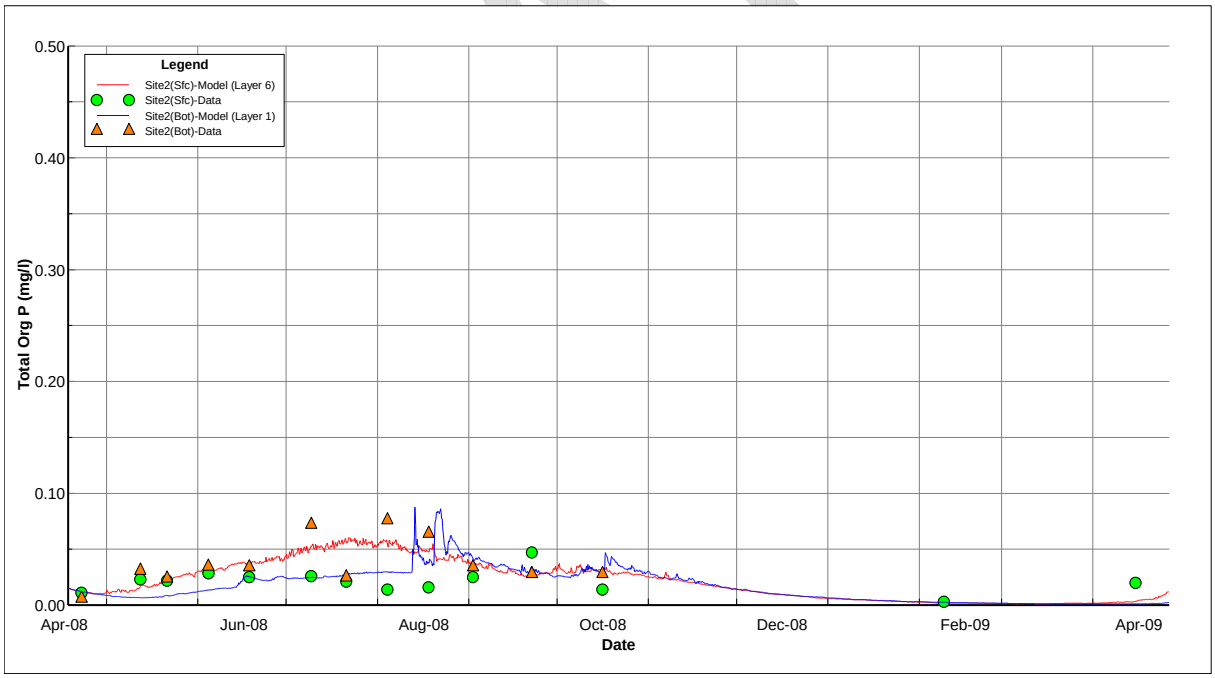

Figure 61 – Total Organic Phosphorus (TOP) calibration results in the lacustrine zone at Site 2

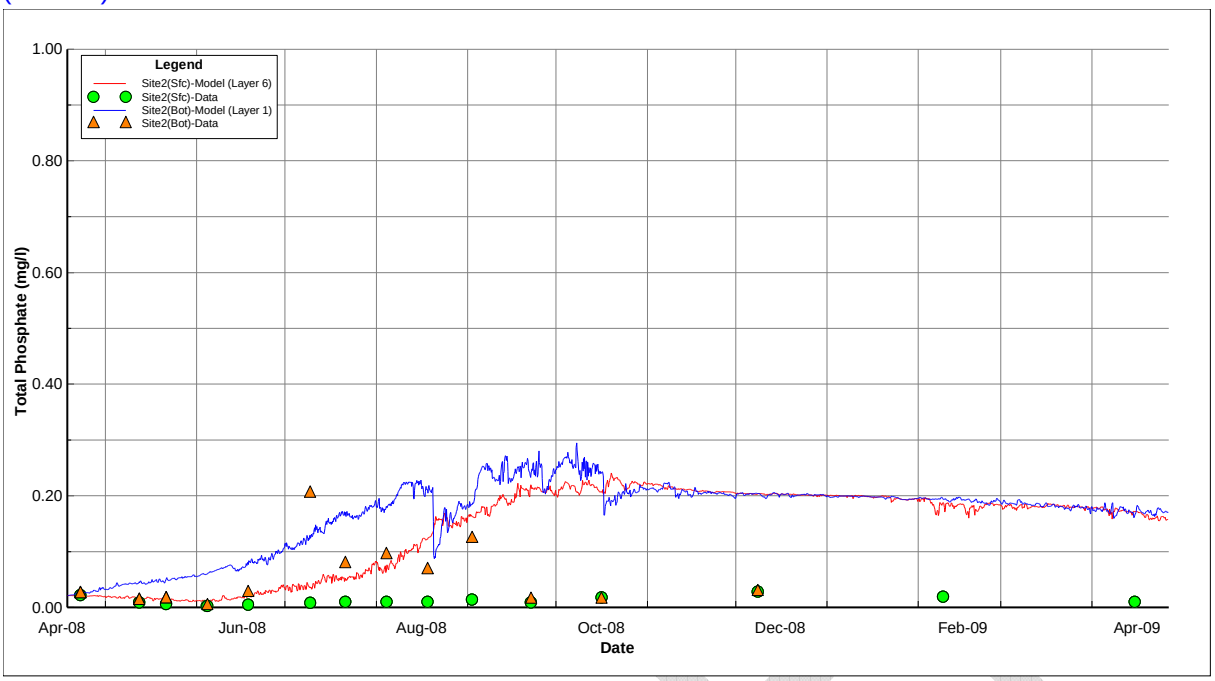

Figure 62 – Total Phosphate (TPO4) calibration results in the lacustrine zone at Site 2

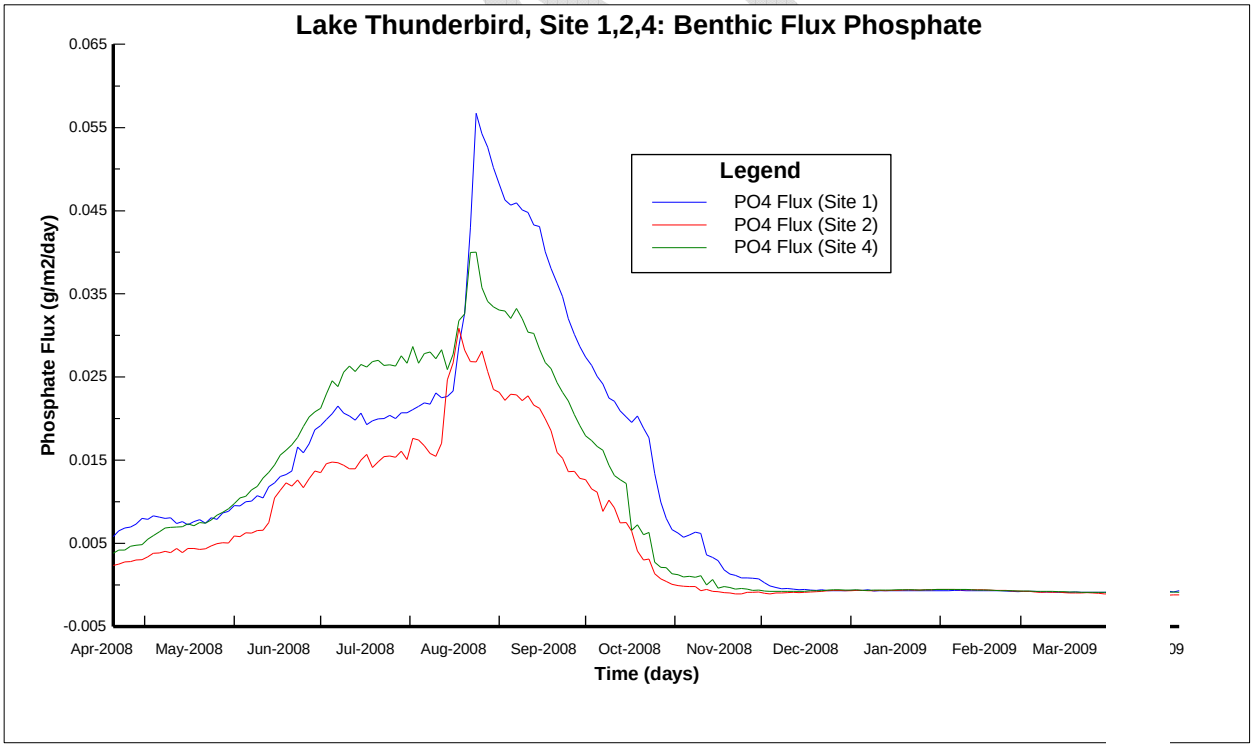

Figure 63 – Sediment flux of phosphate (PO4) calibration results in the lacustrine zone at Site 1, Site 2 and Site 4

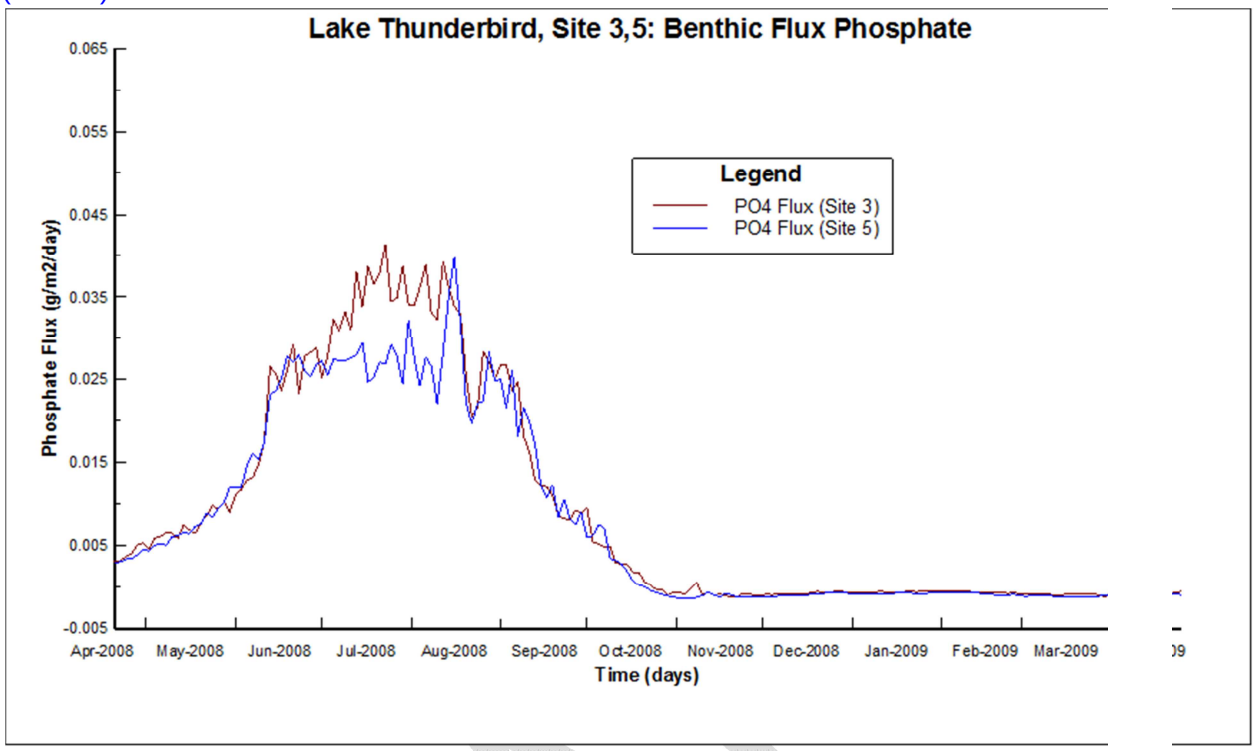

Figure 64 – Sediment flux of phosphate (PO4) (as g/m**2-day) calibration res in the transition zone at Site 3 and Site 5.

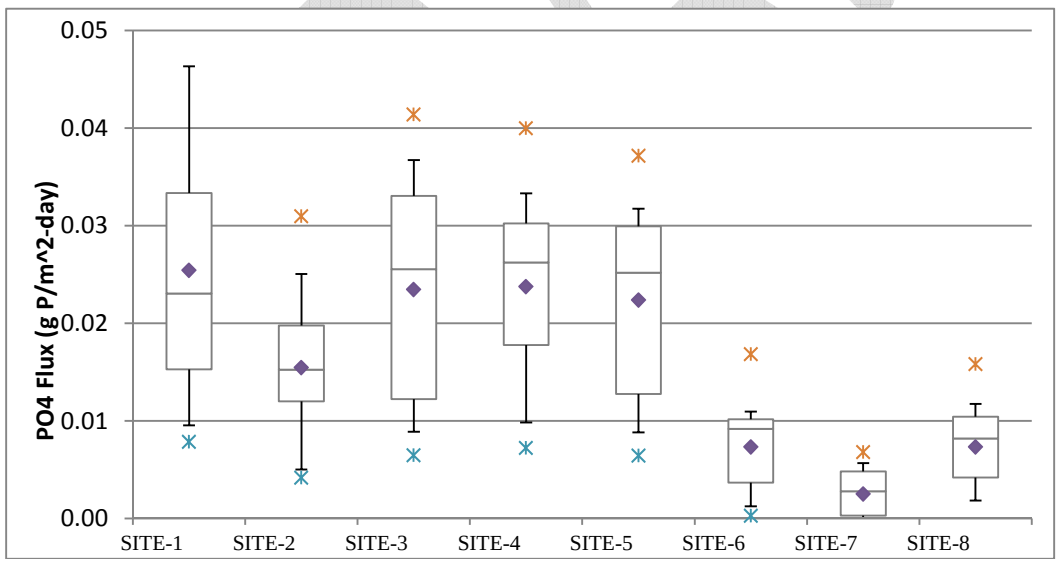

Figure 65 – Sediment flux of phosphate (PO4) (as g/m**2-day) calibration results in Lake Thunderbird across all station sites for stratified conditions (May 15-October 1, 2008). Line within the box represents the median; data point within the box marks mean; edges of the box represent the 25th and 75th percentiles; error bars represent the 10th and 90th percentiles; data points outside the box represent the minimum and maximum values.

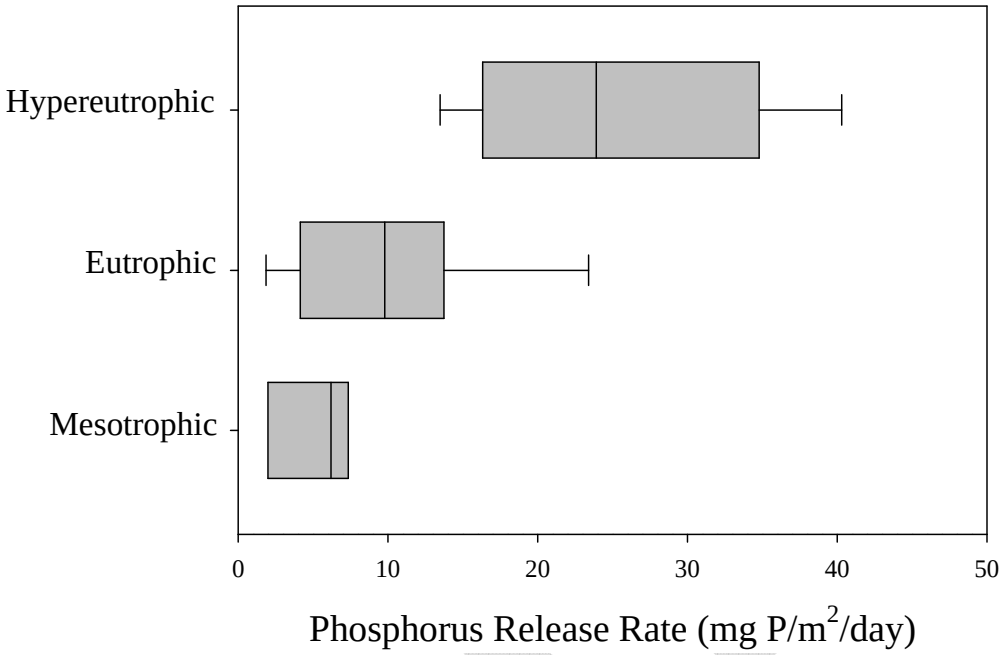

Figure 66 – Comparisons of anoxic release rates of phosphorus (as mg/m**2-day) from mesotrophic (n=3), eutrophic (n=9), and hypereutrophic (n=5) reservoirs in the Central Plains. Line within the box represents the median; edges of the box represent the 25th and 75th percentiles; error bars represent the 10th and 90th percentiles (Dzialowski and Carter, undated).

Section 5 LOAD ALLOCATIONS

5.1 Introduction and Methodology

The Oklahoma Department of Environmental Quality (ODEQ) will develop a TMDL or a watershed-based water quality management plan in lieu of a TMDL for Lake Thunderbird. An important component of the plan will be the identification of potential load reductions needed to control loading of nutrients, organic matter and sediments expected to attain compliance with water quality targets for restoration of Lake Thunderbird to its designated beneficial uses. The calibrated watershed-lake model developed for Lake Thunderbird will be used by ODEQ as a technically credible framework to (a) describe the water quality response within the lake to watershed loading and (b) develop a TMDL or a watershed-based water quality management plan for Lake Thunderbird.

The linked watershed and lake model framework, calibrated to data collected from April 2008 through April 2009 as described in Section 4 of this report, will be used by ODEQ to assess the effectiveness of load reduction scenarios needed to attain compliance with Oklahoma water quality standards and defined water quality targets for turbidity, chlorophyll-a and dissolved oxygen for Lake Thunderbird. The calibrated HSPF watershed runoff model and the EFDC hydrodynamic and water quality model of Lake Thunderbird will provide ODEQ with a scientifically defensible surface water model framework to support development of a TMDL or a water quality management plan for Lake Thunderbird.

The model framework is used to compile a mass-balance budget of TSS, nutrients and organic carbon to identify the magnitude of external controllable sources and internal uncontrollable sources of loading to the lake under the existing conditions of 2008-2009. External sources include tributary inputs, atmospheric deposition and nonpoint source runoff from the watershed. Internal sources include the benthic fluxes of nutrients across the sediment-water interface of the lake. External flow and loading of TSS, organic carbon and nutrients, generated by the HSPF watershed model, is linked for input to the EFDC lake model. Internal loading of inorganic nutrients is simulated with the sediment diagenesis model that is coupled with the water column water quality model.

The model framework is applied to simulate and evaluate the response of Lake Thunderbird to a series of systematic reductions in external loading of nutrients, sediment and organic carbon. Watershed loading rates are decreased for all tributaries and nonpoint source catchments by 95%, 85%, 75% and 50% to represent the overall reduction of external sources from the watershed into the lake. The water quality responses of the lake model to the changes in external loads are evaluated in terms of compliance with water quality criteria and targets for turbidity, chlorophyll-a and dissolved oxygen. The results of each reduction scenario are evaluated to identify the selected load allocation scenario that provides the best response for those water quality parameters -- oxygen, chlorophyll and turbidity – that have been identified as the cause of impairment for Lake Thunderbird. The selected load reduction scenario is then applied for a series of sequential restart runs to simulate initial conditions for the sediment flux model that represent a new quasi-equilibrium condition for the sediment bed in response to the reduction of external loads from the watershed.

Comparisons of the observed data, calibration results and the results for each load allocation scenario are presented in this section as box-whisker plots for turbidity, chlorophyll and oxygen. The box-whisker plots show the lake wide response to a load allocation scenario based on the

overall average of the summary statistics computed for each of the 8 sites. The 10th percentile value shown on a box plot, for example, is the arithmetic average of the 10th percentile values determined for each of the 8 monitoring sites. The box-whisker plots show the summary statistics computed from the observed data and the model results. Minimum and maximum values are shown as "outlier" data points plotted outside the tails of the box (* symbol). The lower and upper tails of the box show the 10th and 90th percentile values. The lower and upper horizontal lines of the box show the 25th and 75th percentile with the 50th percentile shown as the line through the box. The mean value is shown as a data point within the box. A complete set of box-whisker plots for turbidity, chlorophyll and oxygen is presented in **Appendix H** to show the response to each load allocation scenario across each of the eight monitoring sites under annual and seasonal conditions.

5.2 Mass Balance Budgets for Loads for Model Calibration

Using data developed for calibration of the watershed model and the lake model to 2008-2009 conditions, a mass-balance budget for TSS, nutrients and organic carbon is compiled to identify the magnitude of the external and internal sources of pollutant loading to the lake. External sources include tributary inputs, atmospheric deposition and nonpoint source runoff from the watershed. Internal sources include the benthic fluxes of ammonia, nitrate and phosphate across the sediment-water interface of the lake. **Table 17** presents a summary of the mass balance budget for existing 2008-2009 conditions for the HSPF watershed loads. **Table 18** presents a summary and comparison of the external and internal loading rates for the existing 2008-2009 conditions. Mass balance loading rates (as kg/day) are compiled for (a) annual loading from April 2008-April 2009 and (b) seasonal loading from May 15-October 1, 2008 when the water column is stratified and anoxia is observed in the hypolimnion during the summer months.

As can be seen from the data presented in the tables, internal loading of ammonia and phosphate accounts for over 90% of the total loading to the lake for both annual (91-94%) and seasonal (96%) time periods. The spatial distribution (by zone) of the sediment flux loads is presented in **Table 19** for the seasonal stratified period when the internal loading is greatest. Sediment flux data is presented in **Table 19** as the mass loading rate for each zone as kg/day and the sediment flux rate as mg/m**2-day for NH4, NO3 and PO4. Sediment oxygen demand is presented as g/m**2-day.

Table 17. Annual and Seasonal Loading from HSPF Watershed Model for Model Calibration

Model	Annual	Seasonal
Calibration	HSPF	HSPF
	kg/day	kg/day
TSS	70129.3	158872.0
TOC	2066.8	4248.6
TN	370.7	708.5
TP	68.1	113.6
NH4	8.0	14.1
NO3	41.6	75.2
PO4	19.7	19.9

Table 18. Comparison of Annual and Seasonal Loading from Watershed, Atmospheric Deposition and Sediment Flux of Inorganic Nutrients for Model Calibration

Model	Annual	Annual	Annual	Annual
Calibration	HSPF	AtmDep	SedFlux	Total
	kg/day	kg/day	kg/day	kg/day
NH4	8.0	9.2	290.4	307.6
NO3	41.6	15.8	107.2	164.6
PO4	19.7	1.1	209.8	230.6

Model	Annual	Annual	Annual	Annual
Calibration	HSPF	AtmDep	SedFlux	Total
	% Total	% Total	% Total	% Total
NH4	2.6%	3.0%	94.4%	100.0%
NO3	25.3%	9.6%	65.2%	100.0%
PO4	8.6%	0.5%	91.0%	100.0%

Model	Seasonal	Seasonal	Seasonal	Seasonal
Calibration	HSPF	AtmDep	SedFlux	Total
	kg/day	kg/day	kg/day	kg/day
NH4	14.1	13.0	677,85	704.94
NO3	75.2	21.3	367.54	464.03
PO4	19.9	1.5	543.81	565.16

Model	Seasonal	Seasonal	Seasonal	Seasonal
Calibration	HSPF	AtmDep	SedFlux	Total
	% Total	% Total	% Total	% Total
NH4	2.0%	1.8%	96.2%	100.0%
NO3	16.2%	4.6%	79.2%	100.0%
PO4	3.5%	0.3%	96.2%	100.0%

Table 19. Spatial Distribution of Sediment Flux Loading for Seasonal Stratified Period for Model Calibration

Model		NH4	NO3	SOD	PO4
Calibration		kg/day	kg/day	kg/day	kg/day
Zone-1	stream	14.8	21.9	1860.9	11.4
Zone-2	riverine	61.6	37.6	835.2	21.0
Zone-3	transition	158.5	69.3	7782.7	110.0
Zone-4	lake	105.1	66.3	7539.2	138.9
Zone-5	riverine	18.1	17.8	1160.5	3.8
Zone-6	hdw	-2.5	0.5	276.2	3.4
Zone-7	lake	152.7	44.3	7808.5	136.1
Zone-8	lake	31.7	21.7	1924.1	34.6
Zone-9	transition	56.2	27.3	5278.5	54.5
Zone-10	riverine	81.8	60.8	1436.9	30.0
TOTAL	Total Lake	677.9	367.5	35902.6	543.8

Model		NH4	NO3	SOD	PO4
Calibration		mg/m2-d	mg/m2-day	g/m2-d	mg/m2-d
Zone-1	stream	4.60	6.81	0.57	3.53
Zone-2	riverine	19.41	11.86	0.26	6.61
Zone-3	transition	29.16	12.75	1.43	20.24
Zone-4	lake	17.95	11.32	1.28	23.72
Zone-5	riverine	11.22	11.03	0.72	2.39
Zone-6	hdw	-1.26	0.28	0.14	1.71
Zone-7	lake	37.47	10.88	1.91	33.41
Zone-8	lake	16.02	11.00	0.97	17.52
Zone-9	transition	24.99	12.14	2.34	24.25
Zone-10	riverine	19.35	14.37	0.34	7.11
TOTAL	Total Lake	20.05	10.87	1.06	16.09

5.3 Turbidity

Figure 67 presents a comparison of observed turbidity, model calibration results and the response of turbidity for each load allocation scenario over the whole lake. The box-whisker plots show the lake wide response based on the overall averages of the summary statistics computed for each of the 8 sites for each load allocation scenario. The 90th percentile value shown on a box plot, for example, is the arithmetic average of the 90th percentile values determined for each of the 8 monitoring sites. The response for turbidity is directly proportional to the removal of TSS from the watershed loading. The water quality criteria of 25 NTU,

compared to the 90th percentile of the model results, is satisfied for the 95%, 85% and 75% removal scenarios.

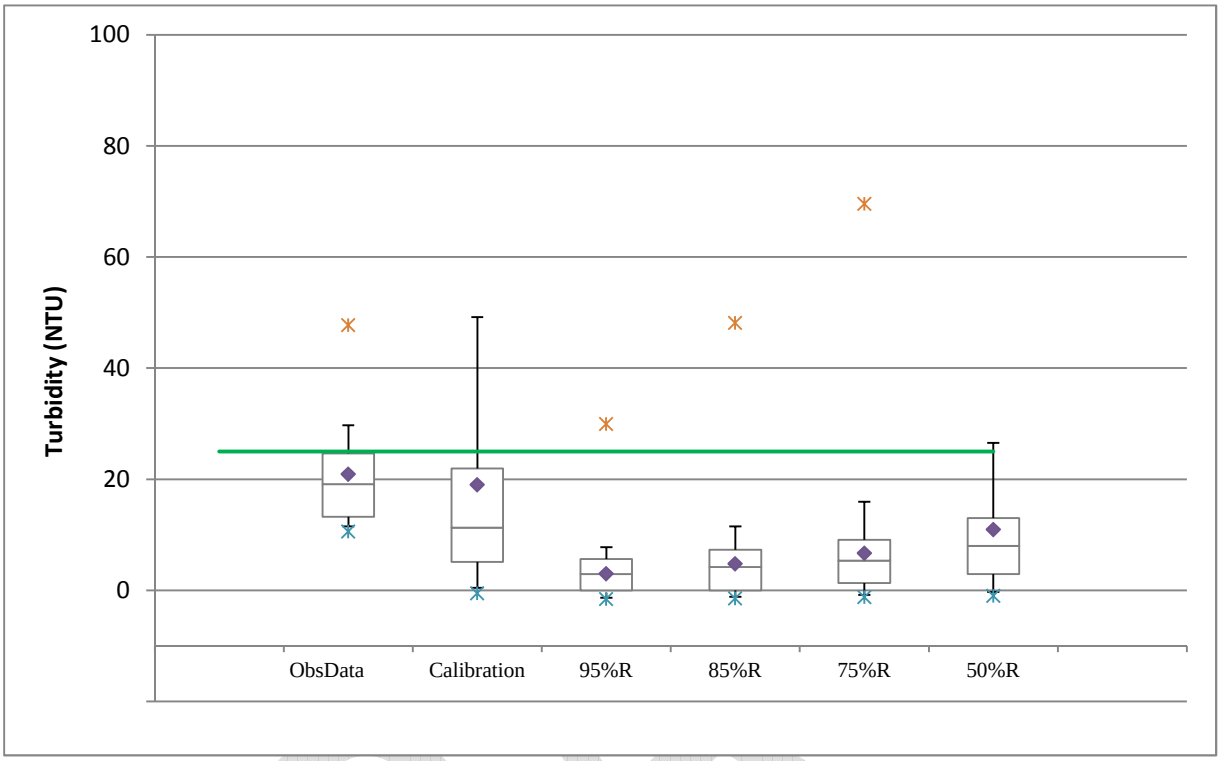

Figure 67 – Box-whisker plot comparison of observed data, calibration results and turbidity response to load allocation scenarios for 95%, 85%, 75% and 50% reduction of watershed loads for surface layer and annual condition. Boxplots show averages of statistics for all 8 Sites.

5.4 Chlorophyll a

Figure 68 presents a comparison of observed chlorophyll, model calibration results and the response of chlorophyll for each load allocation scenario over the whole lake. The box-whisker plots show the lake wide response based on the overall averages of the summary statistics computed for each of the 8 sites for each load allocation scenario. The mean value shown on a box plot, for example, is the arithmetic average of the mean values determined for each of the 8 monitoring sites.The response for chlorophyll is related to the removal of TSS and nutrients from watershed loading via improvements in water clarity, decreases in water column nutrient levels and changes in the sediment flux rates for nutrients. The water quality criteria of 10 ug/L, compared to the average of the model results, fails to be achieved for the 95%, 85%, 75% and 50% removal scenarios. Algae production and biomass is controlled by both light availability and nutrient availability. The largest reduction of TSS for the 95% scenario improves water clarity so that the response for algal productivity is greatest for this scenario. As will be shown for the analysis of the spin up runs, the sediment flux of nutrients, reduced by only a small amount for each of the load allocation scenarios, provides a sufficient nutrient supply to sustain algal production even with reductions in nutrient loads from the watershed. As shown with the

mass balance comparison of loads from the watershed and sediment bed, the sediment bed accounts for most of the nutrient loading to the lake.

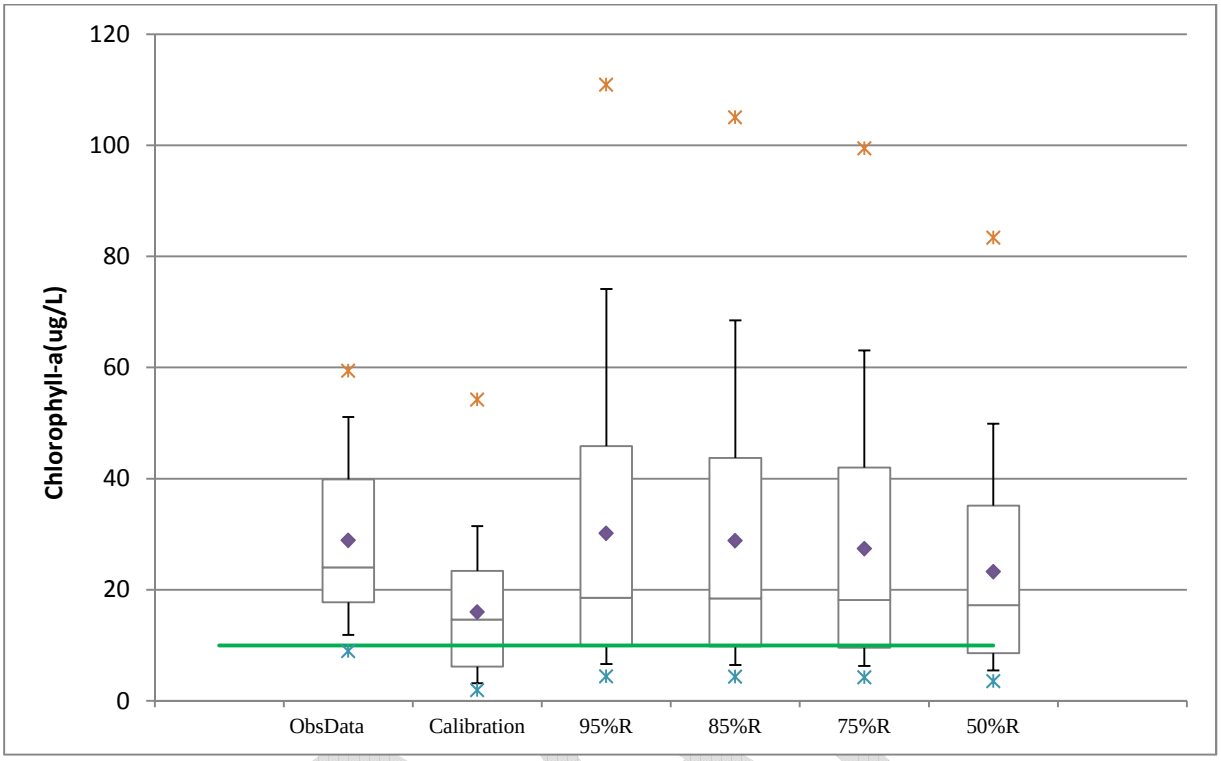

Figure 68 – Box-whisker plot comparison of observed data, calibration results and chlorophyll response to load allocation scenarios for 95%, 85%, 75% and 50% reduction of watershed loads for surface layer and annual condition. Boxplots show averages of statistics for all 8 Sites.

5.5 Dissolved Oxygen

Figure 69 and **Figure 70** presents a comparison of observed oxygen, model calibration results and the response of oxygen in the surface layer and bottom layer for each load allocation scenario for seasonal stratified conditions over the whole lake. The box-whisker plots show the lake wide response based on the overall averages of the summary statistics computed for each of the 8 sites for each load allocation scenario. The 10th percentile value shown on a box plot, for example, is the arithmetic average of the 10th percentile values determined for each of the 8 monitoring sites. As shown in the box-whisker plots for both the surface and bottom layer, the response of oxygen to each load allocation scenario represents a negligible change from the calibration results. For the surface layer, however, the water quality criteria of 5 mg/L, compared to the 10th percentile of the model results, is achieved for the 95%, 85%, 75% and 50% removal scenarios. In the bottom layer, the 10th percentile of the model results are less than 2 mg/L for the 95%, 85%, 75% and 50% removal scenarios. Oklahoma water quality criteria define a reservoir as fully supporting if less than 50% of the volume of the lake is less than 2 mg/L during the period of seasonal stratification. The waterbody is non-supporting, however, if more than 50% of the lake volume is less than 2 mg/L. Dissolved oxygen results of the lake model are post-processed with EFDC_Explorer to display a time series of the percentage of the entire lake

volume that is less than 2 mg/L for comparison to the Oklahoma water quality target of 50% for full-support of beneficial uses. Model results are shown as the anoxic volume percentage of the entire lake for model calibration (Figure71) and the load reduction scenarios for 95% (Figure 72),85% (Figure 73),75% (Figure 74) and 50% (Figure 75). As shown in the time series plot for model calibration (Figure 71), the anoxic volume of the lake during seasonal stratification (May 15-October 1) increases from ~5% in mid-May to a peak of ~35-40% during July through mid-August 2008. The two storm events in August 2008 breakup water column stratification and reduce the anoxic volume of the lake to ~5% until stratification is reestablished in late August and the anoxic volume increases to a high of ~30% in early September.

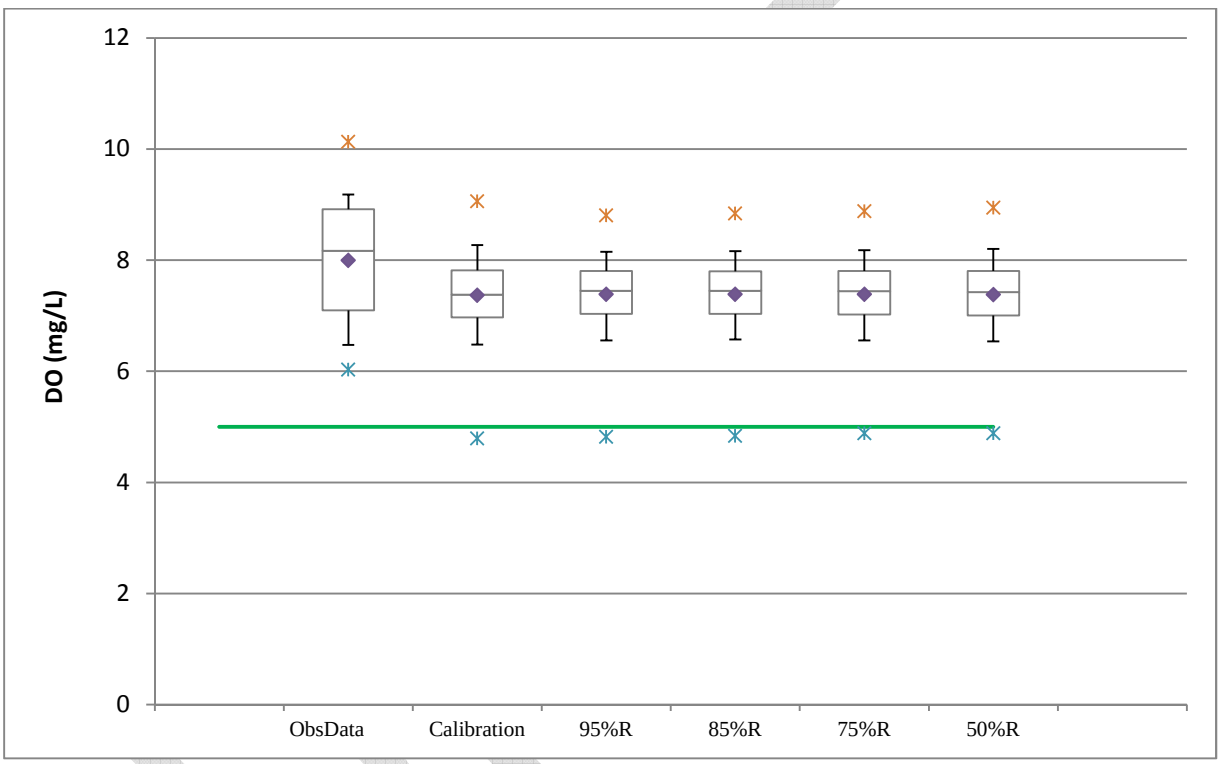

Figure 69 – Box-whisker plot comparison of observed data, calibration results and dissolved oxygen response to load allocation scenarios for 95%, 85%, 75% and 50% reduction of watershed loads for surface layer and seasonal stratified condition. Boxplots show averages of statistics for all 8 Sites.

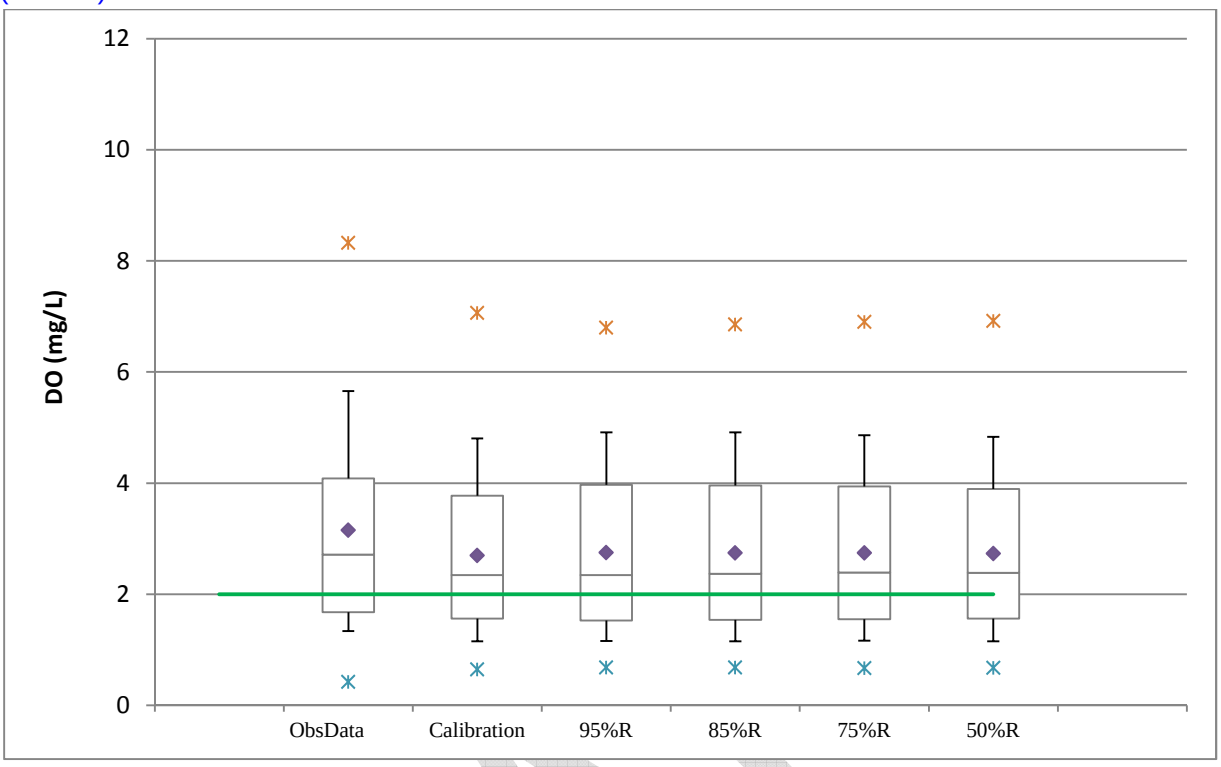

Figure 70 – Box-whisker plot comparison of observed data, calibration results and dissolved oxygen response to load allocation scenarios for 95%, 85%, 75% and 50% reduction of watershed loads for bottom layer and seasonal stratified condition. Boxplots show averages of statistics for all 8 Sites.

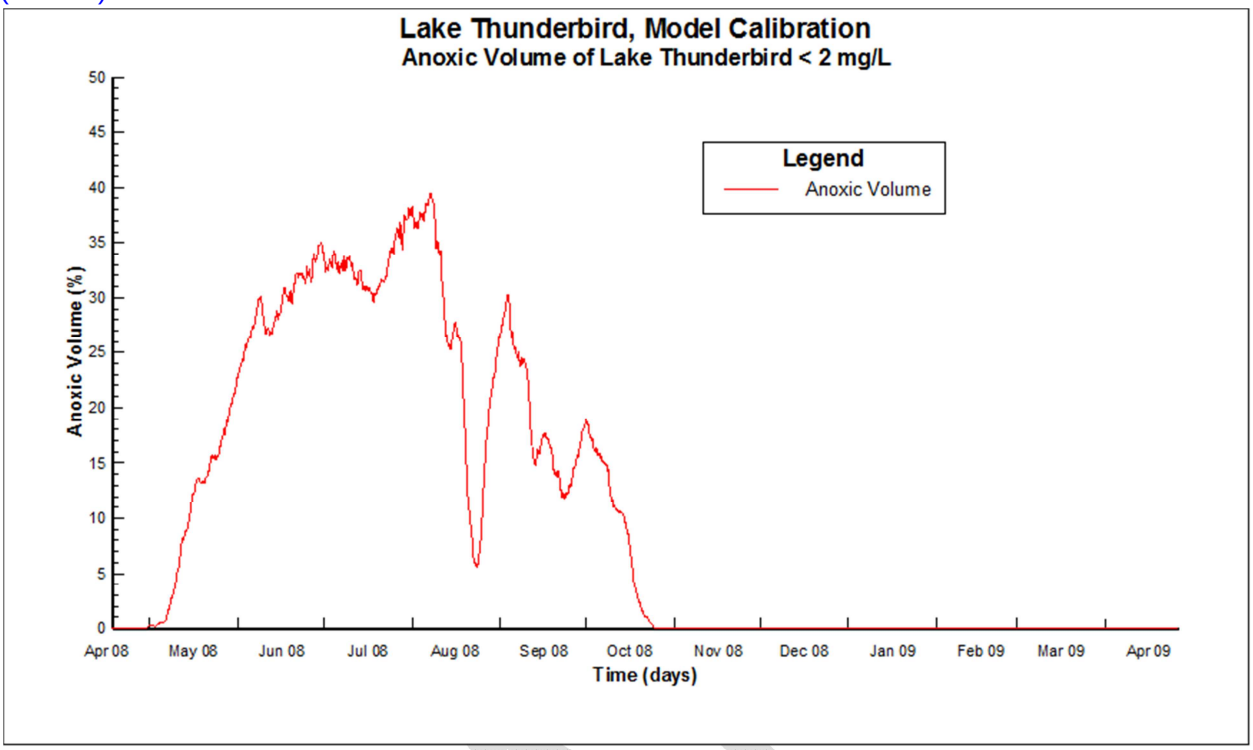

Figure 71 – Time series of anoxic volume of Lake Thunderbird for model calibration.

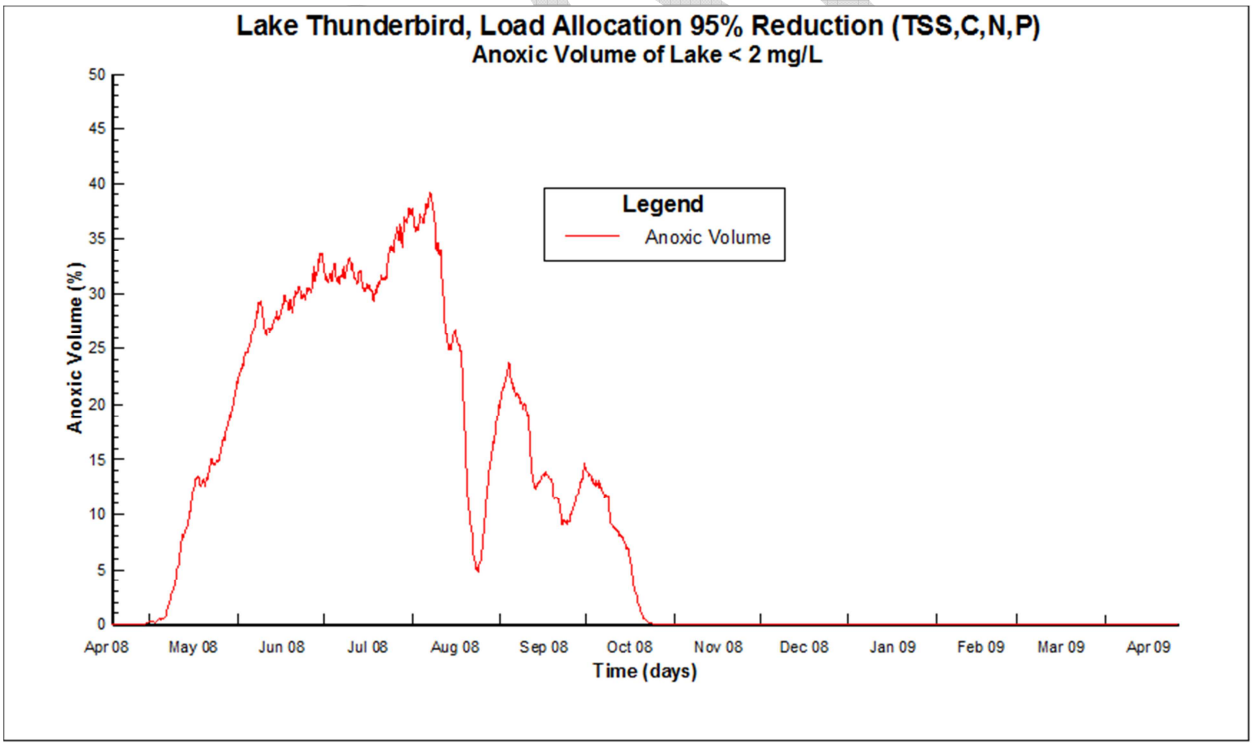

Figure 72 – Time series of anoxic volume of Lake Thunderbird for 95% removal load reduction scenario.

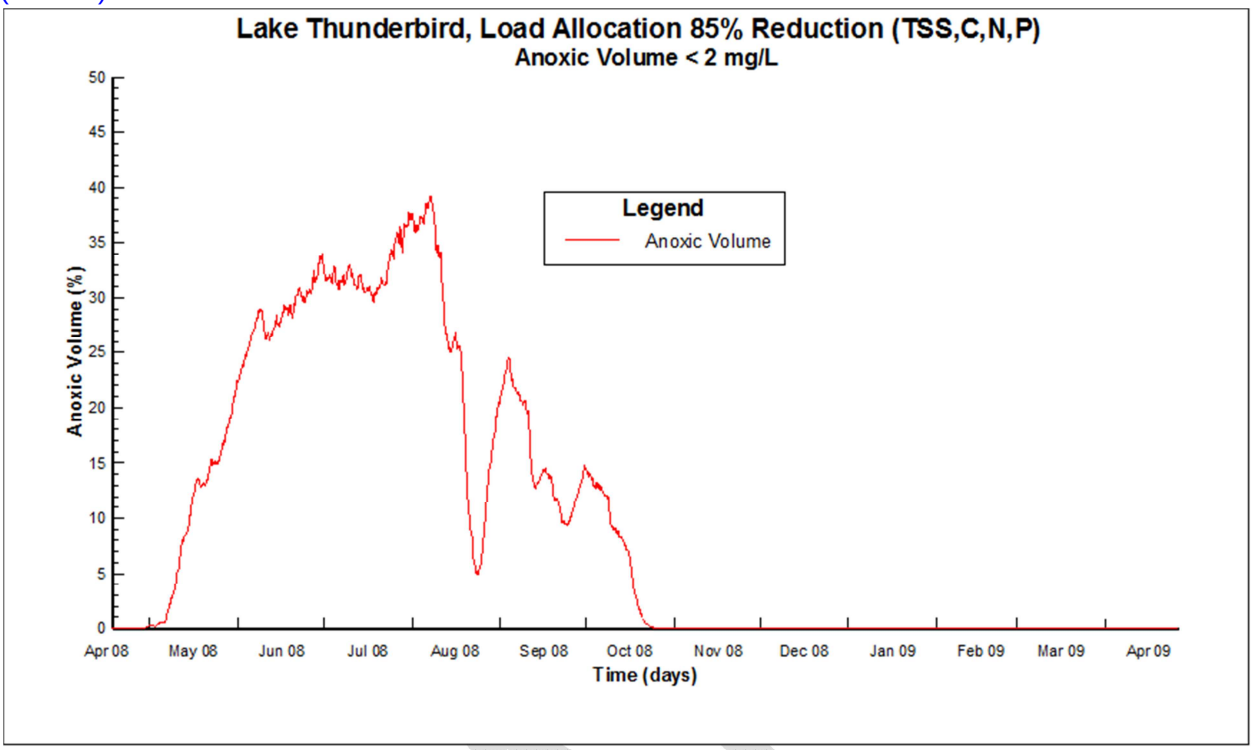

Figure 73 – Time series of anoxic volume of Lake Thunderbird for 85% removal load reduction scenario.

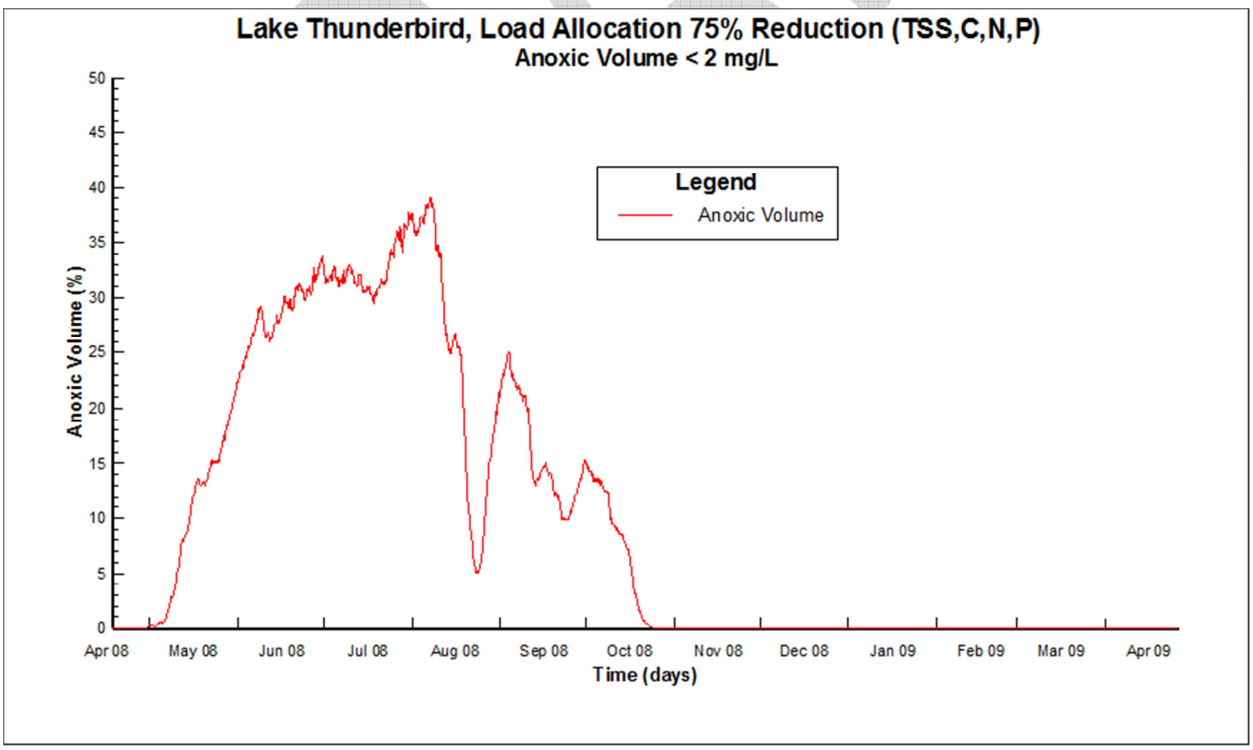

Figure 74 – Time series of anoxic volume of Lake Thunderbird for 75% removal load reduction scenario.

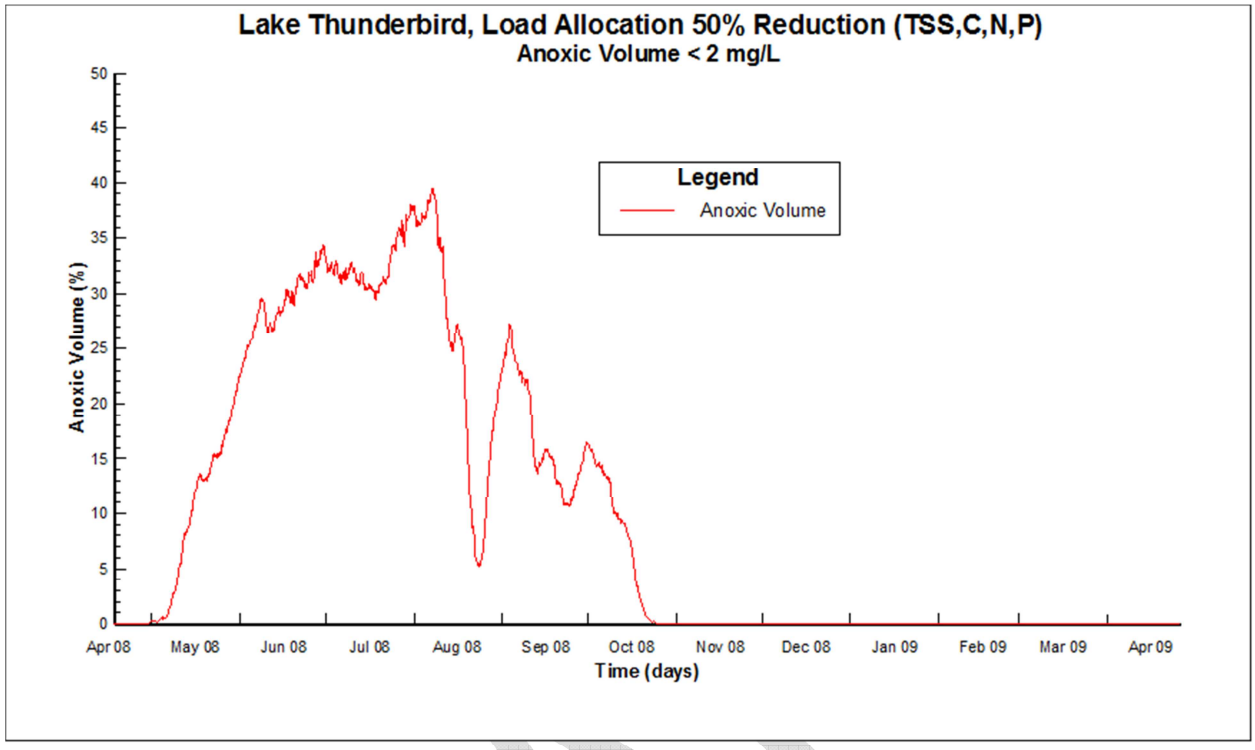

Figure 75 – Time series of anoxic volume of Lake Thunderbird for 50% removal load reduction scenario.

5.6 Sediment Diagenesis Model Spinup of Load Allocation Scenario

Based on an evaluation of the results simulated for each reduction scenario, the 75% removal scenario is selected as the load allocation scenario that provides the best response for chlorophyll and turbidity. As shown in **Figure 67**, water quality criteria for turbidity is expected to be achieved for the 95%, 85% and 75% removal scenarios. The model response for chlorophyll (**Figure 68**), although failing to meet the water quality target of 10 ug/L, is, however, seen to progressively diminish from the 95% to the 50% removal scenario because of increased light limitation for algal production from the smaller reduction of sediment from watershed loading.

The 75% removal load reduction scenario is applied for a series of 5 sequential restart runs to determine the (a) “spin-up” time needed for the sediment flux model to attain a new quasi-equilibrium condition within the sediment bed in response to the reduction of external loads from the watershed; (b) effect of the new internal nutrient loads from the sediment bed on water quality; and (c) changes to the sediment-water flux of nutrients. Since model calibration is defined by the 1 year period from April 2008 to April 2009, the results of the 6 sequential “spin-up” runs with the selected load allocation scenario are reported as Year 0, 1, 2, 3, 4, 5, and 6. Based on simulation of the final 75% removal load allocation scenario (for Year 6) where the results of the Year 5 “spin-up” run are used to assign the initial conditions for the water quality model and the sediment diagenesis model, a mass-balance budget of TSS, nutrients and organic carbon is compiled to determine the magnitude of external controllable sources and

internal uncontrollable sources of loading to the lake under the projected conditions for the 75% removal load allocation scenario.

A comparison of the observed data, calibration results and the results for the spin-up runs for Year 0-6 is presented in this section as box-whisker plots for turbidity (Figure 76), chlorophyll (Figure 77) and oxygen (Figure 78 and 79). The box-whisker plots show the lake wide response based on the overall average of the summary statistics computed for each of the 8 sites. The 10^{th} percentile value shown on a box plot, for example, is the arithmetic average of the 10^{th} percentile values determined for each of the 8 monitoring sites. The box-whisker plots show the summary statistics computed from the observed data and the model results. Minimum and maximum values are shown as "outlier" data points plotted outside the tails of the box (* symbol). The lower and upper tails of the box show the 10^{th} and 90^{th} percentile values. The lower and upper horizontal lines of the box show the 25^{th} and 75^{th} percentile with the 50^{th} percentile shown as the line through the box. The mean value is shown as a data point within the box. The spin-up response for benthic phosphate flux (Figure 80) and sediment oxygen demand (Figure 81) is also presented for comparison to the calibration results for the lake-wide averages of all 8 sites. A complete set of box-whisker plots for turbidity, chlorophyll, oxygen and sediment flux results is presented in **Appendix I** to show the whole lake spin-up response for Year 0-6 for the selected 75% load reduction scenario.

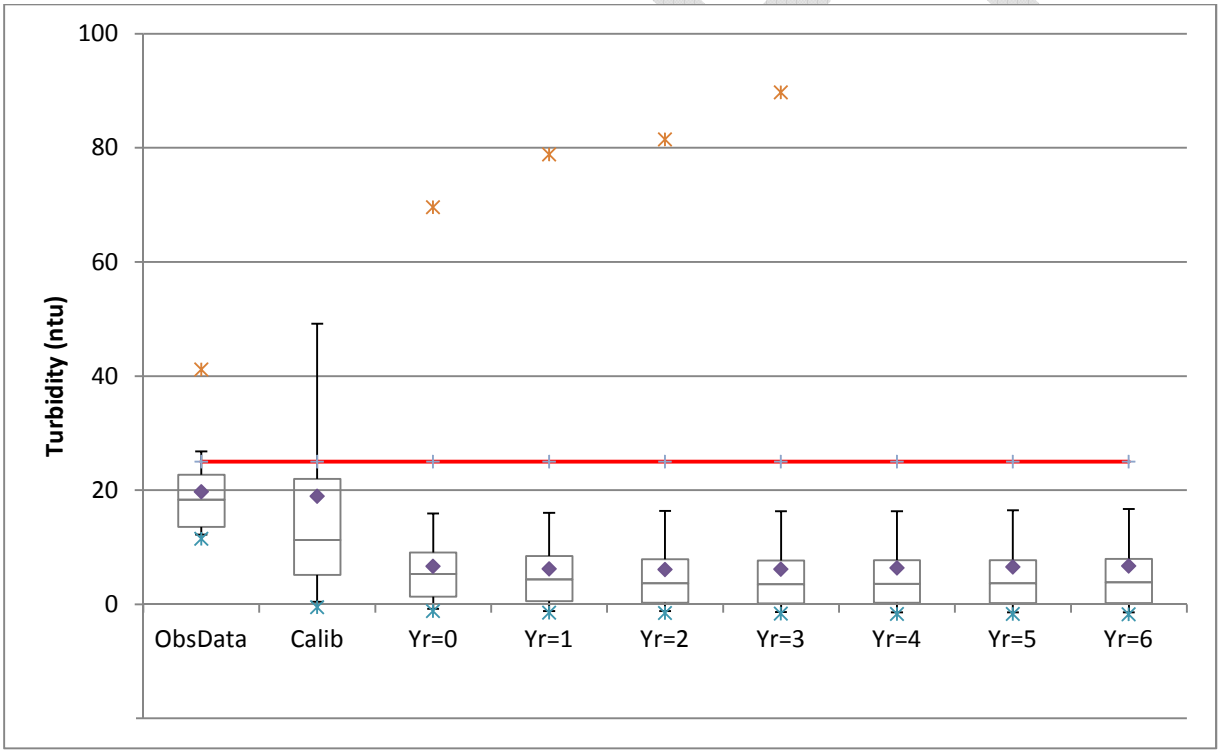

Figure 76 – Box-whisker plot comparison of observed data, calibration results and turbidity response for spin up runs for Year 0-6 for 75% reduction of watershed loads for surface layer and annual conditions. Boxplots show averages of statistics for all 8 Sites.

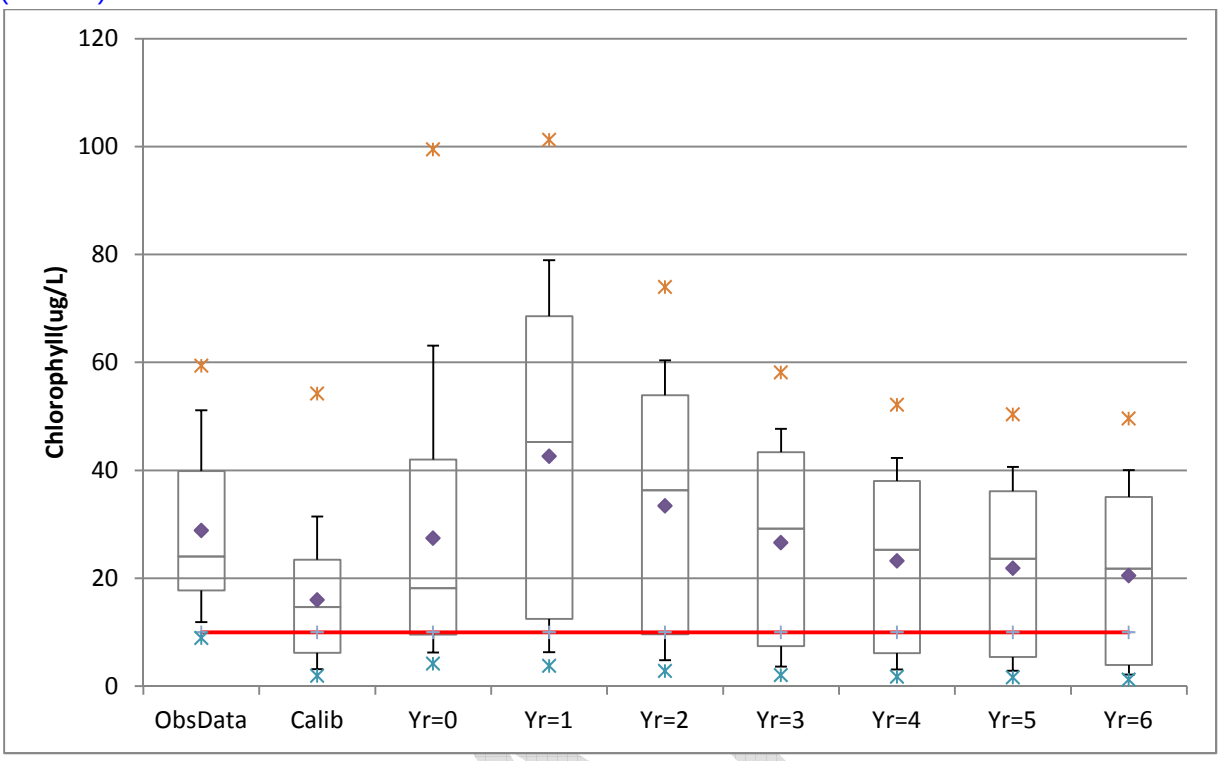

Figure 77 – Box-whisker plot comparison of observed data, calibration results and chlorophyll response for spin up runs for Year 0-6 for 75% reduction of watershed loads for surface layer and annual conditions. Boxplots show averages of statistics for all 8 Sites.

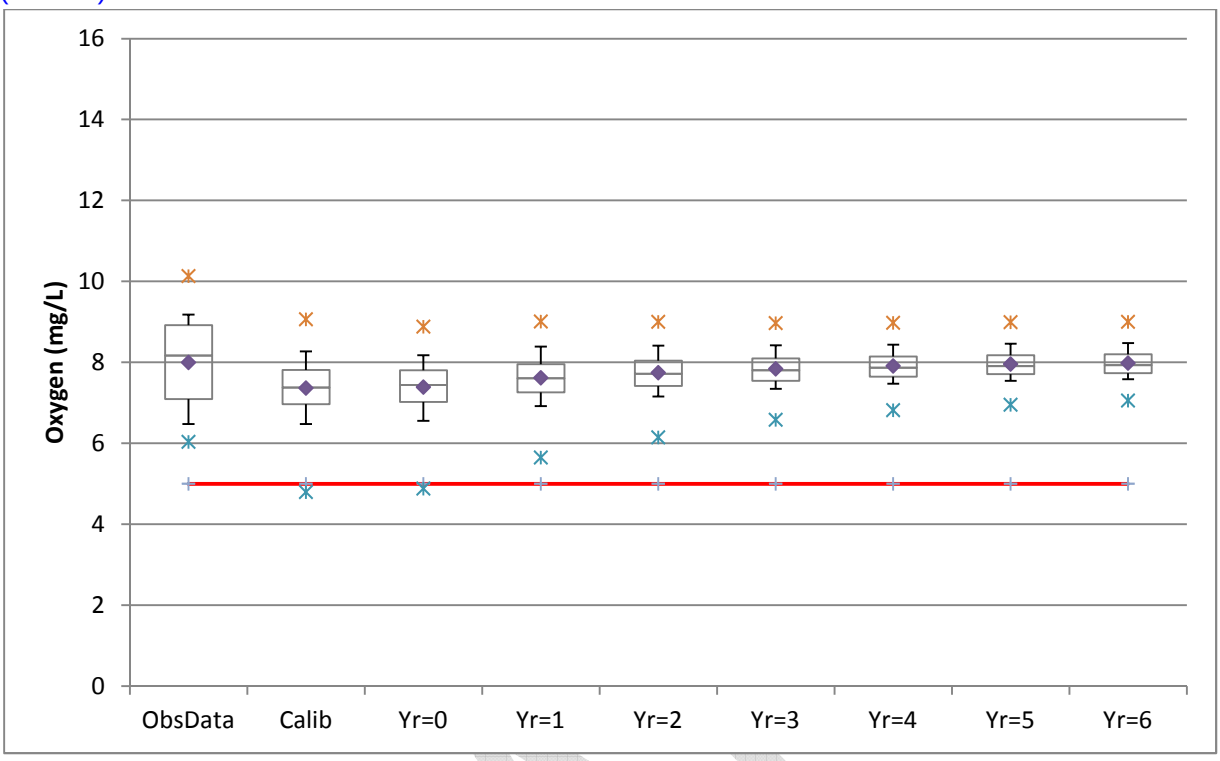

Figure 78 – Box-whisker plot comparison of observed data, calibration results and dissolved oxygen response for spin up runs for Year 0-6 for 75% reduction of watershed loads for surface layer and seasonal stratified conditions. Boxplots show averages of statistics for all 8 Sites.

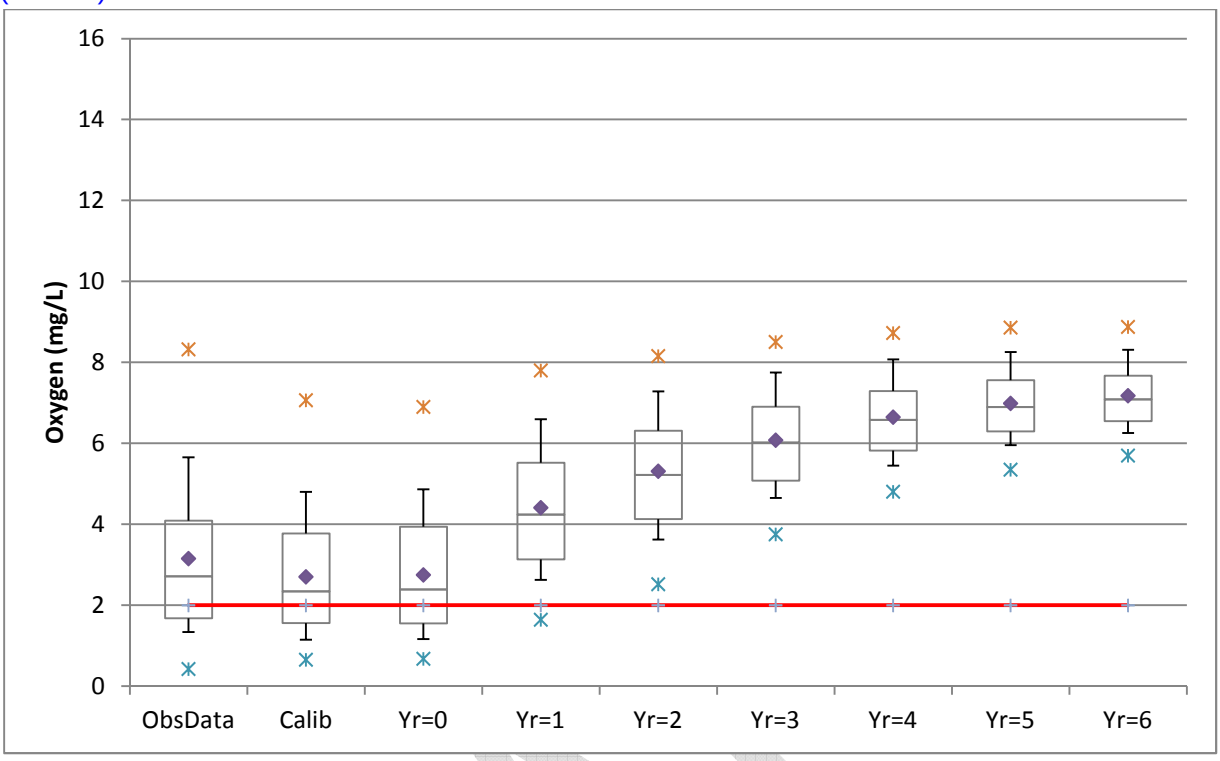

Figure 79 – Box-whisker plot comparison of observed data, calibration results and dissolved oxygen response for spin up runs for Year 0-6 for 75% reduction of watershed loads for bottom layer and seasonal stratified conditions. Boxplots show averages of statistics for all 8 Sites.

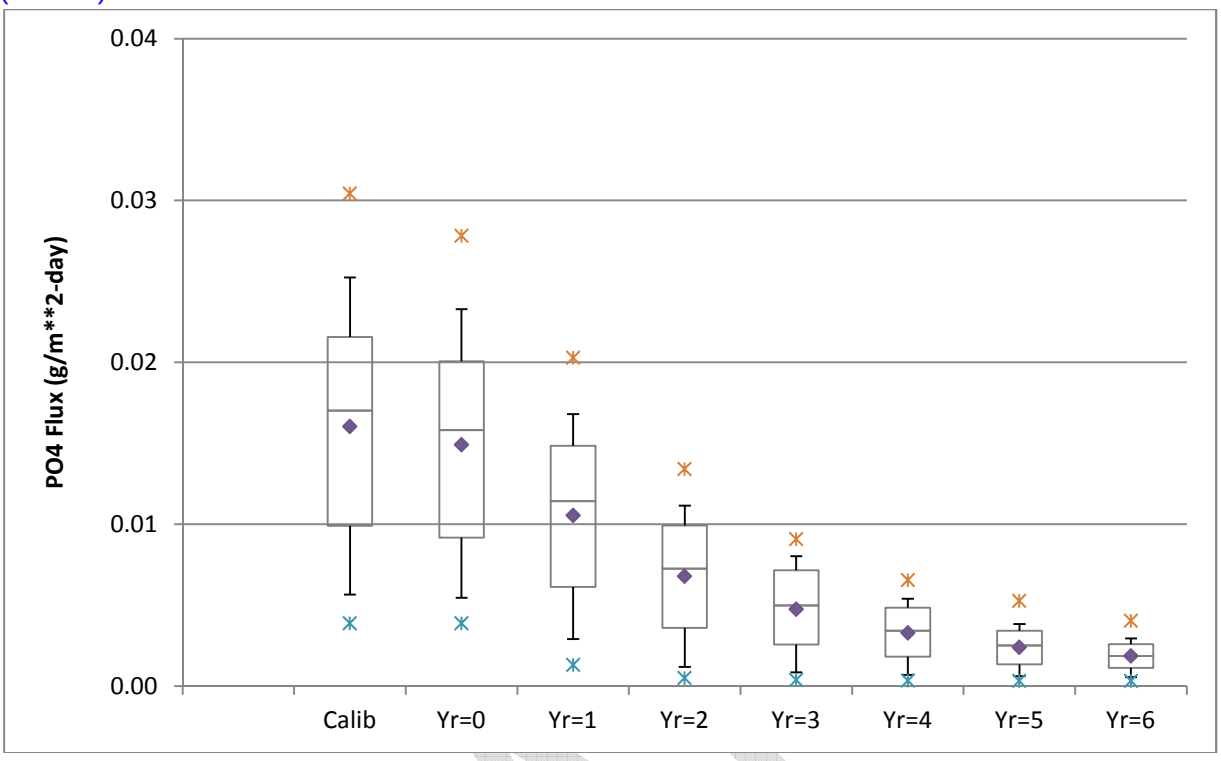

Figure 80 – Box-whisker plot comparison of benthic phosphate flux calibration results and response for spin up runs for Year 0-6 for 75% reduction of watershed loads for seasonal stratified conditions. Boxplots show averages of statistics for all 8 Sites.

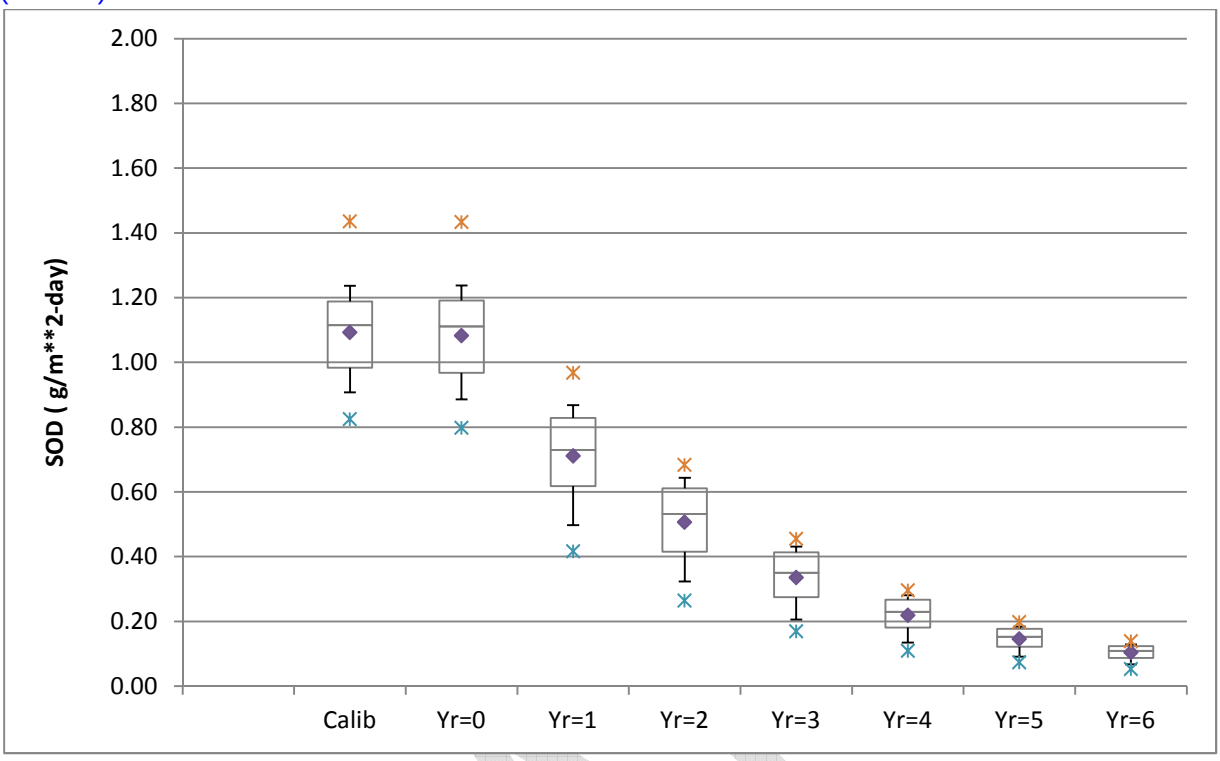

Figure 81 – Box-whisker plot comparison of sediment oxygen demand calibration results and response for spin up runs for Year 0-6 for 75% reduction of watershed loads for seasonal stratified conditions. Boxplots show averages of statistics for all 8 Sites.

5.7 Mass Balance Budget for Loads for 75% Removal Scenario

Using data developed for 75% removal of TSS, nutrients and organic carbon from the watershed model and the spin-up response of the lake model to the 75% removal load scenario, a mass-balance budget for TSS, nutrients and organic carbon is compiled for the projected external and internal sources of loading to the lake. **Table 20** presents a summary of the mass balance budget for the 75% removal scenario for the HSPF watershed loads. Table 21 presents a summary and comparison of the external and internal loading rates for the 75% removal scenario. Mass balance loading rates (as kg/day) are compiled for (a) annual loading and (b) seasonal loading from May 15-October 1 when the water column is stratified and anoxia is observed in the hypolimnion during the summer months.

The results of the spin-up run for the 75% removal scenario indicates that ammonia and nitrate may be lost from the water column to the sediment bed under the new quasi-equilibrium conditions for the sediment bed. A negative sediment flux load represents a loss from the water column (Table 21). Internal loading of phosphate, still accounting for ~79-90% of the total loading to the lake for both annual (79%) and seasonal (90%) time periods, is greatly reduced from the calibration conditions for existing loading shown in Table 18. Overall for the entire lake, the seasonally stratified benthic flux rate for phosphate is reduced from 16.1 mg/m**2-day for the calibration conditions (Table 19) to 1.66 mg/m**2-day under the 75% removal scenario with spin-up of the sediment flux model (Table 22). For Zone 7 where Site 1 is located, the benthic phosphate flux (**Figure 80**) is reduced by more than a factor of 10 from 33.4 mg/m**2-day

(Table 19) for model calibration to 2.48 mg/m**2-day for the 75% removal scenario. Sediment oxygen demand in Zone 7 (Site 1) (**Figure 81**) is seen to be reduced from 1.91 g/m**2-day for the calibration condition (Table 19) to 0.09 g/m**2-day for the 75% removal scenario (Table 22).

Table 20. Annual and Seasonal Loading from HSPF Watershed Model for 75% Removal Scenario (515_75R_S6)

Model	Annual	Seasonal
75%R	HSPF	HSPF
515_75R_S6	kg/day	kg/day
TSS	17532.33	39718.00
TOC	516.70	1062.15
TN	92.68	177.14
TP	17.02	28.40
NH4	1.99	3.52
NO3	10.40	18.79
PO4	4.93	4.98

Table 21. Comparison of Annual and Seasonal Loading from Watershed, Atmospheric Deposition and Sediment Flux of Inorganic Nutrients for 75% Removal Scenario (515_75R_S6)

Model	Annual	Annual	Annual	Annual
75%R	HSPF	AtmDep	SedFlux	Total
515_75R_S6	kg/day	kg/day	kg/day	kg/day
NH4	2.0	9.2	-4.1	0.0
NO3	10.4	15.8	-4.0	0.0
PO4	4.9	1.1	22.7	28.7
Model	Seasonal	Seasonal	Seasonal	Seasonal
75%R	HSPF	AtmDep	SedFlux	Total
515_75R_S6	kg/day	kg/day	kg/day	kg/day
NH4	3.5	13.0	-9.2	0.0
NO3	18.8	21.3	-5.4	0.0
PO4	5.0	1.5	56.0	62.4

Table 22. Annual and Seasonal Projected Sediment Flux Rates for Nutrients and Oxygen for 75% Removal Scenario (515_75R_S6) for Total Lake and Zone 7(Site 1)

	Total	**Zone-7**	**Total**	**Zone-7**	
75% R	**Lake**	**Site-1**	**Lake**	**Site-1**	**SedFlux**
515_75R_S6	**Annual**	**Annual**	**Seasonal**	**Seasonal**	**Units**
NH4	-0.12	-0.25	-0.27	-0.56	mg/m2-day
NO3	-0.12	-0.30	-0.16	-0.47	mg/m2-day
SOD	0.05	0.12	0.09	0.23	g/m2-day
PO4	0.67	0.67	1.66	2.48	mg/m2-day

5.8 Summary

Based on an evaluation of the results simulated for the 95%, 85%, 75% and 50% load reduction scenario, the 75% removal scenario is selected as the load allocation scenario that provides the best response for chlorophyll and turbidity. The 75% removal load reduction scenario was applied for a series of sequential restart runs to simulate the effect of the change in watershed loading on internal nutrient loads from the sediment bed and the response of lake water quality to the changes in sediment-water flux of nutrients and dissolved oxygen. The spin-up results with the model demonstrate a gradual reduction in internal sediment flux loading of nutrients and a significant improvement in water quality conditions under the final 75% removal scenario simulation. The results of the spin-up analysis suggest that compliance with water quality criteria for turbidity and dissolved oxygen may be achieved with 75% removal of TSS, organic matter and nutrients from external watershed loading to the lake. The results for the 75% load reduction indicate that the overall annual average 90^{th} percentile value of 16.7 NTU for turbidity for all 8 stations will be in compliance with the 25 NTU criteria for turbidity. The results also indicate that the overall average 10^{th} percentile concentration of 7.6 mg/L for surface dissolved oxygen for all 8 stations will be in compliance with the 5 mg/L criteria for surface oxygen under stratified conditions. In addition to compliance with the surface layer criteria for oxygen, the model results for the 75% load reduction scenario indicate that the overall hypoxic volume of the lake, defined by a cutoff level of 2 mg/L, is less than 50% during summer stratification. The results for the 75% load allocation indicate that the overall annual average chlorophyll for the 8 station locations (20.5 ug/L), however, exceeds the water quality target of 10 ug/L.The simulation results for the spin-up runs of the 75% removal scenario should not be taken as projections of future water quality conditions in the lake with absolute certainty. The simulation model, does however, provide ODEQ with a technically credible model framework that clearly shows that water quality improvements can be achieved in Lake Thunderbird to support the desired beneficial uses if watershed loading can be controlled to a level based on 75% reduction of the existing loading conditions.

In addition to the application of the model framework for the determination of the selected load allocation scenario, the calibrated lake model can also be applied as a tool to support evaluations of the potential water quality impact of in-lake remediation strategies. Hypolimnetic oxygen injection, designed to decrease phosphorus release from the sediment bed under stratified conditions to control algae production, is one in-lake remediation strategy that has been tested experimentally, and is being considered for operational use in Lake Thunderbird (OWRB, 2011).

Section 6 SUMMARY AND RECOMMENDATIONS

6.1 Summary

Lake Thunderbird is a 6,070-acre reservoir lake located in Cleveland County, Oklahoma within the Little River drainage basin. The lake, constructed in 1965 and owned by the U.S. Bureau of Reclamation, is on Oklahoma's 2008 303 (d) list for impaired beneficial uses of public/private water supply and warm water aquatic community life. Causes of impairment have been identified as low oxygen, high algae biomass, and high turbidity. Lake Thunderbird is classified as a Nutrient Limited Watershed (NLW) in Oklahoma Water Quality Standards based on Carlson's Trophic State Index (TSI). Lake Thunderbird, an important recreational lake for fishing and boating, is also identified as a Sensitive Water Supply (SWS) since the lake serves as a public water supply for the cities of Norman, Midwest City and Del City.

The Oklahoma Department of Environmental Quality (ODEQ) will develop a TMDL or a watershed-based water quality management plan in lieu of a TMDL for Lake Thunderbird. An important component of the plan will be the identification of potential load reductions needed to control loading of nutrients, organic matter and sediments expected to attain compliance with water quality targets for restoration of Lake Thunderbird to its designated beneficial uses. To provide a sound technical basis for the TMDL or a water quality management plan, two EPA-supported public domain models have been selected by ODEQ to describe hydrology, runoff and pollutant loading from the watershed (HSPF); and hydrodynamics and water quality in Lake Thunderbird (EFDC). The linked watershed-lake model, calibrated to data collected in 2008-2009, provides ODEQ with a technically credible framework to (a) describe the water quality response within the lake to existing watershed loading; (b) describe the potential response of in-lake water quality to alternative watershed load reduction scenarios; (c) evaluate the effectiveness of load reduction scenarios on compliance with Oklahoma water quality standards and defined water quality targets for turbidity, chlorophyll-a and dissolved oxygen for Lake Thunderbird; and (d) develop a TMDl or a watershed-based water quality management plan for Lake Thunderbird.

Using external flow and loading data provided by the watershed model and sediment bed data to describe the distribution of solids and nutrients in the lake, the lake model was calibrated for the 374 day period from April 2008 through April 2009, Model results were compared to observations of water temperature, total suspended solids (TSS), dissolved oxygen, chlorophyll-a, nitrogen, phosphorus and organic carbon. A regression relationship for TSS and turbidity was developed for calibration of model results with turbidity observations because Oklahoma water quality criteria for water clarity are defined in terms of turbidity. Model results for water clarity were also calibrated using observations of secchi depth.

The EFDC model incorporates internal coupling of organic matter production and deposition from the water column to the sediment bed with decomposition processes in the sediment bed that, in turn, produce benthic fluxes of nutrients and dissolved oxygen across the sediment-water interface. Lake Thunderbird, like many reservoirs, is seasonally characterized by thermal stratification and hypolimnetic anoxia. Summer anoxic conditions, in turn, are associated with internal nutrient loading from the benthic release of phosphate and ammonia into the water column that is triggered, in part, by low oxygen conditions. The water quality model, calibrated to 2008-2009 data available for Lake Thunderbird, accounts for the cause-effect interactions of water clarity, nutrient cycling, algal production, organic matter deposition, sediment decay, and sediment-water fluxes of nutrients and oxygen.

Using data compiled for the existing calibrated conditions of 2008-2009, the model framework is used to compile annual and seasonal mass-balance budgets of TSS, nutrients and organic carbon to compare the magnitude of external and internal loading to the lake under the existing conditions of 2008-2009. External sources include atmospheric deposition and streamflow and nonpoint source runoff from the HSPF watershed model. Internal sources include the benthic fluxes of nutrients simulated with the EFDC sediment diagenesis model. Internally generated benthic releases of ammonia and phosphate, aggregated over the entire lake, is estimated to account for 96% of the total loading of these nutrients during the summer stratified period from May 15-October 1. On a lake-wide basis, the anoxic period benthic phosphate release rate is 16 mg P/m**2-day, the benthic ammonia release rate is 20 mg N/m**2-day and sediment oxygen demand (SOD) is 1.1 g/m**2-day. The spatial zone in the vicinity of Site 1 at the dam is characterized by the largest nutrient release rates with the phosphate release rate estimated as 33 mg P/m**2-day, ammonia release rate estimated as 37 mg N/m**2-day and SOD estimated as 1.9 g/m**2-day. Although site-specific measurements are not available for Lake Thunderbird, the results of the sediment flux model are consistent with the range of measurements reported for ammonia and phosphate release rates and sediment oxygen demand for lakes and reservoirs characterized as eutrophic and hypereutrophic.

The calibrated model framework was applied to simulate, and evaluate, the response of Lake Thunderbird to a series of reductions in external loading of nutrients, sediment and organic carbon. Watershed loading rates are decreased for all tributaries and nonpoint source catchments by 95%, 85%, 75% and 50% to represent the overall reduction of external sources from the watershed into the lake. The water quality response of the lake model to the changes in external loads is evaluated in terms of compliance with water quality criteria and targets for turbidity, chlorophyll-a and dissolved oxygen. The results of each reduction scenario were evaluated to identify the selected load allocation scenario that provides the best response for those water quality parameters -- oxygen, chlorophyll and turbidity – that have been identified as the cause of impairment for Lake Thunderbird.

Based on an evaluation of the results simulated for the load reduction scenarios, the 75% removal scenario was selected as the load allocation scenario that provided the best response for chlorophyll and turbidity. The effect of the 75% reduction in watershed loading on internal nutrient release from the sediment bed and the response of lake water quality to changes in the sediment-water flux of nutrients and oxygen was determined with a 6-year series of model “spin-up” runs. The model simulations demonstrated a gradual reduction in internal sediment flux loading of nutrients and a significant improvement in water quality conditions under the final 75% removal scenario simulation. The model results suggest that compliance with water quality criteria for turbidity and dissolved oxygen may be achieved with 75% removal of TSS, organic matter and nutrients from external watershed loading to the lake. The results for the 75% load reduction indicate that the overall annual average 90th percentile value of 16.7 NTU for turbidity for all 8 stations will be in compliance with the 25 NTU criteria for turbidity. The results also indicate that the overall average 10th percentile concentration of 7.6 mg/L for surface dissolved oxygen for all 8 stations will be in compliance with the 5 mg/L criteria for surface oxygen under stratified conditions. In addition to compliance with the surface layer criteria for oxygen, the model results for the 75% load reduction scenario indicate that the overall hypoxic volume of the lake, defined by a cutoff level of 2 mg/L, is much less than 50% during summer stratification. The results for the 75% load allocation indicate that the overall annual average surface layer chlorophyll for the 8 station locations (20.5 ug/L), however, exceeds the water quality target of 10 ug/L.It is important to note that the model results for the 75% removal scenario should not be taken as projections of future water quality conditions in the lake with absolute certainty. The model, does however, provide ODEQ with a technically credible model framework that clearly

shows that water quality improvements can be achieved in Lake Thunderbird to support the desired beneficial uses if watershed loading can be controlled to a level based on 75% reduction of the existing loading conditions.

6.2 Conclusions

The EFDC hydrodynamic and water quality model of Lake Thunderbird was calibrated to data available to describe lake water quality conditions from April 2008 through April 2009, Model results, in general, were in good agreement to observations and met model performance targets for water temperature, dissolved oxygen, chlorophyll-a and organic carbon. Model results for TSS and turbidity was in good agreement with observed data except for the period during the two large storm events in August 2008.

The model results clearly demonstrated that internal loading of nutrients from the sediment bed to the water column is the major controlling factor leading to eutrophication of the reservoir. The model results also demonstrate that a 75% reduction in loading from the watershed may be expected to result in gradual decreases in internal loading of nutrients, decreases in sediment oxygen demand and corresponding improvements in lake water quality conditions that should result in attainment of the beneficial uses of Lake Thunderbird for turbidity and dissolved oxygen.

The calibrated HSPF watershed runoff model and the EFDC hydrodynamic and water quality model of Lake Thunderbird will provide ODEQ with a scientifically defensible surface water model framework to support development of a TMDL or a water quality management plan for Lake Thunderbird.

The calibrated watershed-lake model framework can also be applied as a tool to support evaluations of the potential water quality impact of in-lake remediation strategies. Hypolimnetic oxygen injection, designed to decrease phosphorus release from the sediment bed under stratified conditions to control algae production, is one in-lake remediation strategy that has been tested experimentally, and is being considered for operational use in Lake Thunderbird (OWRB, 2011).

6.3 Recommendations

Based on the findings of this study, the following recommendations for data collection efforts for Lake Thunderbird are submitted for consideration by ODEQ:

- Continue the existing program for routine water quality monitoring of the key water quality parameters at the designated monitoring sites in Lake Thunderbird;
- Expand the existing lake monitoring program to periodically include measurements of euphotic zone productivity and respiration;
- Expand the existing lake monitoring program to routinely collect and track phytoplankton species groups. The availability of a database that can be used to track and evaluate physical and water quality conditions that lead to Harmful Algae Blooms (HABs), such

as outbreaks of cyanobacteria, is critical information that is needed for effective management of the lake as a public water supply;

- Initiate surveys coordinated with routine lake monitoring program to collect measurements of (a) sediment bed C,N,P content and porewater nutrients; and (b) benthic release rates for ammonia, nitrate, phosphate and sediment oxygen demand. Surveys conducted in spring, summer and fall at 2-3 year intervals would provide a reasonable time frame to track changes in benthic release rates expected to result from implementation of load reductions within the watershed;
- Install streamflow gages on the Little River and Hog Creek and initiate a routine monitoring program to begin to develop a database to characterize streamflow and water quality loading from the watershed into the lake; watershed data is essential for evaluations of the effectiveness of any BMPs that may be implemented under the TMDL or the water quality management plan to be developed for Lake Thunderbird.

Section 7 REFERENCES

Arhonditsis, G.B. and M.T. Brett. 2005. Eutrophication model for Lake Washington (USA) Part I. Model description and sensitivity analysis. Ecol. Model. 187:140-178.

Bicknell, B., J.C. Imhoff, J.L. Kittle, T.H. Jobes, A.S. Donigian. 2001. *Hydrological Simulation Program–Fortran. HSPF Version 12, User's Manual*. Prepared by AQUA TERRA Consultants, Mountain View, CA in cooperation with Hydrologic Analysis Software Support Program, U.S. Geological Survey, Reston, VA. Prepared for National Exposure Research Laboratory, Office of Research and Development, U.S. Environmental Protection Agency, Athens, GA, EPA-March.

Blumberg, A.F., L.A. Khan and J. St. John .1999. Three-dimensional hydrodynamic model of New York Harbor Region. *Jour. Hydr. Engineering Div. , Proc. ASCE, 125(8):799-816, August.*

Carlson, R.E. 1977. A trophic state index for lakes*. Limnol. Oceanogr*. 22:361-369.

Cerco, C.F. and T.M. Cole. 1995. User's Guide to the CE-QUAL-ICM Three-Dimensional Eutrophication Model: Release 1.0. Prepared for U.S. Army Waterways Experiment Station, Vicksburg, MS. Technical Report 95-15.

Cerco, C.F., B.H. Johnson and H.V. Wang. 2002. Tributary refinements to the Chesapeake Bay Model. US Army Corps of Engineers, Engineer Research and Development Center, ERDC TR-02-4, Vicksburg, MS.

Corral, J., B. Haggard, T. Scott and S. Patterson (2011). Potential alum treatment of reservoir bottom sediments to manage phosphorus release. Poster presentation at Arkansas Water Resources Center 2011 Annual Watershed and Research Conference, July 6-7, 2011, Fayetteville, Arkansas.

Craig, P.M.. 2010. *User's Manual for EFDC_Explorer5: Pre/Post-Processor for the Environmental Fluid Dynamics Code*, Dynamic Solutions, LLC, Knoxville, TN.

Delft Hydraulics 2007. *Generation and manipulation of curvilinear grids for FLOW and WAVE*. Delft, The Netherlands, October.

Di Toro, D.M. 1978. Optics of turbid estuarine waters: approximations and applications. Water Research 12:1059-1068.

Di Toro, D.M. 2001. *Sediment Flux Modeling*. Wiley Interscience, New York, NY.

Donigian,Jr., A.S. 2000. *HSPF Training Workshop Handbook and CD*. Lecture #19. Calibration and Verification Issues, Slide #L19-22. EPA Headquarters, Washington Information Center, 10-14 January 2000. Presented and prepared for U.S. EPA Office of Water, Office of Science & Technology, Washington, DC.

Dynamic Solutions, LLC. 2011. 3-Dimensional Hydrodynamic EFDC Model of Lake Thunderbird, Oklahoma Model Setup and Calibration, Tasks 1A,1B(b) and 1B(c). Technical report prepared by Dynamic Solutions, Knoxville, TN for Oklahoma Dept. Environmental Quality, Water Quality Division, Oklahoma City, OK.

Dzialowski, A.R. and L. Carter (undated). Predicting internal nutrient release rates from Central Plains reservoirs for use in TMDL development. Final Report, Project Number: X7 97703801, Dept. Zoology, Oklahoma State University, Stillwater, OK, Submitted to U.S. Environmental Protection Agency, Region 7, TMDL Program, Water Quality Management Branch, Kansas City, KS.

Haggard, B.E. and T.S. Soerens. 2006. Sediment phosphorus release at a small impoundment on the Illinois River, Arkansas and Oklahoma, USA. Ecol. Eng'r. 28:280-287.

Haggard, B.E., D.R. Smith and K.R. Brye. 2007. Variations in stream water and sediment phosphorus among select Ozark catchments. J. Environ. Qual. 36(6):1725-1734.

Haggard, B.E., P.A. Moore and P.B. DeLaune. 2005. Phosphorus flux from bottom sediments in Lake Eucha, Oklahoma. J. Environ. Qual. 34:724-728.

Haggard, B.E. and J.T. Scott .2011. Phosphorus release rates from bottom sediments at Lake Wister, Oklahoma,Summer, 2010. Arkansas Water Resources Center-University of Arkansas, Tech. Pub. Number MSC 364-Year 2011.

Hamdan, T., T. Scott, D. Wolf and B.E. Haggard 2010. Sediment phosphorus flux in Beaver Lake in Northwest Arkansas. Discovery, Student Journal of Dale Bumpers College of Agricultural, Food and Life Sciences, University of Arkansas, Fayetteville, AR, Volume 11, Fall 2010, pp. 3-12.

Hamrick, J.M. 1992. *A Three-Dimensional Environmental Fluid Dynamics Computer Code: Theoretical and Computational Aspects*. Special Report No. 317 in Applied Marine Science and Ocean Engineering, Virginia Institute of Marine Science, Gloucester Point, VA. 64pp.

Hamrick, J.M. 1996. *User's Manual for the Environmental Fluid Dynamics Computer Code*. Special Report No. 331 in Applied Marine Science and Ocean Engineering, Virginia Institute of Marine Science, Gloucester Point, VA.

Hamrick, J.M. 2007. The Environmental Fluid Dynamics Code Theory and Computation Volume 3: Water Quality Module. Technical report prepared by Tetra Tech, Inc., Fairfax, VA.

Hamon, R.W. 1961. Estimating Potential Evapotranspiration, Proceedings of the American Society of Civil Engineers, *Journal of the Hydraulic Division*, Vol. 87, No. HY3, p 107-120.

Hupfer, M. and J. Lewandowski. 2008. Oxygen controls the phosphorus release from lake sediments- along-lasting paradigm in limnology. Internat. Rev. Hydrobiol. 93:415-432.

Ji, Z-G. 2008. *Hydrodynamics and Water Quality Modeling Rivers, Lakes and Estuaries*. Wiley Interscience, John Wiley & Sons, Inc., Hoboken, NJ, 676 pp.

Kaushai, S. and M. W. Binford. 1999. Relationship between C:N ratios of lake sediments, organic matter sources, and historical deforestation in Lake Pleasant, Massachusetts, US. Jour. Paleolimnology, 22:439-442.

Lick, W. 2009. *Sediment and Contaminant Transport in Surface Waters*. CRC Press, Boca Raton, FL, 398 pp.

Mortimer, C.H. 1941. The exchange of dissolved substances between mud and water in lakes. J. Ecology 29:280-329.

Mortimer, C.H. 1942. The exchange of dissolved substances between mud and water in lakes. J. Ecology 30:147-201.

Nowlin, W.H., J.L. Evarts and M.J. Vanni 2005 Release rates and potential fates of nitrogen and phosphorus from sediments in a eutrophic reservoir. *Freshwater Biology*, 50, 301-322.

ODEQ 2008. *Water Quality in Oklahoma 2008 Integrated Report.* Appendix C: 303 (d) List of Impaired Waters. Oklahoma Department of Environmental Quality, Oklahoma City, OK, 376 pp.

OWRB. 2004. Lake Thunderbird Algae 2003. Oklahoma Water Resources Board, Oklahoma City, OK.

OWRB. 2009. Lake Thunderbird Water Quality 2008. Oklahoma Water Resources Board, Oklahoma City, OK.

OWRB. 2010. Lake Thunderbird Water Quality 2009. Oklahoma Water Resources Board, Oklahoma City, OK.

OWRB. 2008. *2007-2008 Oklahoma's Lakes Report. Beneficial Use Monitoring Program*. Oklahoma Water Resources Board, Oklahoma City, OK. www.owrb.ok.gov/quality/monitoring/bump/pdf_bump/CurrentLakesReport.pdf

OWRB. 2011. Developing in-lake BMPs to enhance raw water quality of Oklahoma's Sensitive Water Supply. Final Report, CA# 2P-96690801, Project 4, Oklahoma Water Resources Board, Oklahoma City, OK.

Park, R, A.Y. Kuo, J. Shen and J. Hamrick.2000. *A Three-Dimensional Hydrodynamic-Eutrophication Model (HEM-3D): Description of Water Quality and Sediment Process Submodels.* Special Report 327 in Applied Marine Science and Ocean Engineering, School of Marine Science, Virginia Institute of Marine Science, the College of William and Mary, Gloucester Point, Virginia.

Sen, S., B.E. Haggard, I. Chaubey, K.R. Brye, T.A. Costello and M.D. Matlock. 2007. Sediment phosphorus release at Beaver Reservoir, northwest Arkansas, USA, 2002-2003: a preliminary investigation. Water, Air & Soil Pollution 179:67-77.

Thomann, R.V. and J.A. Mueller. 1987. *Principles of Surface Water Quality Modeling and Control*. Harper Collins Publishers,New York, NY.

Veenstra, J.N. and S. L. Nolen. 1991. *In-situ* sediment oxygen demand in five southwestern U.S. lakes. Water Research, 25(3):351-354.